

**UNIVERSITY OF TURKISH AERONAUTICAL ASSOCIATION  
INSTITUTE OF SCIENCE AND TECHNOLOGY**

**SIMULATION AND COMPARISON AMONG CONVENTIONAL BUCK-  
BOOST, Z-SOURCE AND QUASI Z-SOURCE POWER INVERTERS**

**MASTER THESIS**

**Israa Ismael HUSSEIN**

**A THESIS SUBMITTED IN PARTIAL FULFILLMENT OF THE  
REQUIREMENTS FOR THE DEGREE OF  
MASTER OF SCIENCE IN  
ELECTRICAL AND ELECTRONICS ENGINEERING**

**NOVEMBER, 2016**

**UNIVERSITY OF TURKISH AERONAUTICAL ASSOCIATION  
INSTITUTE OF SCIENCE AND TECHNOLOGY**

**SIMULATION AND COMPARISON AMONG CONVENTIONAL BUCK-  
BOOST, Z-SOURCE AND QUASI Z-SOURCE POWER INVERTERS**

**MASTER THESIS**

**Israa Ismael HUSSEIN**

**1406030006**

**A THESIS SUBMITTED IN PARTIAL FULFILLMENT OF THE  
REQUIREMENTS FOR THE DEGREE OF  
MASTER OF SCIENCE IN  
ELECTRICAL AND ELECTRONICS ENGINEERING**

**Supervisor: Assist. Prof. Dr. Ibrahim MAHARIQ**

**NOVEMBER, 2016**

Israa Ismael HUSSEIN, having student number 1406030006 and enrolled in the Master Program at the Institute of Science and Technology at the University of Turkish Aeronautical Association, after meeting all of the required conditions contained in the related regulations, has successfully accomplished, in front of the jury, the presentation of the thesis prepared with the title of: "SIMULATION AND COMPARISON AMONG CONVENTIONAL BUCK-BOOST, Z-SOURCE AND QUASI Z-SOURCE POWER INVERTERS".

**Supervisor : Assist. Prof. Dr. Ibrahim MAHARIQ**  
**University of Turkish Aeronautical Association** .....



**Jury Members : Assist Prof. Dr. Ozan KEYSAN**  
**Middle East Technical University**



**: Assist. Prof. Dr. Javad RAHEBI**  
**University of Turkish Aeronautical Association** .....



**: Assist. Prof. Dr. Ibrahim MAHARIQ**  
**University of Turkish Aeronautical Association** .....



**Thesis Defense Date: 14.11.2016**

**UNIVERSITY OF TURKISH AERONAUTICAL ASSOCIATION  
INSTITUTE OF SCIENCE AND TECHNOLOGY**

I hereby declare that all the information in this study I presented as my Master's Thesis, called: SIMULATION AND COMPARISON AMONG CONVENTIONAL BUCK-BOOST, Z-SOURCE AND QUASI Z-SOURCE POWER INVERTERS has been presented in accordance with the academic rules and ethical conduct. I also declare and certify with my honor that I have fully cited and referenced all the sources I made use of in this present study.



**14.11.2016**

**Israa Ismael HUSSEIN**

## **ACKNOWLEDGEMENTS**

First of all, I am grateful to The Almighty God for helping me to complete this thesis.

I would like to acknowledge my thesis advisor Assist. Prof. Dr. Ibrahim Mahariq at University of Turkish Aeronautical Association for his guidance and encouragement through my research for this thesis.

I would also like to acknowledge general director of general directorate of middle region in Iraqi Ministry of Electricity Eng. Qasim Abbood Mezaal for his valuable supports, helped me in one way or another in bringing out this work and advices me toward finishing my thesis in a good way.

Finally, I would present my fully gratitude to Eng. Raad Salih Jawad for all his efforts to help me in my thesis.

**November, 2016**

**Israa Ismael HUSSEIN**

## TABLE OF CONTENTS

ACKNOWLEDGEMENTS .....	iv
TABLE OF CONTENTS .....	v
LIST OF TABLES .....	viii
LIST OF FIGURES.....	ix
LIST OF ABBRIVIATIONS .....	xii
LIST OF PUPULICATIONS .....	xiv
ABSTRACT .....	xv
ÖZET.....	xvi
<b>CHAPTER ONE</b> .....	1
<b>1. INTRODUCTION</b> .....	1
1.1 Background.....	1
1.2 Purpose of The Study.....	2
1.3 Significance of The Study .....	2
1.4 Material and Method.....	3
1.5 Organization of The Thesis .....	4
<b>CHAPTER TWO</b> .....	5
<b>2. LITERATURE REVIEW</b> .....	5
2.1 Literature Review .....	5
2.2 DC and AC Current .....	9
2.3 Power Inverters .....	10
2.4 Pulse Width Modulation .....	11
2.4.1 Basic Operation of Three Phase PWM .....	13
2.4.2 Sinusoidal Pulse Width Modulation Techniqe (SPWM) .....	14
2.5 Insulated Gate Bipolar Transistors (IGBTs).....	15
2.6 LC-Filter .....	15
<b>CHAPTER THREE</b> .....	17
<b>3. INVERTERS TOPOLOGIES</b> .....	17

3.1	Traditional Inverter .....	17
3.2	Types of Traditional Inverters .....	18
3.2.1	Three Phase Voltage Source Inverters (VSIs).....	18
3.2.2	Three Phase Current Source Inverters (CSIs) .....	21
3.3	Buck-Boost Converter .....	22
3.4	Z-source inverter.....	25
3.4.1	Impedance Network .....	26
3.4.2	Equivalent Circuit and Operating Principle .....	26
3.4.3	Analysis of Impedance Network .....	31
3.4.4	Advantages of Z-Source Inverter .....	33
3.5	Quasi Z-Source Inverter .....	34
3.5.1	Quasi Z-Source Inverter Circuit.....	35
3.5.2	Circuit Analysis of Quasi Z-Source Inverter.....	37
3.5.3	Advantages of Quasi Z-Source Inverter.....	38
<b>CHAPTER FOUR.....</b>		<b>40</b>
<b>4. CONTROL METHODS.....</b>		<b>40</b>
4.1	Literature Overview .....	40
4.2	PWM Control Methods of Z-Source Inverter.....	41
4.2.1	Simple Boost Control Method.....	41
4.2.2	Maximum Boost Control Method .....	42
4.2.3	Modified Space-Vector Modulation Control Method.....	43
4.2.4	Maximum Constant Boost Control Method .....	44
4.2.4.1	Principle of operation of the maximum constant boost control method .....	46
4.3	Efficiency Comparison .....	49
<b>CHAPTER FIVE.....</b>		<b>51</b>
<b>5. CALCULATIONS AND RESULTS .....</b>		<b>51</b>
5.1	Arrangement of Results .....	51
5.2	Results of Three Phase Conventional Two Stage VSI .....	51
5.2.1	Matlab Simulink Model of Buck-Boost System.....	51
5.2.2	Calculations and Results of Conventional BB.....	53
5.3	Results of Three Phase Z-Source Inverter .....	65
5.3.1	Matlab Simulink Model of ZSI System .....	65

5.3.2	Calculations and results of ZSI .....	67
5.4	Results of Three Phase Quasi Z-Source Inverter.....	81
5.4.1	Matlab Simulink Model of QZSI System .....	81
5.4.2	Calculations and Results of QZSI.....	82
5.5	Comparison Among Conventional Two Stage BB VSI, ZSI AND QZSI....	87
<b>CHAPTER SIX</b>	.....	<b>89</b>
<b>6. CONCLUSIONS AND FUTURE WORKS</b>	.....	<b>89</b>
6.1	Conclusions.....	89
6.2	Future Works .....	92
<b>REFERENCES</b>	.....	<b>93</b>
<b>CURRICULUM VITAE</b>	.....	<b>100</b>

## LIST OF TABLES

<b>Table 3.1</b>	: Valid switch vectors for a three-phase VSI.....	20
<b>Table 4.1</b>	: The summary of different ST control methods expressions. ....	48
<b>Table 5.1</b>	: DC link voltage vs modulation index of conventional BB VSI.....	54
<b>Table 5.2</b>	: Duty cycle vs input voltage of conventional BB VSI. ....	54
<b>Table 5.3</b>	: Voltage stress vs input voltage of conventional BB VSI. ....	56
<b>Table 5.4</b>	: Simulation results of conventional BB VSI. ....	56
<b>Table 5.5</b>	: Modulation index vs input voltage of ZSI. ....	67
<b>Table 5.6</b>	: Modulation index vs shoot through duty Cycle of ZSI. ....	67
<b>Table 5.7</b>	: Modulation index vs boost factor of ZSI. ....	68
<b>Table 5.8</b>	: Voltage stress vs input voltage of ZSI. ....	68
<b>Table 5.9</b>	: Theoretical calculations of ZSI. ....	68
<b>Table 5.10</b>	: Simulation results of ZSI.....	69
<b>Table 5.12</b>	: The comparison results of conventional BB, ZSI and QZSI.....	87
<b>Table 5.13</b>	: Comparison the input voltage and the voltage stress. ....	88

## LIST OF FIGURES

<b>Figure 2.1</b> : Basic power electronic system. ....	6
<b>Figure 2.2</b> : Pulse width modulation. ....	12
<b>Figure 2.3</b> : Three-phase PWM inverter. ....	13
<b>Figure 2.4</b> : Three-phase single layer PWM inverter. ....	13
<b>Figure 3.1</b> : Traditional V-source converter. ....	19
<b>Figure 3.2</b> : Three-phase VSI model. ....	20
<b>Figure 3.3</b> : Traditional I-source converter. ....	21
<b>Figure 3.4</b> : Buck-boost power stage schematic. ....	23
<b>Figure 3.5</b> : Conventional two stage buck-boost VSI. ....	25
<b>Figure 3.6</b> : ZSI using the antiparallel combination of switch and diode. ....	25
<b>Figure 3.7</b> : Equivalent circuit of the ZSI in one of the six active states. ....	28
<b>Figure 3.8</b> : Equivalent circuit of the ZSI in one of the two traditional zero states. ....	28
<b>Figure 3.9</b> : Equivalent circuit of the ZSI in the non shoot-through states. ....	29
<b>Figure 3.10</b> : Equivalent circuit of the ZSI in the shoot-through state. ....	29
<b>Figure 3.11</b> : Traditional carrier-based PWM control without shoot-through zero states. ....	30
<b>Figure 3.12</b> : Modified carrier-based PWM control with shoot-through zero states. ....	31
<b>Figure 3.13</b> : Voltage fed ZSI. ....	36
<b>Figure 3.14</b> : Voltage fed QZSI. ....	36
<b>Figure 3.15</b> : Equivalent circuit of the QZSI in non-shoot-through vectors. ....	36
<b>Figure 3.16</b> : Equivalent circuit of the QZSI in shoot-through vectors. ....	36
<b>Figure 4.1</b> : Waveforms of simple boost control strategy (SBC). ....	42
<b>Figure 4.2</b> : Waveforms of maximum boost control strategy (MBC). ....	43
<b>Figure 4.3</b> : Switching form of MSVPWM-1. ....	44
<b>Figure 4.4</b> : Switching form of MSVPWM-2. ....	44

<b>Figure 4.5</b> : Waveforms of maximum constant boost control strategy (MCBC) with third harmonic injection.....	45
<b>Figure 4.6</b> : Shoot through pulses. ....	47
<b>Figure 4.7</b> : Voltage gain against modulation index of PWM control strategies.....	49
<b>Figure 4.8</b> : Voltage stress against voltage gain of PWM control strategies. ....	49
<b>Figure 5.1</b> : Simulink model of conventional buck-boost DC-AC VSI.....	52
<b>Figure 5.2</b> : Sinusoidal PWM controller.....	53
<b>Figure 5.3</b> : Output DC voltage at $M=0.755$ , $V_{in}=98$ v.....	59
<b>Figure 5.4</b> : Load current at $M=0.755$ , $V_{in}=98$ v. ....	59
<b>Figure 5.5</b> : Three phase load voltage at $M=0.755$ , $V_{in}=98$ v. ....	60
<b>Figure 5.6</b> : Line to line load voltage at $M=0.755$ , $V_{in}=98$ v. ....	60
<b>Figure 5.7</b> : Total Harmonic at $M=0.755$ , $V_{in}=98$ v.....	61
<b>Figure 5.8</b> : Output DC Voltage at $M=0.812$ , $V_{in}=120$ v.....	61
<b>Figure 5.9</b> : Load Current at $M=0.812$ , $V_{in}=120$ v.....	62
<b>Figure 5.10</b> : Three Phase Load Voltage at $M=0.812$ , $V_{in}=120$ v. ....	62
<b>Figure 5.11</b> : Line to Line Load Voltage at $M=0.812$ , $V_{in}=120$ v. ....	62
<b>Figure 5.12</b> : Total Harmonic at $M=0.812$ , $V_{in}=120$ v. ....	63
<b>Figure 5.13</b> : Output DC Voltage at $M=1.0$ , $V_{in}=176$ v.....	63
<b>Figure 5.14</b> : Load current at $M=1.0$ , $V_{in}=176$ v. ....	64
<b>Figure 5.15</b> : Three phase load voltage at $M=1.0$ , $V_{in}=176$ v.....	64
<b>Figure 5.16</b> : Line to line load voltage at $M=1.0$ , $V_{in}=176$ v.....	64
<b>Figure 5.17</b> : Total harmonic at $M=1.0$ , $V_{in}=176$ v. ....	65
<b>Figure 5.18</b> : Simulink model of ZSI.....	66
<b>Figure 5.19</b> : Maximum constant boost strategy with 3 <sup>rd</sup> harmonic injection controller. ....	66
<b>Figure 5.20</b> : The DC link voltage at $M=0.755$ , $V_{in}=98$ v.....	72
<b>Figure 5.21</b> : The voltage across $C1$ and $C2$ at $M=0.755$ , $V_{in}=98$ v.....	72
<b>Figure 5.22</b> : The Inductors current at $M=0.755$ , $V_{in}=98$ v.....	72
<b>Figure 5.23</b> : The load current at $M=0.755$ , $V_{in}=98$ v.....	73
<b>Figure 5.24</b> : Three phase load voltage at $M=0.755$ , $V_{in}=98$ v.....	73
<b>Figure 5.25</b> : Line to Line load Voltage at $M=0.755$ , $V_{in}=98$ v.....	73
<b>Figure 5.26</b> : Total harmonic at $M=0.755$ , $V_{in}=98$ v. ....	74

<b>Figure 5.28</b> : The voltage across $C1$ and $C2$ at $M=0.812$ , $V_{in}=120$ v. ....	75
<b>Figure 5.29</b> : The inductors current at $M=0.812$ , $V_{in}=120$ v. ....	75
<b>Figure 5.30</b> : The load current at $M=0.812$ , $V_{in}=120$ v. ....	75
<b>Figure 5.31</b> : Three phase load voltage at $M=0.812$ , $V_{in}=120$ v. ....	76
<b>Figure 5.32</b> : Line to line load voltage at $M=0.812$ , $V_{in}=120$ v. ....	76
<b>Figure 5.33</b> : Total harmonic at $M=0.812$ , $V_{in}=120$ v. ....	76
<b>Figure 5.34</b> : The voltage across $C1$ and $C2$ at $M=1.0$ , $V_{in}=176$ v. ....	77
<b>Figure 5.35</b> : The inductors current at $M=1.0$ , $V_{in}=176$ v. ....	77
<b>Figure 5.36</b> : The DC link voltage at $M=1.0$ , $V_{in}=176$ v. ....	77
<b>Figure 5.37</b> : The load current at $M=1.0$ , $V_{in}=176$ v. ....	78
<b>Figure 5.38</b> : Three phase load voltage at $M=1.0$ , $V_{in}=176$ v. ....	78
<b>Figure 5.39</b> : Line to line load voltage at $M=1.0$ , $V_{in}=176$ v. ....	78
<b>Figure 5.40</b> : Total harmonic at $M=1.0$ , $V_{in}=176$ v. ....	79
<b>Figure 5.41</b> : The DC link voltage at $M=1.1$ , $V_{in}=198$ v. ....	79
<b>Figure 5.42</b> : The voltage across $C1$ and $C2$ at $M=1.1$ , $V_{in}=198$ v. ....	80
<b>Figure 5.43</b> : The Inductors Current at $M=1.1$ , $V_{in}=198$ v. ....	80
<b>Figure 5.44</b> : The Load Current at $M=1.1$ , $V_{in}=198$ v. ....	80
<b>Figure 5.45</b> : Three phase load voltage at $M=1.1$ , $V_{in}=198$ v. ....	80
<b>Figure 5.46</b> : Line to Line load Voltage at $M=1.1$ , $V_{in}=198$ v. ....	81
<b>Figure 5.47</b> : Total harmonic at $M=1.1$ , $V_{in}=198$ v. ....	81
<b>Figure 5.48</b> : Simulink model of QZSI. ....	82
<b>Figure 5.49</b> : The DC link voltage at $M=0.755$ , $V_{in}=98$ v. ....	83
<b>Figure 5.50</b> : The voltage across $C1$ and $C2$ at $M=0.755$ , $V_{in}=98$ v. ....	83
<b>Figure 5.51</b> : The inductors current at $M=0.755$ , $V_{in}=98$ v. ....	83
<b>Figure 5.52</b> : The DC link voltage at $M=0.812$ , $V_{in}=120$ v. ....	84
<b>Figure 5.53</b> : The voltage across $C1$ and $C2$ at $M=0.812$ , $V_{in}=120$ v. ....	84
<b>Figure 5.54</b> : The inductors current at $M=0.812$ , $V_{in}=120$ v. ....	84
<b>Figure 5.55</b> : The DC link voltage at $M=1.0$ , $V_{in}=176$ v. ....	85
<b>Figure 5.56</b> : The voltage across $C1$ and $C2$ at $M=1.0$ , $V_{in}=176$ v. ....	85
<b>Figure 5.57</b> : The inductors current at $M=1.0$ , $V_{in}=176$ v. ....	85
<b>Figure 5.58</b> : The DC link voltage at $M=1.1$ , $V_{in}=198$ v. ....	86
<b>Figure 5.59</b> : The voltage across $C1$ and $C2$ at $M=1.1$ , $V_{in}=198$ v. ....	86
<b>Figure 5.60</b> : The inductors current at $M=1.1$ , $V_{in}=198$ v. ....	86

## LIST OF ABBRIVIATIONS

<b>PWM</b>	: Pulse Width Modulation
<b>DC</b>	: Direct Current
<b>AC</b>	: Alternating Current
<b>SPWM</b>	: Sinusoidal Pulse Width Modulation
<b>EMI</b>	: Electromagnetic Interference
<b>CM</b>	: Common Mode
<b>IGBTs</b>	: Insulated Gate Bipolar Transistors
<b>CSIs</b>	: Current Source Inverters
<b>SVPWM</b>	: Space Vector Pulse Width Modulation
<b>ASDs</b>	: Adjustable Speed Drives
<b>FACTS</b>	: Flexible Alternating Current Transmission Systems
<b>HVDC</b>	: High Voltage Direct Current
<b>CMV</b>	: Common Mode Voltage
<b>CMC</b>	: Common Mode Current
<b>MOSFET</b>	: Metal Oxide Semiconductor Field Effect Transistor
<b>GUI</b>	: Graphical User Interface
<b>R</b>	: Resistor
<b>L</b>	: Inductor
<b>C</b>	: Capacitor
<b>P</b>	: Power
<b>THD</b>	: Total Harmonic Distortion
<b>VSI</b>	: Voltage Source Inverters
<b>ZSI</b>	: Z Source Inverter
<b>ST</b>	: Shoot Through
<b>QZSI</b>	: Quasi Z Source Inverter
<b>SPWM</b>	: Sinusoidal Pulse Width Modulation
<b>MSVPWM</b>	: Modified Space Vector Pulse Width Modulation

<b>MBC</b>	: Maximum Boost Control
<b>MCBC</b>	: Maximum Constant Boost Control
<b>SBC</b>	: Simple Boost Control
<b>BB</b>	: Buck Boost
<b>G</b>	: Gain
<b>M</b>	: Modulation Index
<b>PV</b>	: Photovoltaic
<b>ZCS</b>	: Zero Current Switching
<b>ZVS</b>	: Zero Voltage Switching
<b>GTO</b>	: Gate Turn Off thyristor
<b>IPMs</b>	: Intelligent Power Modules
<b>PFC</b>	: power factor correction
<b>D</b>	: Duty cycle
<b>SCR</b>	: Silicon Controlled Rectifier
<b>BJT</b>	: Bipolar Junction Transistor
<b>MOSFET</b>	: Metal Oxide Semi-Conductor Field Effect Transistor
<b>SVPWM</b>	: Space Vector Pulse Width Modulation
<b>BBVSI</b>	: Buck Boost Voltage Source Inverter
<b>V<sub>s</sub></b>	: Voltage stress
<b>D<sub>o</sub></b>	: Shoot through duty cycle
<b>F<sub>s</sub></b>	: Switching Frequency
<b>B</b>	: Boost factor
<b>SI</b>	: Source Inverter

## LIST OF PUPULICATIONS

**Raad S. Jawad, Israa I. Hussein, I. Mahariq** , "Design and Simulation of Three Phase and Single Phase Z-Source Inverters", ICEEPIV, researchgate.net, pp. 58-64, 6-7 April 2016.

Online paper link:

[https://scholar.google.com.tr/scholar?q=Design+And+Simulation+Of+Three+Phase+And+Single+Phase+ZSource+Inverters&hl=en&as\\_sdt=0&as\\_vis=1&oi=scholar&sa=](https://scholar.google.com.tr/scholar?q=Design+And+Simulation+Of+Three+Phase+And+Single+Phase+ZSource+Inverters&hl=en&as_sdt=0&as_vis=1&oi=scholar&sa=)

**Raad S. Jawad, Israa I. Hussein, I. Mahariq** , "FACTS Technology: Current Challenges and Future Trends", ICEEPIV, researchgate.net, pp. 45-50, 6-7 April 2016.

Online paper link:

[https://scholar.google.com.tr/scholar?q=FACTS+Technology%3A+Current+Challenges+And+Future+Trends&btnG=&hl=en&as\\_sdt=0%2C5&as\\_vis=1](https://scholar.google.com.tr/scholar?q=FACTS+Technology%3A+Current+Challenges+And+Future+Trends&btnG=&hl=en&as_sdt=0%2C5&as_vis=1)

## ABSTRACT

### SIMULATION AND COMPARISON AMONG CONVENTIONAL BUCK-BOOST, Z-SOURCE AND QUASI Z-SOURCE POWER INVERTERS

Hussein, Israa

Master, Department of Electrical and Electronics Engineering

Supervisor: Assist. Prof. Dr. Ibrahim Mahariq

November 2016, 100 pages

This thesis investigated the modeling and simulation of three types of voltage source inverters, conventional two stage buck-boost dc-ac VSI controlled by sinusoidal pulse width modulation control, Z-source and Quasi Z-source topologies controlled by maximum constant boost with third harmonic injection control. The work in this thesis is based on three-phase voltage source inverters having 120V output peak phase voltage, 60 HZ, and with a switching frequency of 10 KHz to drive a resistive load of 10  $\Omega$ . The output voltage, current ripple and their harmonics are varied with modulation index at various input voltages. In addition, the thesis focuses on the effect of shoot through in the traditional Z-source and Quasi Z-Source inverters.

The simulation is implemented by MATLAB-Simulink software. The Insulated Gate Bipolar Transistor (IGBTs) is utilized as a switching device. The duty cycle variation is achieved by using pulse width modulation.

**Keywords:** Buck-Boost, Matlab Simulink, Shoot through, Power Inverter, Z-Source.

## ÖZET

### GELENEKSEL BUCK-BOOST (DÜŞÜRÜCÜ-YÜKSELTİCİ), Z-SOURCE VE QUASI Z-SOURCE GÜÇ EVİRGEÇLERİ ARASINDA SİMULASYON VE KARŞILAŞTIRMA

Hussein, Israa

Yüksek Lisans, Elektrik ve Elektronik Mühendisliği

Tez Danışmanı: Yrd. Doç. Dr. Ibrahim Mahariq

Ekim 2016, 100 sayfa

Bu tezde, üç farklı tipte gerilim kaynak evirgeçlerinin modelleme ve simülasyonunu incelenmiş bulunmaktadır; geleneksel iki aşamalı, sinüzoidal atış aralığı modülasyonu kontrollü buck-boost dc-ac VSI ile üçüncü harmonic enjeksiyonlu maksimum sabit yükseltme kontrollü Z-source ve Quasi Z-source topolojileri. Bu tezdeki çalışmalar, 120 V çıkış tepe faz gerilimi, 60 Hz'te 10  $\Omega$  direnç yükünü tahriklemek üzere 10 KHz anahtarlama frekansına sahip üç-fazlı gerilim kaynak evirgeçlerine dayanmaktadır. Çıkış gerilimi, akım dalgalanması ve bunların harmonikleri çeşitli giriş gerilimleri altında modülasyon endeksi ile çeşitlendirilmiştir. Buna ilaveten, tez geleneksel Z-source ve Quasi Z-source evirgeçlerindeki shoot-through etkisine odaklanmaktadır.

Simulasyon MATLAB-Simulink yazılımı ile uygulanmıştır. Yalıtımlı Geçitli Bipolar Tranzistör (Insulated Gate Bipolar Transistor - IGBTs) ise anahtarlama cihazı olarak kullanılmıştır. Görev çevrimi varyasyonuna, atış aralığı modülasyonu kullanılarak ulaşılmıştır.

**Anahtar Kelimeler:** Buck-Boost, MatlabSimulink, Shoot-Through, Güç Evirgeci, Z-Source

## **CHAPTER ONE**

### **INTRODUCTION**

#### **1.1 Background**

Today, the most of small size commercial inverters that found in the markets have been covered up well in confidential way either in single phase or three phase applications. This is to guarantee that the item will not be reproduce or duplicated by others. The process applied also to avoid the competition.

Mostly DC-AC inverters have been widely utilized in electrical power applications, for example, AC motor drives, static frequency changes, uninterruptible power supplies ...etc. Recently, the inverters have importance as they represent backbones of the renewable energy applications as they are used to link a photovoltaic or wind system to power grids.

In this era, the advances in solid-state semiconductors, power electronics devices and microprocessors helped many Pulse Width Modulation (PWM) techniques to develop for industrial applications. One of these applications is PWM based three phase voltage source inverters (VSI), that convert DC power to AC power with various voltage in magnitude and/or frequency. The most widely utilized PWM schemes for three phase voltage source inverters are Sinusoidal PWM (SPWM).

These days, many studies have been done concentrating on renewable energy as an alternative to produce the electricity. Renewable energy is generally derived from either solar, wind, hydro, geothermal or biomass.

By using inverters, fuel consumption cost is decreased and hence the maintenance wanted for generators is decreased as well, and this results in less pollution to the environment.

## **1.2 Purpose of The Study**

Inverters have been gaining more attention and importance in power electronics systems especially after the implementation of high voltage DC (HVDC) systems in 1950s. They have even more importance nowadays because they are considered as the main part of renewable energy systems from the sense that they are responsible for converting voltages from DC to AC form.

This study focuses on voltage source inverters, mainly conventional two stage buck-boost dc-ac VSI and Z-Source inverter by taking into account the mostly applied topologies: ZSI and quasi ZSI. An intensive comparison based on the analysis and simulation results among all of these topologies is presented in the current study.

For purposes of comparison, the total losses resulted in the power switching devices of each of these inverters were calculated, in addition to the calculation of total harmonic distortion, voltage stress and the efficiency of the inverters. It is important to note that MATLAB/Simulink simulation model is utilized in this study.

There are many scholars who studied the ZSI topologies and more than a hundred of papers that had been presented in the literature. However, in our study we intend to give intensive comparison supported by circuit analysis and simulation all by MATLAB/Simulink software and present a deep discussion for most of the advantages and disadvantages that determine the limitation for each topology. Thus, such a comparison will lead to develop one or more of studied topologies to satisfy the requirements of supply voltage and to overcome the most issues, and as it's clear from literature survey which consists all studies and research paper that published from 2003 till now, there is no study that covers these objectives.

## **1.3 Significance of The Study**

Many studies which intend to study the VSI or ZSI and quasi-ZSI present the advantages and disadvantages for the studied topology. In our study, we will present all advantages and disadvantages and issues that limit the use of each topology and suggesting some developments for each topology. In addition, we also specify the field of applications that mostly fit each topology.

In this thesis, a comparison among conventional two stage buck-boost dc-ac VSI, Z-Source inverter and quasi ZSI inverter by taking into account the following factors are to be considered in order to meet the requirement:

- The cost of equipment.
- Power losses.
- Voltage stress.
- Size of passive elements of filters.
- Reliability.
- Total harmonic distortion (THD).

Based on this work, an engineer will be able to get a clear insight to each topology and will be able to choose the suitable one for the intended application.

#### **1.4 Material and Method**

We will study every topology based on specific values of voltage and power and applying the same control strategy for two topologies Z-source and Quasi Z-source inverters , Maximum Constant Boost Control (MCBC) method with third harmonic injection will be used, and sinusoidal pulse width modulation control used with conventional two stage buck-boost dc-ac VSI. Circuit analysis and simulation are performed by using MATLAB/Simulink software.

We intend to use the standard networks that presented by the original research. We will study all under the same conditions and for three phase systems by applying star resistive load. Our work is based on the American standard (120 volt –peak phase voltage, 60 Hz,10-ohm resistive load), and on using an LC-filter to obtain the desired output voltages and currents.

In order to fulfill the requirements, the switching technique had been used in this thesis, namely SPWM which is generated with combination of high frequency triangular wave and a sinusoidal wave. Then an LC filter is used which will provide a nearly constant output current which stabilizes system rapidly and reduces harmonics generated by inverters.

## **1.5 Organization of The Thesis**

The thesis consists of six chapters. A short explanation is introduced here:

### **1. Chapter 1: Introduction**

This chapter presents the background of the thesis objectives, purpose and significance of the study, methodology and research structure.

### **2. Chapter 2: Literature Review**

This chapter presents a literature review and the widely used power inverters, and techniques of sinusoidal pulse width modulation. Some of literature regarding the thesis topic is also included in this chapter.

### **3. Chapter 3: Inverters Topologies**

The Chapter introduces classification of converters, different power inverter topologies, types of traditional inverter and applications. In addition, circuit analysis of the DC-DC buck- boost converter and conventional two stage dc-ac VSI are also presented. Z-Source inverter and Quasi Z-Source inverters topologies and there principles of operation was presented in this chapter.

### **4. Chapter 4: Control Methods**

This chapter presents different control strategies, sinusoidal carrier based PWM and focuses on the maximum constant boost with third harmonic injection control method which proposed as a controller used in this thesis.

### **5. Chapter 5: Calculations and Results**

In this chapter, all the calculations required to determine the parameters related to the three types of inverters topologies are stated. The results of testing the three models that are implemented in MATLAB /SIMULINK software are stated and organized in tables for each topology.

### **6. Chapter 6: Conclusions and Future Works**

Finally, a conclusion on the obtained results is presented. This also includes the contribution of this thesis and suggestions for future works.

## **CHAPTER TWO**

### **LITERATURE REVIEW**

#### **2.1 Literature Review**

With the development of human populace of the world and the fast increment of the worldwide economic, the request of the energy in every one of its assets, particularly electricity confronted a huge increment.

As per the U.S. Energy Information Administration in the International Energy Outlook 2009 said that the era in worldwide power is predicated to be expanded from 18 trillion kWh in 2006 to 23.2 trillion kWh in 2015 and will much further increment to 31.8 trillion kWh for the following five years. With such sharp increment in power request, utilizing customary power era by blazing the fossil fuel to coordinate the power request is no more drawn out ready to satisfy the request. Other than that, blazing the fossil fuel will bring about various natural issues.

The emission of gases such carbon dioxide, methane and other nursery gasses will prompt to a worldwide temperature alteration issue. Besides, after agreement of the Kyoto and Copenhagen accord by a large portion of the nations in the world, this customary strategy is presently on more extended the correct approach to produce power.

This has given a few open doors for the renewable energy assets and innovation to assume control over the procedure of power generation. One of the renewable and accepted to be boundless energy assets is from the sun or normally known as the solar energy. Photovoltaic, PV is an innovation first discovered by Alexander-Edmond Becquerel in 1839, the technology changes over or converts solar energy or solar power to electric energy or electric power. From that point forward, the PV innovation had gone over with huge advancement and change, beginning from few watts in

standalone systems to few megawatts in grid connected systems. The late advancements in power semiconductors made PV technology more efficient thus saved approach to produce energy [1].

The semiconductors act as the heart of the cutting edge of power electronics, and are being widely utilized as a part of power electronics converters as a matrix of ON or OFF switches, and consequently convert power from one shape to another. There are four fundamental types of conversion that regularly can be actualized, that is, AC to AC, AC to DC, DC to AC and DC to DC. Inverter considered as one of the converter classifications which are called DC to AC converter. It changes over DC energy to a symmetric AC output voltage at requested voltage and frequency.

Inverters are broadly utilized as a part of industrial applications, for example, AC motor drives, standby power supplies, induction heating, and uninterruptible power supplies. The input power of an inverter is gotten from the power supply network, it can be a battery, photovoltaic, wind energy, fuel cell or other DC sources [2].

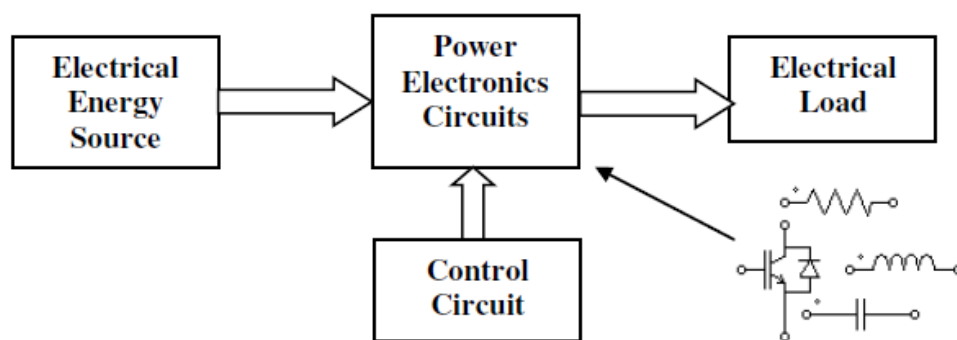


**Figure 2.1:** Basic power electronic system.

This thesis concentrates on DC to AC inverters, which plan to effectively change DC voltage to AC voltage. Inverters are utilized for some applications, for the most part in circumstances where low voltage DC sources, for example, solar panels, fuel cell and batteries must be changed over, thus devices can keep running off of AC power.

The technique in which the DC voltage is reversed, is finished by two stages. The first is the transformation of the low voltage DC energy to a high voltage DC source, and the second stage is the change of the high DC source to an AC voltage by applying pulse width modulation. Another technique to get the wanted result is change

over the low voltage DC energy to AC, and after that use a transformer to step it up. This thesis concentrates on the first strategy that mentioned above.

Among the variant DC-AC inverters, today in the market, there are basically two types of AC output, pure sine wave and modified sine wave. A modified sine wave can be viewed as a square wave more than a sine wave, that is, it passes the high DC voltage for indicated amounts of time so that the mean power and rms voltage are the same as though it were a sine wave. These kinds of inverters are less expensive than pure sine wave inverters, therefore they are be an attractive choices [3].

Yan Z. et al. [4] investigated the wide range voltage modulation, low cost, high efficiency and high power density DC/AC power conversion in renewable energy applications. Omar E. et al. [5] presented a simulation and experimental comparative analysis of the Z-source inverter (ZSI) with four different shoot-through (ST) control methods, namely: the simple boost control, the maximum boost control, the maximum constant boost control and the modified space vector modulation boost control methods.

H. Rostami [6] compared voltage gain of control methods for the Z-source inverter at a given boost factor and simulated the circuit in MATLAB. The control methods of the Z-source inverter are simple boost control, maximum boost control and maximum constant boost control, respectively. Ref. [7] presented three different inverters: traditional PWM inverter, dc/dc boosted PWM inverter, and Z-source inverter for fuel cell vehicles. In addition, the total switching device power of each of these inverters was calculated.

In Ref. [8], an Impedance Source Inverter for A.C electrical drives was studied. The impedance source inverter employs a unique impedance network coupled with inverter main circuit and rectifier by controlling the shoot-through duty cycle.

Mohd. S. B. et al. [9] compared three PWM control methods on a single-phase Z-source inverter (ZSI), traditional, simple boost (SB-PWM), and modified-reference (MR-PWM). Ref. [10] proposed two constant boost-control methods for the Z-source inverter, which can obtain maximum voltage gain at any given modulation index without producing a low-frequency ripple that is related to the output frequency and hence, minimize the voltage stress at the same time.

Selva Kumar and Priyaa Dharshini [11] discussed Photovoltaic source (PV) as it has become one of the most promising DC sources of the future. It utilizes an inverter to convert the dc output of the PV in order to utilize it for AC appliances. Anh-V. et al. [12] proposed an active switched quasi-Z-source inverter (AS-qZSI) topology, which is based on the classical qZSI. The proposed AS-qZSI adds only one switching device and diode to the classical qZSI in order to increase the boosting ability.

Ref. [13] discussed multilevel inverters and the reason why they have drawn significant attention in research and high power applications such as AC Transmission systems (FACTS), power quality devices, renewable energy resources, etc. Such power converters have been the prime focus of power electronics researches in order to improve their reliability, performance and energy efficient at minimum cost.

M. Aswini K. and Mukti B. [14] presented the performance analysis of various control and modulation methods of Z-source inverter (ZSI). Miaosen et al. [15] proposed two maximum constant boost control methods for the Z-source inverter, which can obtain maximum voltage gain at any modulation index without producing low-frequency ripple that is related to the output frequency. Ref. [16] discussed the possible operating states of an impedance network of a Z-source inverter. The authors identified and analyzed the inverter with the objective of deriving design guidelines.

Ref. [17] proposed a drive system for a symmetrical two-phase motor using Z-source inverter. The modulation technique applied to proposed system combines the theory of space-vector PWM with the ease of implementation of a triangular-comparison PWM including the shoot-through zero vectors inherent of Z-source inverter. In Ref. [18] a Z-source inverter with a modified carrier based-pulse width-modulation technique is proposed for photovoltaic systems is presented. In this new technique, two carrier waves and three reference waves were used to produce the switching pulses.

Refs. [19, 20, 28] presented a novel 3-phase Z-source inverter with six switches. The proposed system has different PWM techniques i.e., simple boost, maximum boost, maximum constant boost, modified space vector PWM etc. All are reviewed and compared for Z-source inverter and traditional Z-source inverter. Ref. [21] focuses on step by step development of MATLAB/SIMULINK model of Z-source inverter followed by harmonics study as compared to traditional inverters; i.e., voltage and current source inverter.

Sumedha and Lakumana [22] showed that in addition to the desired three dynamic states, an operating cycle may contain another three static states that do not contribute to the power conversion process. Vinnikov et al. [23] discussed the efficiency and gain of the qZSI and showed that they are limited and comparable with the conventional system of a voltage source inverter with the auxiliary step up DC/DC converter in the input stage.

Sunpho and Jani [24] presented the quasi Z source inverters and proposed an alternative to power conversion concepts as it can both buck or boost input voltage and explored various modulation technique. Ref. [25] discussed that by using the quasi-Z-Source topology, the inverter draws a constant current from the PV array and is capable of handling a wide input range. It also features reduced source stress and lower component ratings compared to the traditional ZSI. Ref. [26] reviewed various converter topologies that have been reported in the literature to overcome the limitations and problems of the traditional current source, voltage source as well as various classical buck–boost, bidirectional and unidirectional converter topologies. For further discussions, the reader may refer to references [27-32].

## 2.2 DC and AC Current

There are two types of electrical transmission, Direct Current (DC) and Alternating Current (AC). Each have advantages and disadvantages. DC power is essentially the use of a constant voltage over a circuit which cause to flow a constant current. A battery is regularly main source of DC voltage which allows DC current to flow through the load.

Most circuits today is keep running off of DC energy to give either a constant high or low voltage, by enable digital logic, process executes code. Power was first commercially transmitted as a DC power line by Thomas Edison, however, this power was limited to low magnitude due to voltage level, and dc voltage had got difficult to stepping up or down, and for these reasons ,it have not the capability to transmit dc voltage over long lines.

$$V = I * R \tag{2.1}$$

$$P = I * V = I^2 * R \tag{2.2}$$

From the equations above, we observed that the power loss can be gotten from the current squared and the resistance ( $R$ ) of a transmission line. At the point when the voltage is raised up, the present declines and appropriately the power loss reduces exponentially; that means by getting high voltage transmission, the power loss will minimize.

Electrical transmission has been based upon AC power, providing most American homes with a 120 volt AC. It ought to be noticed that since 1954 there have been many high voltage DC transmission systems constructed around the world with the appearance of DC/DC converters, permitting the simple way to step up or down of DC voltages [33].

### **2.3 Power Inverters**

Power inverter is a combination of power electronics elements which have the ability to convert electrical energy of DC frame into that of AC. Power inverters have been implemented in all sizes and shapes. Inverter circuits can be exceptionally mind boggling so the target here is to present a portion of the internal workings of inverters without losing some details. "Inverter" with regards to power electronics represents for a class of power converters circuits that is worked from a dc voltage source or a dc current source and converts it into AC voltage or current. Despite, the fact that contribution to an inverter circuit is a dc source, it is normal to have this dc got from an AC source. Accordingly, for example, the mainly source of input power might be utility AC supply that is rectified to dc by an AC to dc converter and then inverted to AC power secondly by an inverter, the output might be less or greater than AC input of the supply.

Nowadays, there two types of power inverters are available, pure sine wave and modified sine wave inverters. These inverters contrast in the related outputs, giving shifting levels of productivity and mutilation that effect on electronic devices in various ways.

Inverters, according to the kind of the topology relationship of the power circuit, can be classified to two categories, current source inverters (CSIs) and voltage source inverters (VSIs) [34]. In this thesis only the voltage source inverter will be studied.

## 2.4 Pulse Width Modulation

In electronic power converters and motors, pulse width modulation is utilized as a means of powering alternating current (AC) devices extensively with an existing direct current (DC) source or for advanced DC to AC conversion. Variation of duty cycle in the signal of PWM to give a DC voltage through the load in a particular form will appear to the load as an AC source, or can control the speed of motors that would run only at rated speed or off. The form at which the duty cycle of a pulse width modulation waveform changes can be produced during a digital microcontroller, analog components, or specific integrated circuits.

Many PWM control schemes, strategies, and realization techniques recently have been advanced. Pulse width modulation technique plays a significant role in the decreases in harmonics and switching losses of the converters, particularly in three phase applications. The first modulation techniques were advanced in the mid of 1960s by Heinrick, Kirnnich, and Bowes. The study in PWM schemes has increased in the last three decades. The main goal of any modulation technique is to get a varying output with a maximum fundamental component with minimum harmonics [3].

Analog PWM control is implemented by generating control and carrier waveforms that is applying on a comparator inputs that resulting an output based on the difference between the two waveforms. The control waveform is a sinusoidal waveform and set at the frequency of the required output, and the carrier waveform is either a saw tooth waveform or triangular waveform has a high frequency which greater than the control waveform frequency. When the carrier waveform is larger than the control waveform, the comparator gives output waveform at one case, and when the control signal is at a larger voltage, the output is at its second case. This procedure is appeared in figure 2.2 with the triangular carrier signal colored in red, sinusoidal control signal colored in blue, modulated and unmodulated sine pulses colored in blue and green respectively.

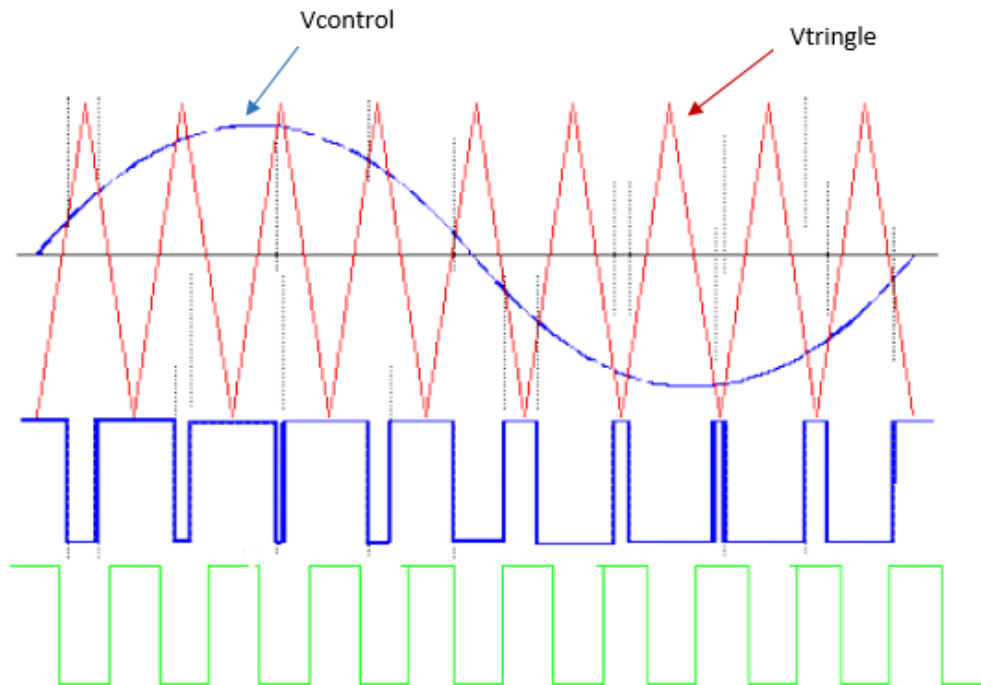


**Figure 2.2:** Pulse width modulation.

So as to create an output with a PWM signal, transistor, IGBTs or other switching technologies are regularly used to associate the source to the load. Half or full bridge configurations techniques are commonly used in power electronics.

The most features of the inverter output voltage can be written as following:

- PWM frequency is same as the frequency of  $V_{tri}$ .
- Amplitude is controlled by of  $V_{control}$  peak value.
- Fundamental frequency is controlled by frequency of  $V_{control}$ .

Modulation index ( $M$ ) can be written as:

$$M = \frac{V_{control}}{V_{triangle}} \quad (2.3)$$

The benefits of PWM are:

- No extra parts are required.
- The output voltage control can be eliminated or minimized the lower order harmonics.

Therefore, the filtering requirements has been minimized that's lead to simplify the process of filtering of higher order harmonics [34].

### 2.4.1 Basic Operation of Three Phase PWM

Figure 2.3 illustrate the three-phase PWM inverter circuit and figure 2.4 shows the signals of carrier wave ( $V_{tri}$ ) and the control wave ( $V_{control}$ ), inverter output phase voltage ( $V_{A0}, V_{B0}, V_{C0}$ ) and inverter output line to line voltages.

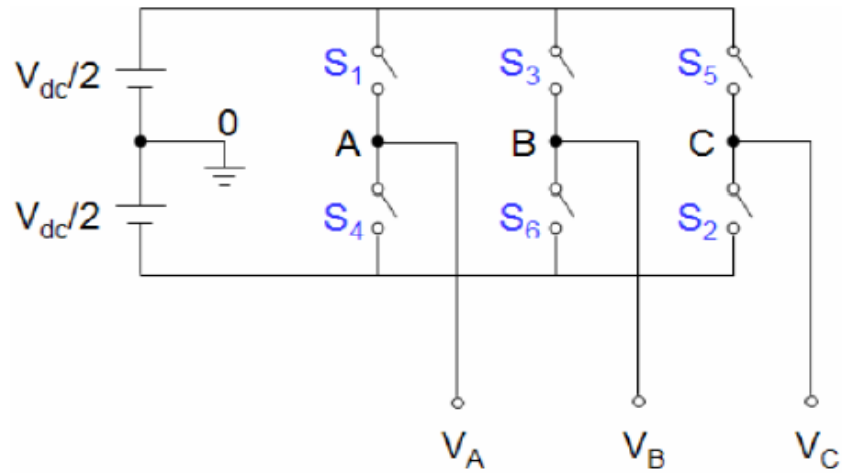


Figure 2.3: Three-phase PWM inverter.

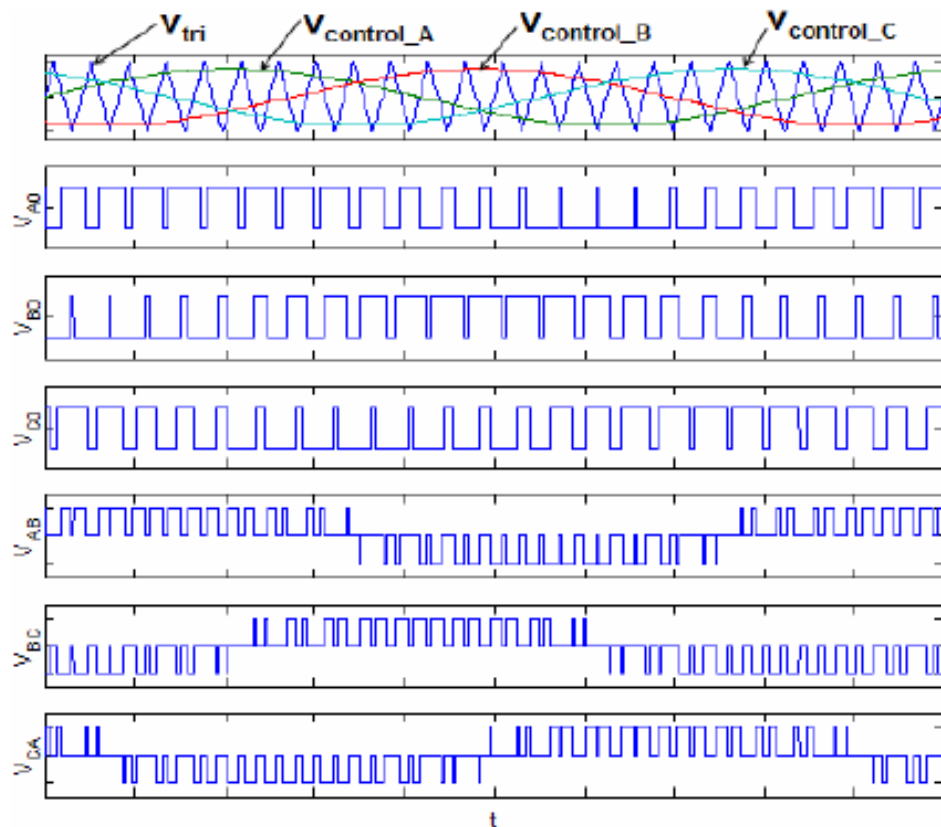


Figure 2.4: Three-phase single layer PWM inverter.

As described in figure 2.4, the frequency of  $V_{tri}$  and  $V_{control}$  is:

- Frequency of  $V_{tri} = fs$
- Frequency of  $V_{control} = f1$

Where,  $fs$  = PWM frequency and  $f1$  = Fundamental frequency.

The inverter output voltages are determined as follows:

- When  $V_{control} > V_{tri}$  ,  $VA0 = V_{dc}/2$
- When  $V_{control} < V_{tri}$  ,  $VA0 = -V_{dc}/2$

Where,  $V_{AB} = VA0 - VB0$ ,  $V_{BC} = VB0 - VC0$ ,  $V_{CA} = VC0 - VA0$

### 2.4.2 Sinusoidal Pulse Width Modulation Technique (SPWM)

Sinusoidal pulse width modulation (SPWM) is utilized in power electronics, it is widely used to digitize the power. By applying this technique, a sequence of voltage pulses can be produced by the ON and OFF of the power switching devices. The PWM inverters have been the major choices in power electronic for the last three decades, because of its circuit simplicity and rugged control scheme. SPWM switching strategy is utilized commonly in industrial applications. SPWM strategies are described by amplitude of pulses with variant duty cycle for each cycle and the width of these pulses are modulated to get output voltage control and to decrease its harmonic components [35].

This thesis deals with Sinusoidal Pulse Width Modulated (SPWM) inverters, by using this type of modulation, several pulses are generated in every half cycle of sinusoidal control signal. A high frequency triangular carrier signal ( $V_c$ ) is compared with a sinusoidal control (reference) signal ( $V_r$ ) of the output frequency. The switching instants and commutation of the modulated pulse are determined by the intersection between ( $V_c$ ) and ( $V_r$ ) waves.

The carrier and reference signals are fed into a comparator inputs. When the sinusoidal signal is higher, then the comparator output is high, else it is low. The comparator output is processed by a trigger pulse generator in such a way that the output wave has a pulse width in match with the comparator pulse width.

## 2.5 Insulated Gate Bipolar Transistors (IGBTs)

An IGBT inherits all the features of both BJTs and MOSFETs. An IGBT has low on-state conduction losses and high input impedance. There is no second breakdown problem as in BJTs. An IGBT is turned on by injecting a positive gate voltage to force the channel to be open for n-carriers. It is also turned off by disconnecting the gate voltage. It has lower switching and conduction losses because of the above reasons. So an IGBT is faster than a BJT inherently. The current rating for a single IGBT can be up to 1200V, 400A at a switching frequency of 20 KHz.

## 2.6 LC-Filter

The LC-filter, classified as a second order filter, is used to attenuate the ripple in the output. Since the L-filter obtains low attenuation of the inverter switching devices, a shunt capacitor is required to additionally attenuate the switching frequency components; this shunt capacitor should be chosen carefully in order to get low reactance at the switching frequency. But within the control frequency range, that element must give a high magnitude impedance, a capacitor is utilized for this purpose. The resonant frequency is given from the equation:

$$f_o = \frac{1}{2\pi\sqrt{LC}} \quad (2.4)$$

This LC-filter is suited to configurations where the load impedance across (C) is high at and above the switching frequency. The cost and the reactive power consumption of the LC-filter are more than those of the L-filter because of the addition of the shunt capacitor.

The LC low pass filter has the ability to attenuate most of the low order harmonics in the output voltage signals. To decrease the distortion to an acceptable magnitude, for linear or nonlinear loads, the inverter output impedance should be decreased. Therefore, the capacitance should be increased and the inductance is decreased when specifying the cut off frequency. This decreases the total cost, volume and weight.

However, by increasing the capacitance, the inverter rating will be increased due to the reactive power increase due to the filter. The switching frequency in high power applications is chosen according to inverter efficiency. Since switching losses are a significant part of the overall losses, it is desirable to decrease the size and cost of the

filtering elements by increasing the switching frequency. However, efficiency sets a limit (a design trade off should be made). The related module cannot be connected to the power grid unless the high frequency components are attenuated from the output voltage. An LC-filter of the topology has been used in each phase to decrease the distortion of the current and voltage signals of the load [33].

## **CHAPTER THREE**

### **INVERTERS TOPOLOGIES**

#### **3.1 Traditional Inverter**

In traditional DC to AC power converters, the input voltage is a dc voltage that supplied to three-phase PWM inverters and every power switches of the inverter should operate into two states ON and OFF. Therefore, high switching stresses are applying on them also, as a result for that, the switching power losses will increase linearly when the switching frequency of PWM increase.

The high rate of switching power losses not only limit the switching frequency but also decrease the overall efficiency of the system and increase the internal heat of the inverter. This will cost the manufacturers to utilize larger heat sinks, that's leading to increasing volume and weight of the system. The extra restrictions are acoustic noise and Electromagnetic Interference (EMI) [36].

The researchers were pushed to design special converters with the ability to operate at a higher switching frequency to satisfy the demand increasing for high power density converters. The applications are related to aerospace, telecommunications, and defense. Every one of these applications has special requirements with weight, volume and size to fit the field which used for. The researchers face challenges to decrease the side effects of PWM converters.

The advantages of high-frequency converters have been proved and their significance has widely increased over last three decades. Notable efforts have been made recently in the development of high-frequency zero-current switching (ZCS) and zero-voltage switching (ZVS) for dc to ac power applications, hence, power supplies that are highly dynamic, high performance with negligible noise were realized.

In these converters, resonance state is utilized in order to adapt the soft-switching techniques (ZVS/ZCS) for many elements in the resonant link and the inverter. The resonant links are regularly embedded in different locations of the inverters based on their configuration. Soft switching techniques have gained some progress through various stages during the last two decades [36].

For the traditional PWM inverter, the output phase RMS voltage at peak demand is:

$$V_{ph} = \frac{V_{in}}{2\sqrt{2}} M \quad (volt) \quad (3.1)$$

In which ( $V_{in}$ ) represents the input dc voltage, ( $V_{ph}$ ) stand for the rms output phase voltage, and ( $M$ ) is the modulation index.

### 3.2 Types of Traditional Inverters

There are two types of traditional converters, that is; voltage source inverters (VSI) and current source inverters (CSI). The inputs are dc voltage source and dc current source respectively.

#### 3.2.1 Three Phase Voltage Source Inverters (VSIs)

Figure 3.1 shows the three-phase VSI. The dc voltage source can represent a battery, fuel cell stack, diode rectifier, and capacitor. The main circuit consists of six switches. Each of them is composed of a power transistor and an antiparallel diode in order to provide bi-directional current flow and capability of unidirectional voltage blocking. Although it is widely used, it has several limitations:

- Firstly, the output AC voltage is constrained underneath and can't exceeds the dc rail voltage, otherwise, the dc rail voltage must be higher than the source voltage. Therefore, the V-source inverter performs as a buck inverter over dc-to-ac conversion mode, and it is a boost converter during ac-to-dc conversion mode. In some applications, where overdrive is wanted and the available dc voltage is limited, an additional dc-dc boost converter will be needed to obtain the desired ac output. This extra stage may increase the system cost and lower the system efficiency.

- Secondly, intention and electromagnetic interference (EMI) noise may cause a shoot-through problem when the upper and lower devices in each phase leg cannot be gated on simultaneously. When a shoot-through would occur, it will completely destroy the devices. Misgating-on states caused a major decrease in the converter's reliability. Dead time or a delay to block both upper and lower devices has to be provided in the case of V-source converter, however, this causes waveform distortion.
- To get the desired output waveform with less distortion an *LC* filter must be used, these additional components cause extra power losses and made the control of the converter more complex.

Three phase voltage source inverters are meagerly used with AC drives to give high motion control quality and increase the utilization of energy so that clean current signal can be obtained and prevent breaking in AC-DC power converter applications and increase the quality of AC power in uninterruptible power supply [37].

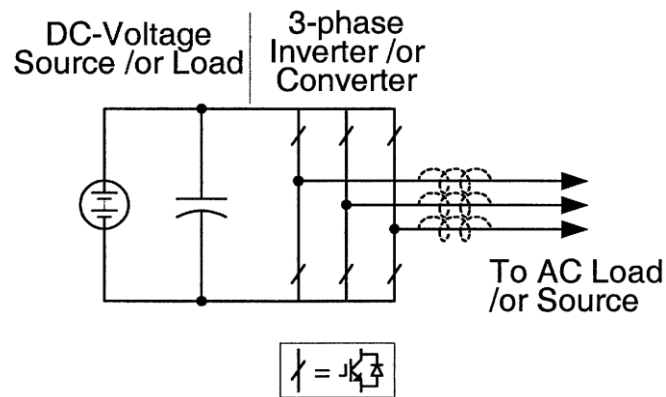


Figure 3.1: Traditional V-source converter.

Three-phase VSIs can be implemented for both medium and high-power applications. The objectives of these topologies are to provide a three-phase voltage source converters having voltage amplitude, frequency, and phase shift being controlled. The pure sinusoidal voltage signal is required for most of the power converters applications, some examples of these are flexible AC transmission systems (FACTS), Adjustable Speed Drives (ASD) and uninterruptible power supplies.

Figure 3.2 shows the standard model of three-phase voltage source inverter topology, and table 3.1 presented the valid switch vectors. For this model the upper and lower switches of any leg: S1 and S4, S3 and S6, or S5 and S2 cannot be conducted simultaneously because this will lead to a short circuit across the terminal of the dc link voltage source.

Likewise, in order to prevent the undefined vectors in the VSI, that cause undefined output AC line voltages, the upper and lower switches of any leg of the inverter shouldn't be turn off simultaneously. If this case occurred, this will lead the voltage to depend on the respective line current polarity.

Among the eight vectors, two of them 7 and 8 in table 3.1 create zero AC line voltages. For this situation, the line currents are freewheeling during either the upper or lower devices. The residual of the vectors 1 to 6 in table 3.1 create non-zero output AC voltages. In order to produce the required output waveform, the inverter moves from one vector to another. Thus, the resulting output AC line voltages consist of discrete values of voltages that are  $V_i$ , 0, and  $-V_i$  for the topology illustrates in figure 3.2. The determination of the states to produce the required signal is finished by the adjusting system to guarantee the utilization of just valid states [34].

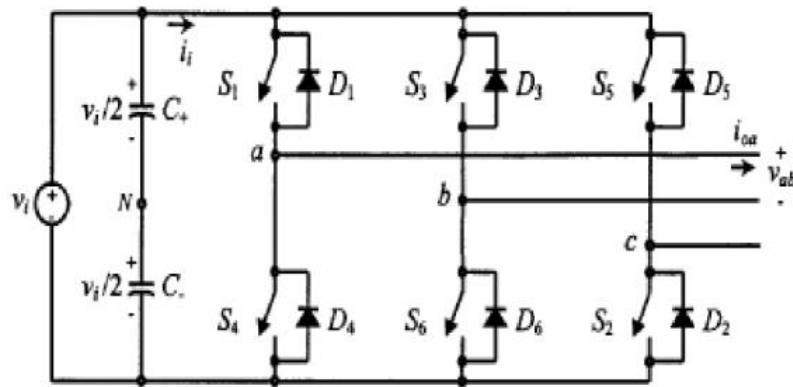


Figure 3.2: Three-phase VSI model.

Table 3.1: Valid switch vectors for a three-phase VSI.

State	Switches		Vab	Vb	Va
1	1, 2 & 6 are ON	4, 5 and 3 are OFF	V	0	-V
2	2, 3 & 1 are ON	5, 6 and 4 are OFF	0	V	-V
3	3, 4 & 2 are ON	6, 1 and 5 are OFF	-V	V	0
4	4, 5 & 3 are ON	1, 2 and 6 are OFF	-V	0	V
5	5, 6 & 4 are ON	2, 3 and 1 are OFF	0	-V	V
6	6, 1 & 5 are ON	3, 4 and 2 are OFF	V	-V	0
7	1, 3 & 5 are ON	4, 6 and 2 are OFF	0	0	0
8	4, 6 & 2 are ON	1, 3 and 5 are OFF	0	0	0

For this study, all simulation has been executed for voltage source inverters.

### 3.2.2 Three Phase Current Source Inverters (CSIs)

Figure 3.3 represents three-phase CSI. The dc current source is consists of a relatively large inductor fed by a voltage source such as a fuel cell stack, diode rectifier, battery, or a thyristor converter. The main circuit of converter consists of six switches are reverse block capability such as a gate-turn-off thyristor (GTO) and SCR or a power transistor with a series diode in order to give rout for unidirectional current and bi-directional voltage blocking. However, the current source converter has the following features and disadvantages:

- The output AC voltage must be larger than the dc original voltage that feeds the inductor or the dc voltage produced is always smaller than the input AC voltage. Along this, the CSI acts as a boost inverter for dc-to-ac power conversion and acts as buck converter for ac-to-dc power conversion. For the applications where a wide voltage range is required, an extra dc–dc buck or boost converter is required. This extra power conversion stage increases the cost of the system and decreases systems efficiency.
- At least one of the upper switches and one of the lower switches must be in on state and remained on at any time. Something else, an open circuit of the dc inductor would happen and damage the switches. The open-circuit issue by EMI noise’s misgating-off is a worst matter that affect the converter’s reliability. Overlap time for safe current commutation is required in the I-source converter, which also results signal distortion.
- The main devises of the CSIs have to block reverse voltage by a series diode to be utilized in set with high-speed transistors for example insulated gate bipolar transistors (IGBTs). This avoids in turn, the direct utilize of low-cost and high-performance IGBT modules and intelligent power modules (IPMs) [37].

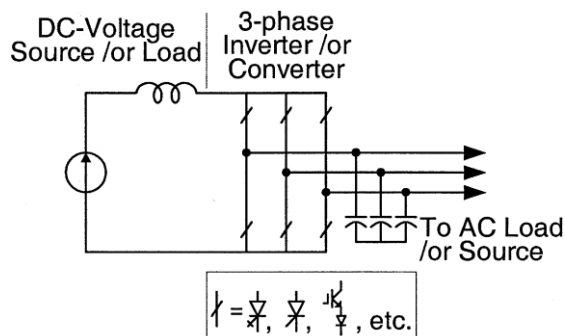


Figure 3.3: Traditional I-source converter.

Moreover, the two types of VSI and CSI have the following main issues:

- Either a buck converter or boost converter cannot acts as buck-boost converter. These limitations that constraint the output voltage to either larger or smaller than the input voltage.
- Their main circuits are not interchangeable. In another meaning, neither the V-source converter main circuit can be utilized for the I-source converter, nor vice versa.
- Both are weak against EMI noise in terms of reliability [37].

The VSI can just execute the buck conversion, while the current-source inverter executes the boost conversion. In applications for example the renewable energy generating system, such as in the photovoltaic power conditioning system, where the input voltage is change with a wide range. Therefore, the inverters systems requests to execute either both the boost and buck conversion.

Hence, the traditional voltage source inverter can't deal with this wide range without over-rating of the inverter, for the reason that the output of VSIs are limited and they are buck converters that the dc input voltages must be higher than the peak output voltages. For that reason, we utilized a buck-boost converter.

### **3.3 Buck-Boost Converter**

The fact that is widely known that the boosting topology is exceptionally successful in power factor correction (PFC) rectifier applications, delivered that the output dc voltage is close to, but slightly higher than, the peak line voltage. Therefore, boost converters that intended and designed for universal-input PFC applications are heavily oversized compared to a converters designed for a narrow range of input line voltages.

Addition to the above, the boost converters have suffering from the inrush current problem due to the large capacitor which is one of the output filter components. This problem mitigated if an additional elements are used. In universal-input PFC applications, the ability of giving both boost and buck conversion is required because the dc output voltage can be fixed to any value. On the other hand, conventional single-switch buck-boost topologies, containing the buck-boost: flyback, Cuk and SEPIC

converters, have significantly increased stresses and element sizes compared to the boost converters.

As a rule, if its conversion specification match the input/output specifications, the advantage of buck converter or the boost converter is that having the lowest stresses. This is a consequence to transfer the direct energy from the input to the output in one of the switching subintervals in the two converter topologies.

For both types of converters topologies, they need the minimum indirect energy supply, and hence, have the lowest component stresses at a specified voltage conversion ratio. Depend on this fact, it is of importance to study buck-boost converter topologies that can operate as boost or as buck converters during portions of an AC line cycle as illustrated in figure 3.4 [38]. The buck-boost DC-DC converter presents a better ability than the buck converter or boost converter individually. As predictable, additional components may be needed to give the level of functionality which required.

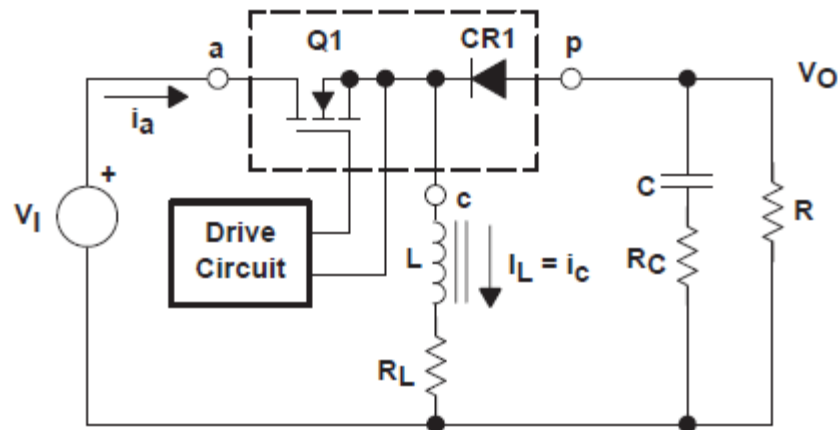


Figure 3.4: Buck-boost power stage schematic.

The buck-boost topology is a nonisolated inverting power stage, it is also known as a buck/boost power stage. Buck boost power stage are usually chosen by power supply designers because it has a wide range of the output voltages that inverted from the input voltage. It gives outputs either higher or lower than the input voltage and the topology gets its name from this feature. On the other hand, the polarity of the output voltage is opposite to the input voltage, the input current for a BB power stage can be intermittent because of the power switch Q1, this switch passes current when switched ON and blocks it while switched OFF and the current pulsates from zero to  $I_L$  every one switching cycle. The output current of a BB stage is likewise intermittent due to

the second switch (diode-CR1), it conducts just through a part of the switching cycle. The output capacitor feeds the entire load current for the remains of the switching cycle.

Figure 3.4 demonstrates the rearranged schematic of the buck-boost stage with a drive circuit block contained within. The power switch, Q1, is selected as an n-channel MOSFET, the output diode is CR1, the inductor is L, and the capacitor is C, the LC combination acts as the effective output filter. The Equivalent Series Resistance (ESR) of the capacitor is RC, and the inductor resistance is RL, are taken in the account in this analysis. The resistor R is acts as a load as observed by the power stage output.

Through ordinary process of the buck-boost stage, the control circuit which determines the cycle duration and numbers of times that Q1 switches ON and OFF. This process provides few pulses to get ricing at the junction of Q1, CR1, and L. In spite of the fact that the inductor is associated to the output capacitor, only when CR1 conducts, an active LC output filter is constructed. It filters the sequence of pulses to generate a typical DC output voltage.

- Voltage Transfer Ratio

For the converter buck boost system, the transfer ratio of the converter can be found from:

$$G = \frac{V_{ac}}{V_{dc}/2} = BM \quad (3.2)$$

Where:

$V_{ac}$ : Is the output peak phase voltage.

$B$ : Is the boost factor of the first stage.

$M$ : Is the modulation index of the second stage.

- Conventional Two Stage Buck-Boost VSI

Figure 3.5 illustrates conventional two stage buck-boost voltage source inverter. For conventional two stage buck-boost VSIs with sinusoidal pulse width modulation control when the modulation index is ( $0 < M < 1$ ), the voltage transfer ratio will be obtained and the maximum obtainable gain in the voltage at a specified on vector duty ratio of S1 ( $D_{on}$ ) are given by [39]:

$$G = BM = \frac{M}{1 - D_{on}} \quad (0 \leq M \leq 1) \quad (3.3)$$

$$G_{max} = B = \frac{1}{1 - D_{on}} \quad (M = 1) \quad (3.4)$$

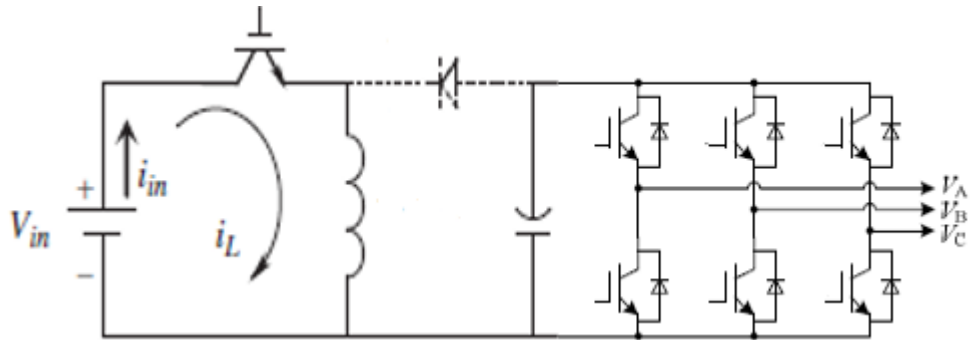


Figure 3.5: Conventional two stage buck-boost VSI.

### 3.4 Z-source inverter

The most goal of any static power converter is that to perform alternating voltage output from a DC voltage supply. Impedance source inverter has gain its name from the impedance network which connected to the inverter main circuit. This impedance network (Z-network) is set back a Power input source, this inverter (z-source inverter) has the capability of buck down or boost up the output voltage which is considered as distinguished or unique feature in compared with the traditional inverter. The network consists of a two split inductors and two capacitors that are connected in a cross shape. This connection provides an impedance source coupling the inverter to the dc source, or another converter. The DC source/load can be act as a current source or a voltage source/load. Therefore, the DC source can be a battery, Thyristor converter, diode rectifier, fuel cell, PV cell, a capacitor, an inductor, or a combination of those [37]. The switches of the converter can be a combination of switching devices and anti-parallel diode as presented in figure 3.6.

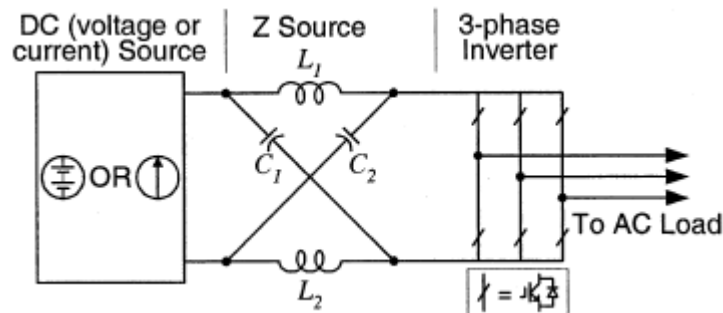


Figure 3.6: ZSI using the antiparallel combination of switch and diode.

The circuit has six switches, every one of these devices is a combination of a power transistor and an antiparallel (or freewheeling) diode to provide bidirectional current flow and unidirectional voltage blocking ability. The common types of semiconductors power switches have been utilized to implement Z-source inverter can be Insulated Gate Bipolar Transistor (IGBT), Metal Oxide Semi-Conductor Field Effect Transistor (MOSFET), Bipolar Junction Transistor (BJT), Gate Turn Off Thyristor (GTO), and Silicon Controlled Rectifier (SCR), etc. The above circuit is used IGBT as the switch combines all advantages of both MOSFET and BJT [39].

### **3.4.1 Impedance Network**

The Z-network can be connected to all DC-to-AC, AC-to-DC, AC-to-AC and DC-to-DC power conversion. Z source converter consists of DC input voltage, impedance network, and conventional three phase inverter providing an AC load. If the source power supply is an AC voltage, it is rectified to DC voltage by a rectifier, the rectifier part contains of six diodes, which are applied in a bridge form and the rectified output (DC voltage) applied to the impedance network.

An impedance network contains of two identical inductors (L1, L2) and two identical capacitors (C1, C2). The network capacitors are coupled diagonally and the inductors are linked in series arms. This impedance source network is utilized to step-up (boost) or step-down (buck) the input voltage related to the boosting factor. The impedance network appears as a filter and it requires a bit small inductors that minimize the size. Also, capacitors needs less capacitance. Therefore, constant impedance output voltage is provide to the inverters main circuit in this network. Related to the obtaining signal, the inverter works and the output is applied to the three phase AC load.

### **3.4.2 Equivalent Circuit and Operating Principle**

The analysis of The Z-source inverter is doing by using VSI. It has the unique feature is that the AC output voltage can take any value from zero to infinity irrespective to the DC input voltage. The Z-source inverter has a buck–boost capability in one stage that gives a wide range of the output voltage. This feature cannot included in the traditional V- and I-source inverters.

This capability of Z-source converter is got by applying control pulses containing the shoot through state into switching cycle. A method to inject this shoot through state which determines the type of the control method. When applying a shoot through state, a short circuit across the inverter bridge occurs then the output terminals are shorted and the output voltage across the load is zero. At shoot through state, the output voltage is zero, which is similar to the zero vectors in the conventional inverters. In this way the duty ratio of the active states must be created so that an output of a sinusoidal signal is gotten, which means that shoot-through replaces a few or the majority of the conventional zero vectors.

To study the structure of the three-phase Z-source inverter shown in figure 3.6, it has nine allowable switching vectors which do not exist in the conventional three-phase VSI that has eight. Six active vectors are presented in the conventional three phase VSI when the DC voltage is to appear through the load and two zero vectors when the output terminals are shorted along either the lower or upper three legs, respectively.

However, in the Z-source inverter, an additional zero vector is obtained at shoot through vector, that means if both the upper and the lower switches of any one leg or any two legs or all three legs are shorted such as both switches are conduct at the same time, this conduction will cause a short at load terminals. This shoot through zero vector is strictly ignored in the conventional VSI because it would cause a damage. Hence, this third zero state is called the shoot-through zero vector, which can be created by seven different ways as explained earlier.

The Z-source network does the shoot-through probable. This shoot-through vector gives the unique buck-boost feature to the inverter. The Z-source inverter can be worked in the modes which are explained below.

Mode I: Figure 3.7 presents the equivalent circuit of mode 1, when the inverter bridge achieves one of the six traditional active vectors.

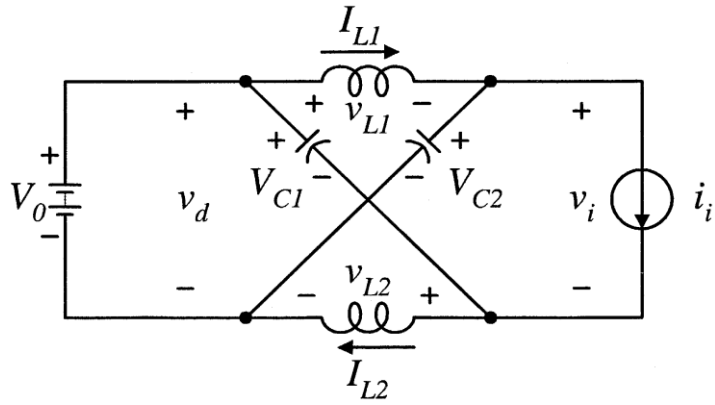


Figure 3.7: Equivalent circuit of the ZSI in one of the six active states.

It viewed from the DC link side that the inverter bridge works as a current source. The two inductors have a same current value due to the symmetry. This feature broadens the line current conducting intervals, therefore, it results a reduction from harmonic currents.

Mode II: Figure 3.8 presents the equivalent circuit of mode 2, when the inverter bridge achieves one of the two traditional zero vectors.

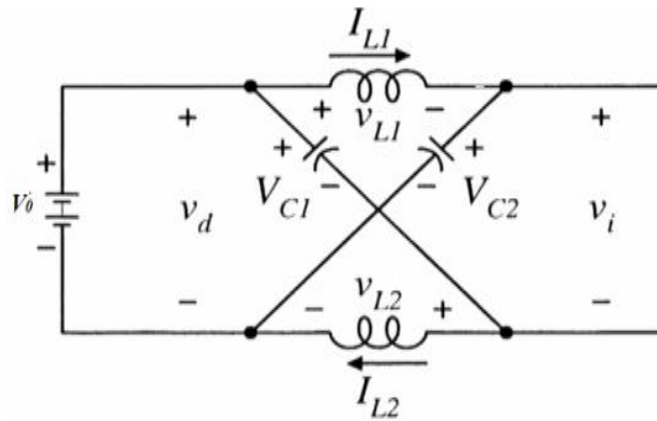


Figure 3.8: Equivalent circuit of the ZSI in one of the two traditional zero states.

When the inverter circuit is working in one of the two traditional zero vectors and shorting a long either the upper or lower three legs, thus performing as an open circuit when showed from the Z-source circuit. Also, in this mode of the operation, the inductor carries current, which involve to the decreasing harmonics as presented in figure 3.9.

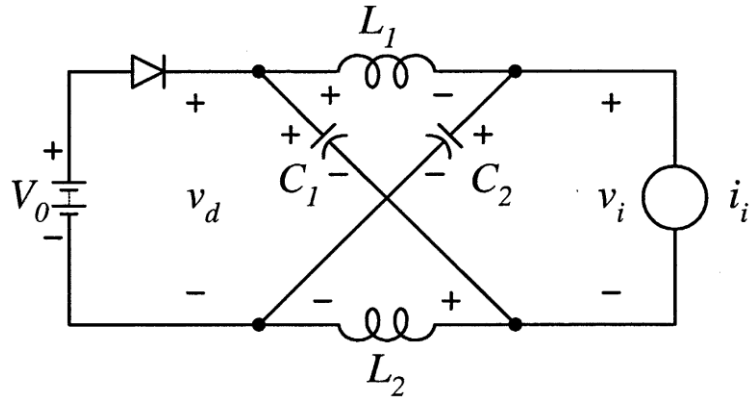


Figure 3.9: Equivalent circuit of the ZSI in the non shoot-through states.

Mode III: Figure 3.10 showed the equivalent circuit of mode 3, when the inverter bridge works in one of the seven shoots through vectors. The shoot-through mode must be utilized in each switching cycle through the traditional zero state interval created by the PWM .according to the boosting that needed, then the duty cycle  $T_o/T$  at the shoot-through period  $T_o$ , can be is estimated. It can be show that the shoot-through interval is just a little division of the switching cycle.

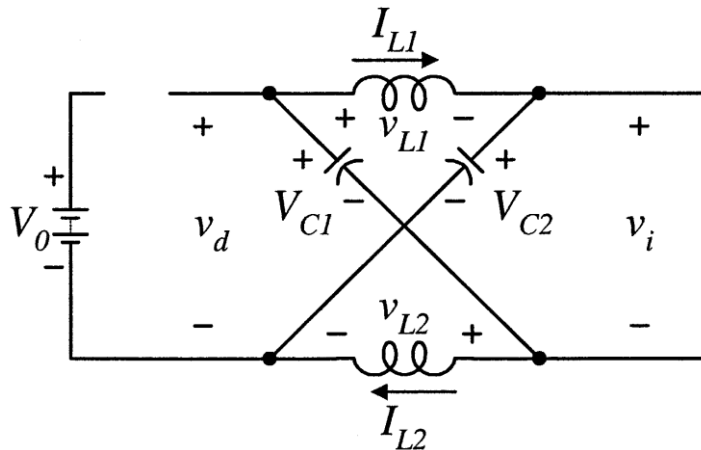
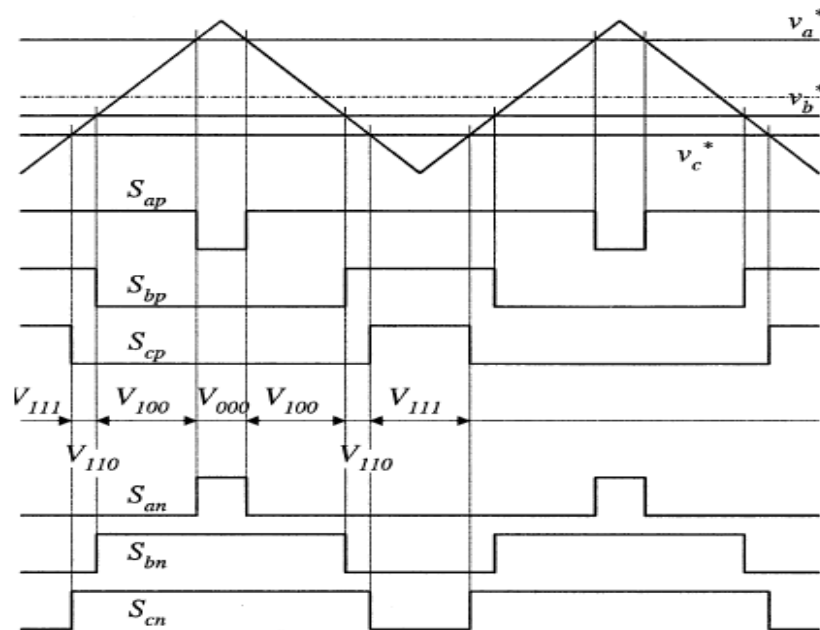


Figure 3.10: Equivalent circuit of the ZSI in the shoot-through state.

All strategies of the traditional pulse-width-modulation (PWM) can be implemented to control the Z-source inverter and their theoretical relationships that relate the input to output are still valid. Fig. 3.11 presents the traditional pulse width modulation switching sequence based on the triangular carrier. In each switching cycle, the two non-shoot-through zero vectors are utilized through a two adjacent active vectors to produce the wanted voltage. When the voltage is sufficiently high to

produce the wanted AC output voltage, the traditional pulse width modulation of fig. 3.11 is utilized.



**Figure 3.11:** Traditional carrier-based PWM control without shoot-through zero states.

At a time whereas the dc voltage is so low a limit to create the wanted output voltage, a modified pulse width modulation with shoot-through zero vectors can be utilized as presented in fig. 3.12 in order to step-up the voltage. It should be observed that every of the legs still turns on and off once per cycle and without alteration the whole time of the zero-vector period, the ST zero vectors are equitably distributed. Specifically, the active vectors are unaltered. Anywise, the equivalent dc-link voltage is stepped-up for the shoot-through vectors. All the relationships will be fully explained in section 3.4.3.

We can observed, that the equivalent switching frequency showed from the Z-source circuit is greater by six times the switching frequency of the main inverter circuit, which decreases the inductance of the Z-source network to significantly value.

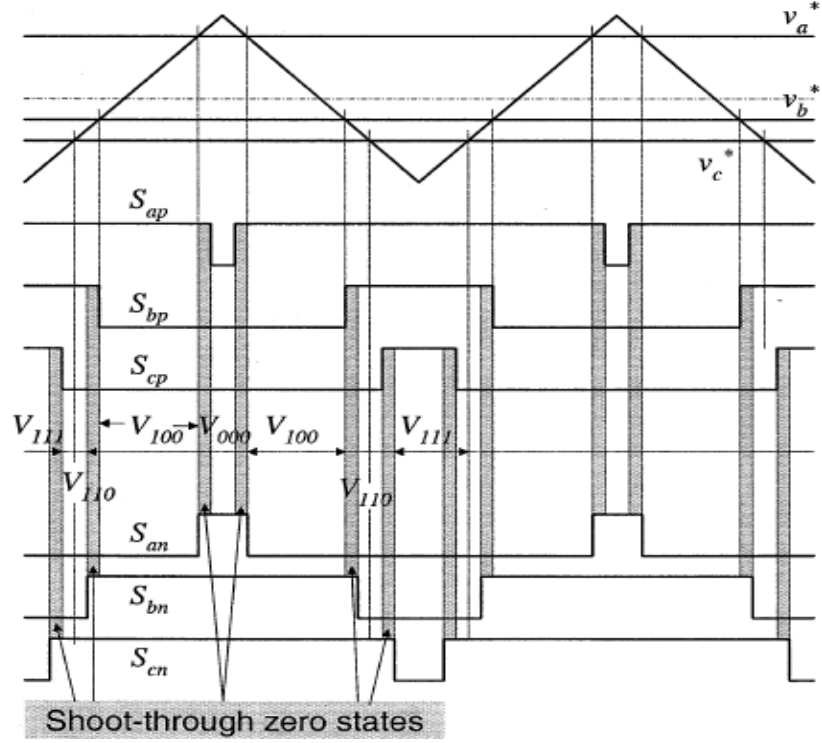


Figure 3.12: Modified carrier-based PWM control with shoot-through zero states.

### 3.4.3 Analysis of Impedance Network

Figure 3.9 presented the equivalent circuit of the impedance network [39]. To do simple analysis, supposing that the inductors  $L_1$  and  $L_2$  and the capacitors  $C_1$  and  $C_2$  have the identical inductance and capacitance respectively, the network of the Z-source network gets to be symmetrical. So that, from fig. 3.7 and the symmetry, we obtained:

$$V_{C_1} = V_{C_2} = V_C \quad ; \quad v_{L_1} = v_{L_2} = v_L \quad (3.5)$$

Figure 3.10 presented the equivalent circuit of inverter bridge in the shoot-through zero vector. Given that the shoot through period is  $(T_o)$  through a switching cycle  $(T)$ , we can obtain:

$$v_L = V_C \quad ; \quad v_d = 2V_C \quad ; \quad v_i = 0 \quad (3.6)$$

Figure 3.7 showed the equivalent circuit of the inverter bridge at any one of the eight non-shoot-through vectors for a period of  $(T_i)$  through the switching cycle  $(T)$ , it can be get:

$$v_L = V_o - V_c \quad ; \quad v_d = V_o \quad ; \quad v_i = V_c - v_L = 2V_c - V_o \quad (3.7)$$

Where ( $V_o$ ) is the dc input voltage of the source, and ( $T = T_o + T_1$ ).

In steady state, the mean value of the inductor voltage over a switching cycle ( $T$ ) should be zero, from the equations (3.6) and (3.7), we obtained:

$$V_L = \bar{v}_L = \frac{T_o \cdot V_c + T_1 \cdot (V_o - V_c)}{T} = 0 \quad (3.8)$$

$$\frac{V_c}{V_o} = \frac{T_1}{T_1 - T_o} \quad (3.9)$$

Similar to the above, we can find that the mean value of the dc-link voltage across the inverter bridge by the relationship as below:

$$V_i = \bar{v}_i = \frac{T_o \cdot 0 + T_1 \cdot (2V_c - V_o)}{T} = \frac{T_1}{T_1 - T_o} V_o = V_c \quad (3.10)$$

From (3.7), we can obtain the peak dc-link voltage on the bridge and it can be modified to express as:

$$\tilde{v}_i = V_c - v_L = 2V_c - V_o = \frac{T}{T_1 - T_o} V_o = B \cdot V_o \quad (3.11)$$

Where ( $B$ ) is the boost factor resulting from the shoot-through zero vector.

$$B = \frac{T}{T_1 - T_o} = \frac{1}{1 - 2\frac{T_o}{T}} \geq 1 \quad (3.12)$$

The peak dc-link voltage ( $\tilde{v}_i$ ) is the equivalent dc-link voltage. Then again, the output peak phase voltage from the inverter can be obtained as:

$$\tilde{v}_{ac} = M \cdot \frac{\tilde{v}_i}{2} \quad (3.13)$$

By using (3.11), (3.13), we can obtain an additional forma as:

$$\tilde{v}_{ac} = M \cdot B \cdot \frac{V_o}{2} \quad (3.14)$$

For the conventional voltage source pulse width modulation inverter, we have the well-known relationship:

$$\tilde{v}_{ac} = M \cdot V_o / 2.$$

Equation (3.14) demonstrates that the output voltage can be boosted and bucked (stepped-up or down) by selecting a suitable buck–boost factor ( $BB$ ).

$$BB = M \cdot B = (0 \sim \infty). \quad (3.15)$$

From (3.5), (3.9) and (3.12), the voltage on the capacitor can be calculated as:

$$V_{c_1} = V_{c_2} = V_c = \frac{1 - \frac{T_o}{T}}{1 - 2\frac{T_o}{T}} V_o \quad (3.16)$$

The buck boost factor ( $BB$ ) is estimated from the modulation index ( $M$ ) and the boost factor ( $B$ ). The boost factor ( $B$ ) is determine as in (3.12), it can be controlled by duty cycle of the ST zero vector over the no ST states of the inverter pulse width modulation.

It is observed that the ST zero vector does not affect the pulse width modulation of the inverter, due to the production of similar zero voltage to the output terminal. The existing shoot through interval is restricted by the zero vector interval that is calculated by the modulation index [37].

#### **3.4.4 Advantages of Z-Source Inverter**

The following are the advantages and features of Z-source inverter when compared to the conventional inverters both types voltage source and current source inverters:

- Execute the function of maximizing and minimizing of the voltage in one stage energy processing for buck and boost conversions, that is lead to lowering the costs and decreasing the losses.
- No short circuits on branches occur.
- Improve switching reliability and Electromagnetic Interference (EMI) distortions.
- It has a relatively simple start-up (voltage surges and minimize inrush currents).
- Secures ride-through during voltage sags without extra costs.
- Improves power factor and decreases common-mode voltage and harmonic current.
- Provides more reliable and efficient conversion.
- Has low or no inrush current compared to conventional voltage source inverter [37].

### **3.5 Quasi Z-Source Inverter**

Due to demand in better efficiency and reduction in losses, the input LC circuit is adapted to reduce harmonics and thus the efficiency of the converter is getting better. The quasi ZSI (q-Impedance Source Inverter) has the capability for working in two modes as voltage and current fed mode. It can be used in boost or buck operation depending on the mode of operation. The reliability of QZSI is high due to the shoot-through capability and lower inrush currents. These inverters are used widely in high voltage gains such as renewable energy systems or motor controllers.

By using the shoot through technique, it is possible to make conduction of phase switches of the same leg. To treat or overcome some issues that appear in the traditional inverters, the Z-source inverter was standed out that it has been joined with dc – dc converter. Furthermore, it gives higher efficiency, low cost for its buck or boost power conversion capability and more reliability [37, 52, and 53].

QZSIs, is a another promising power conversion technology that is exactly appropriate for interfacing of renewable energy which derived from photovoltaic, wind turbines, geothermal ,biomass and different fuel cells energy sources [41-43]. The QZSIs have been recently suggested as another option to power conversion as they can both step-up or down input voltage (i.e. boost or buck power conversion).

QZSI topology has been presented recently to treat some of the drawbacks and issues of the ZSI. The quasi z-source inverter offers some benefits over the ZSI as simple control strategy, lower component ratings, continuous input current and higher reliability. This topology of the inverter is known as one of the greatest appropriate power interfaces between the PV system and the power grid [44-47].

The QZSIs have been gotten from the traditional z-source inverter [50] and have all the features and benefits of the z-source inverter. It can execute boost (step-up) and/or buck (step-down) power conversion with a wide range of voltage gain by one stage of conversion that is highly appropriate for applications in PV generation systems. Besides, the quasi z-source has the feature of decreased source stress when compared with the traditional ZSI.

### **3.5.1 Quasi Z-Source Inverter Circuit**

Figures 3.13 and 3.14 present the conventional voltage fed z-source inverter [37] and the suggested quasi z-source inverter respectively. In a similar way, as the z-source inverter, the quasi z-source inverter has two kinds of operational vectors at the dc side, the first is; eight non-shoot through vectors they are six traditional active vectors and two traditional zero vectors. And the second operational state is the shoot-through vector (i.e. the upper and lower switches in one leg are gated ON simultaneously).

At non-shoot-through vectors, the equivalent circuit of the inverter bridge which is showed from the dc-side, appeared as a current source.

Figures 3.15 and 3.16, illustrated the equivalent circuits to the two types of operational vectors are non-shoot through vector and shoot through vector respectively. The ST vector is ignored in the conventional voltage source inverter due to a short circuit of the source occurs and causes damage the devices. With two topology of quasi z-source and z-source inverter, the diode network and unique LC are linked to the inverter, this allow to perform the process of the circuit, permitting occurrence of the shoot through vector.

If the shoot-through vector occurs, this network (i.e. diode and LC) will keep the circuit effectively from the damage and by utilizing the shoot though vector, the quasi z-source boosts (step-up) or bucks (step-down) the dc-link voltages [25].

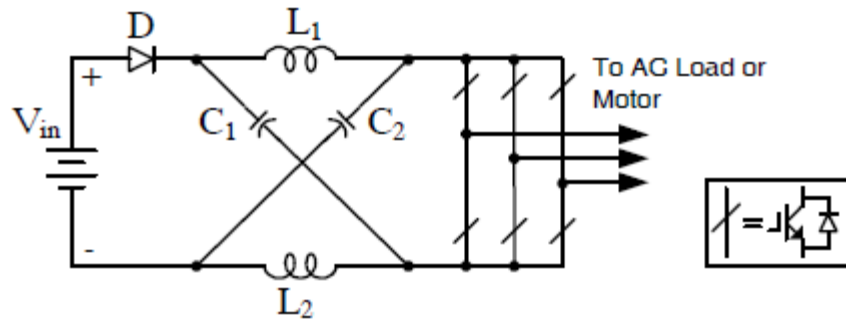


Figure 3.13: Voltage fed ZSI.

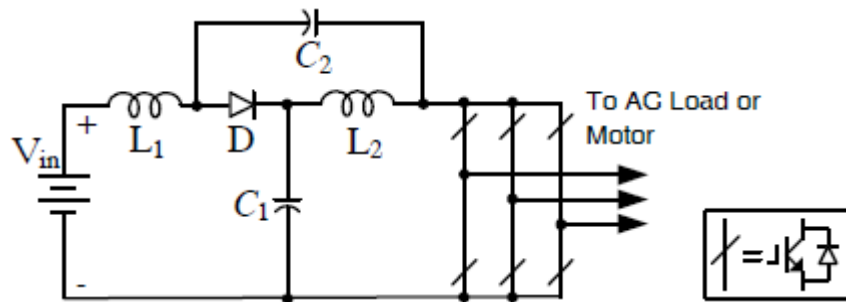


Figure 3.14: Voltage fed QZSI.

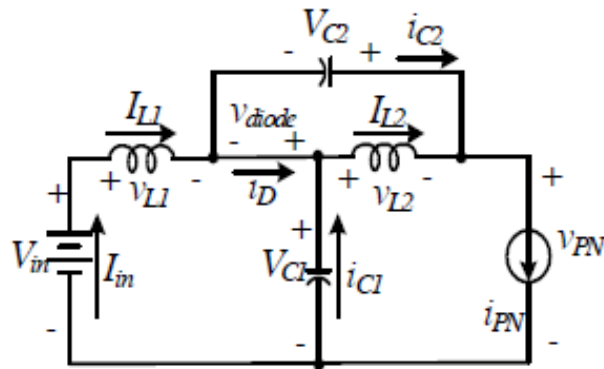


Figure 3.15: Equivalent circuit of the QZSI in non-shoot-through vectors.

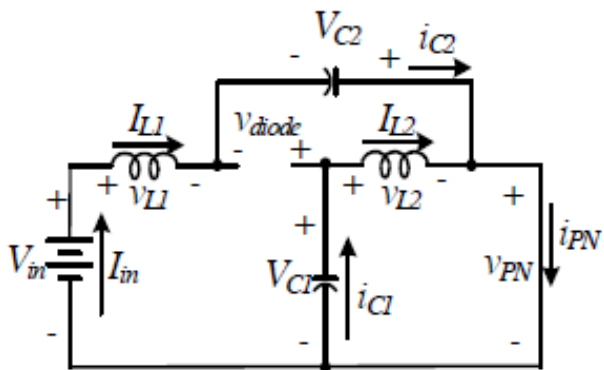


Figure 3.16: Equivalent circuit of the QZSI in shoot-through vectors.

The main differences between the quasi z-source and z-source are:

- The quasi z-source has a continuous input current which significantly reduces input stress. But the z-source has a discontinuous input current.
- In quasi z-source, the voltage across capacitor  $C_2$  is lower than  $C_1$  voltage therefore lower capacitor rating is required, while the voltage across the capacitors  $C_1$  and  $C_2$  have equal values in z-source.
- The continuous and constant dc input current drawn from the voltage source of quasi z-source makes this system well-appropriate for PV power systems.
- In the QZSI, a common dc rail exists between the source and the inverter, and this is easier to assemble and reduces EMI problems [25].

### 3.5.2 Circuit Analysis of Quasi Z-Source Inverter

Figures 3.15 and 3.16 showed and defined all the voltages and the currents. The associated polarities are represented with arrows. Supposing that through one switching cycle ( $T$ ), the period of the shoot-through vector is ( $T_o$ ) and the period of non-shoot through vectors is ( $T_i$ ); where switching cycle ( $T = T_o + T_i$ ) and the ST duty ratio ( $D = T_o / T$ ).

Figure 3.15 showed the equivalent circuit of the inverter through a period of the non-shoot through vectors ( $T_i$ ), we can obtain:

$$v_{L1} = V_{in} - V_{C1} \quad ; \quad v_{L2} = -V_{C2} \quad (3.17)$$

$$v_{PN} = V_{C1} - v_{L2} = V_{C1} + V_{C2} \quad ; \quad v_{diode} = 0 \quad (3.18)$$

Figure 3.16 illustrates the equivalent circuit of the inverter through a period of the shoot-through vectors, ( $T_o$ ), can be obtained:

$$v_{L1} = V_{C2} + V_{in} \quad ; \quad v_{L2} = V_{C1} \quad (3.19)$$

$$v_{PN} = 0 \quad ; \quad v_{diode} = V_{C1} + V_{C2} \quad (3.20)$$

At steady state conditions, the mean value of the inductor voltage over a switching cycle should be zero. From (3.17), (3.19), we can obtain:

$$V_{L1} = \bar{v}_{L1} = \frac{T_o (V_{c2} + V_{in}) + T_1 (V_{in} - V_{c1})}{T} = 0$$

$$V_{L2} = \bar{v}_{L2} = \frac{T_o (V_{c1}) + T_1 (-V_{c2})}{T} = 0$$

Hence:

$$V_{c1} = \frac{T_1}{T_1 - T_o} V_{in} \quad ; \quad V_{c2} = \frac{T_o}{T_1 - T_o} V_{in} \quad (3.21)$$

From (3.18), (3.20) and (3.21), the peak dc-link voltage through the bridge is:

$$\bar{v}_{PN} = V_{c1} + V_{c2} = \frac{T}{T_1 - T_o} V_{in} = \frac{1}{1 - 2 \frac{T_o}{T}} V_{in} = B \cdot V_{in} \quad (3.22)$$

Where ( $B$ ) is the boosting factor of the quasi z-source. In fact, this is the peak voltage through the diode's terminals.

The mean value of the current across both inductors  $L_1$ ,  $L_2$  can be obtained from the system power rating ( $P$ ):

$$I_{L1} = I_{L2} = I_{in} = P / V_{in} \quad (3.23)$$

By using Kirchoff's current law and (3.23), can be obtained:

$$I_{c1} = I_{c2} = IPN - I_{L1} \quad ; \quad ID = 2 I_{L1} - IPN \quad (3.24)$$

We can find that the quasi z-source inverter keeps all the benefits of the z-source inverter. It can boost or buck a voltage at any boosting factor. It is capable to do a ST vector, and hence it is more reliable than the traditional voltage source inverters.

### 3.5.3 Advantages of Quasi Z-Source Inverter

- Execute the function of maximizing and minimizing of the voltage in one stage energy processing for buck and boost conversions, that is lead to lowering the costs and decreasing the losses.

- Quasi z-source inverter has continuous input current (i.e. input current remains far from zero), that's lead to decrease the stress of the input voltage source.
- Better reliability because of the shoot through carrying capability and efficient conversion.
- It has a relatively simple start-up (voltage surges and minimize inrush currents).
- Improve switching reliability and minimize the Electromagnetic Interference (EMI) distortions.
- No short circuits on branches occur.
- Improves power factor and decreases common-mode voltage and harmonic current.
- Low common mode noise [48].
- Has low or no inrush current compared to conventional voltage source inverter [37].
- Secures ride-through during voltage sags without extra costs.

However, the voltage gain and efficiency of the QZSI are limited and close to the traditional system of a VSI with the auxiliary step-up DC/DC converter in input stage [49].

As seen from the discussion above, the quasi z-source inverter inherits all the benefits and features of the z-source inverter. It can do boost (step-up) and/or buck (step-down) conversion in one stage with a wide range of voltage gain that is appropriate for application in PV power systems. As well as, the suggested quasi z-source inverter has continuous dc input current, lower component ratings, and reduced source stress when compared to the traditional ZSI.

## CHAPTER FOUR

### CONTROL METHODS

#### 4.1 Literature Overview

Many control schemes of pulse width modulation control have been improved and utilized for the VSIs. The VSI has eight operational states, six of them are active vectors, and two zero vectors. When the six active vectors mode utilized, the dc voltage fed to the output terminals, while in the second mode the load terminals are shorted across the upper or lower devices. The z-source inverter has an extra zero vector, that is the shoot-through vector.

A method to inject this shoot through state which determines the type of the control method. When applying a shoot through state, a short circuit across the inverter bridge occurs then the output terminals are shorted and the output voltage across the load is zero. At shoot through state, the output voltage is zero, which is similar to the zero vectors in the conventional inverters. In this way the duty ratio of the active states must be created so that an output of a sinusoidal signal is gotten, which means that the shoot-through replaces a few or the majority of the conventional zero vectors.

Since the time when the first research in z-source inverter was issued in 2003, several modified topologies with developed modulation and control techniques have been suggested and issued to develop the performance in different applications in this field, particularly for shoot-through control schemes [37, 51-60].

Different shoot through control schemes/methods have been suggested, they are:

1. Simple boost control (SBC) [51].
2. Maximum-boost control (MBC) [52].
3. Maximum constant-boost control (MCBC) [10].
4. Modified space vector modulation boost control (MSVM) [53, 54].

Some of these are, for instance but not limited to, Jin et al., "Loss Oriented Evaluation and Comparison of Z-Source Inverters Using Different Pulse Width Modulation Strategies", [55]. Ref. [56] introduced a comparison of the Z-source inverter and traditional two-stage buck-boost inverter in grid tied renewable energy generation.

In [55, 56], the authors present a simulation efficiency comparison between two different shoot-through control schemes/methods, which are: two shoot through vectors insertion per switching cycle and six shoot-through vectors insertion per switching cycle. Therefore the authors did not distinguish between the maximum boost, the simple boost, and the maximum constant boost control schemes/methods.

Omar E., Joeri Van M. and Philippe L., "Comparison between Different PWM Control Methods for Different Z-Source Inverter Topologies", the authors present a simulation comparison between the above four mentioned shoot-through control schemes for different ZSI topologies (the basic, the bidirectional and the high-performance ZSI) [57].

Jacek R. presented an improvement of Z-source inverter properties by using advanced PWM methods. The author proposed the application of the discontinuous PWM modulation schemes for improving the efficiency of the ZSI, but the paper did not discuss the effect of the application of these modulation schemes on the voltage gain, output current and switch voltage stress and voltage harmonic content [58].

Rostami and Khaburi, "Voltage Gain Comparison of Different Control Methods of the Z-Source Inverter", A simulation comparison of the voltage gain of different shoot-through control methods of the ZSI, without the modified space vector modulation method, was presented in this paper [59]. Meenakshi and Rajambal, "Identification of an Effective Control Scheme for Z-source Inverter", the simple-boost and the maximum constant-boost control are compared by simulation in terms of voltage gain and voltage stress in this study [60].

## **4.2 PWM Control Methods of Z-Source Inverter**

### **4.2.1 Simple Boost Control Method**

Figure 4.1 illustrates the scheme of the Simple Boost Control (SBC) strategy [51]. In a conventional sinusoidal pulse width modulation, utilizes two straight lines

positive ( $V_p$ ) and negative ( $V_n$ ) voltages, higher than or equal to the peak value of the three phase references -three phase control waveform are necessary to control the shoot through duty time. When the triangular carrier waveform is less than the bottom line ( $V_n$ ), or more than the upper line ( $V_p$ ), the circuit turns into shoot through vector. Else it works similarly as the conventional carrier based pulse width modulation. This strategy is very straight forward. So that, the resulting voltage stress that occurs across the switches is comparatively high due to the some zero vectors are not used.

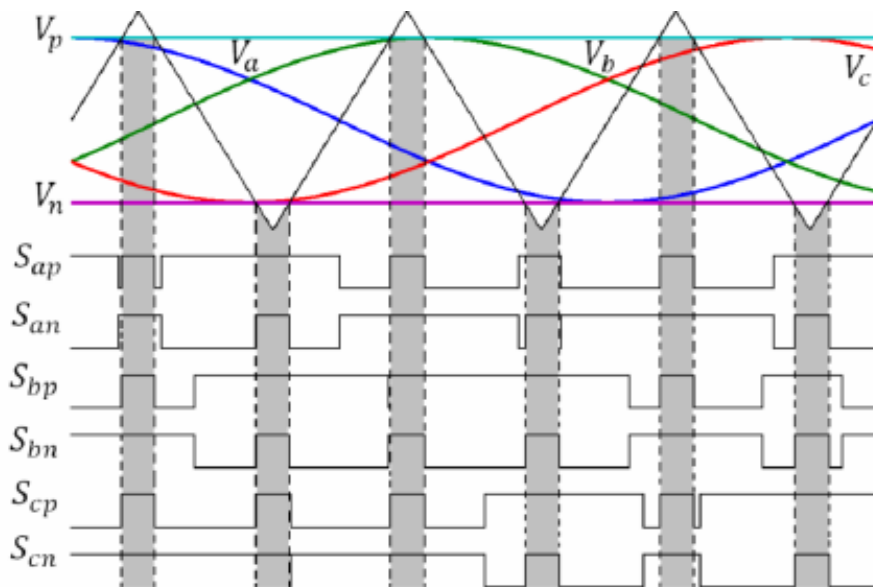


Figure 4.1: Waveforms of simple boost control strategy (SBC).

#### 4.2.2 Maximum Boost Control Method

Figure 4.2 showed the scheme of the Maximum Boost Control (MBC) strategy [52]. To decreasing the voltage stress under a wanted voltage gain is being more important to control ZSI, this can be maintained by creating the shoot through duty as could be allowed, and MBC turns all the conventional zero vectors into shoot-through vector. As illustrates in fig. 4.2, when the triangular signal is either higher than the greatest curve of the references-three phase control signals are ( $V_a$ ,  $V_b$  and  $V_c$ ) or less than the least of these references, therefore the circuit is in shoot-through vector.

Shoot through duty ratio changes as much as six times of the output frequency, and the ripples in the shoot through duty ratio lead to the ripple in the inductor's current and the capacitor's voltage. This will need greater ratings of the passive elements when

the output frequency goes to be low. Consequently, the maximum ST-boost control strategy is appropriate for applications that have a comparatively high or fixed output frequency.

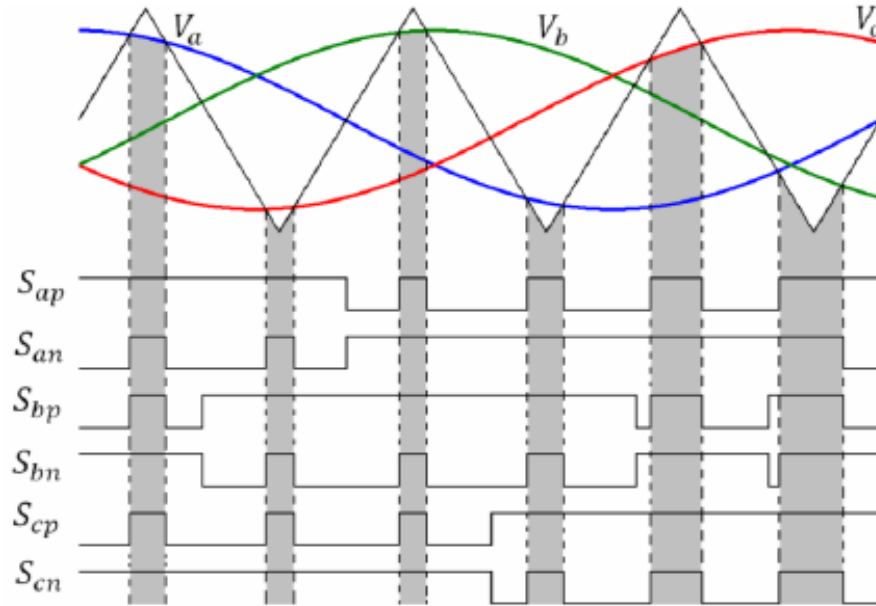


**Figure 4.2:** Waveforms of maximum boost control strategy (MBC).

#### 4.2.3 Modified Space-Vector Modulation Control Method

Space Vector Pulse Width Modulation (SVPWM) control strategy are broadly used in industrial applications of the pulse modulation inverter as a result of the lower current harmonics and greater modulation indices. The space vector pulse width modulation is appropriate to control z-source inverters. Unlike the traditional SVPWMs.

Modified Space Vector Modulation (MSVM) has an extra shoot through time ( $T_o$ ), to step-up (boost) the dc link voltage of the inverter alongside the time periods ( $T_1$ ), ( $T_2$ ) and ( $T_z$ ).

The shoot through vectors are equally given to each phase with ( $T_o / 6$ ) within zero voltage interval ( $T_z$ ). The zero voltage interval should be reduced for producing the shoot through time, as well as the active vectors ( $T_1$ ) and ( $T_2$ ) are unaltered. In this way, the shoot through time does not affect on the pulse width modulation control of the inverter, and it is restricted to zero state time ( $T_z$ ).

MSVM can be executed by utilizing two forms. Figure 4.3 illustrates MSVPWM-1 control strategy. At this switch form, the shoot through time ( $T_o$ ) is restricted to  $(3/4)$  of  $T_z$ , and for this the interval  $(T_z/4 - 2T_s)$  should be higher than zero. Figure 4.4 showed MSVPWM-2 control strategy, where the apportionment of zero vector time is altered into  $(T_z/6)$  and  $(T_z/3)$ . The max. shoot through time is expanded to the zero vector time ( $T_z$ ) [53, 54].

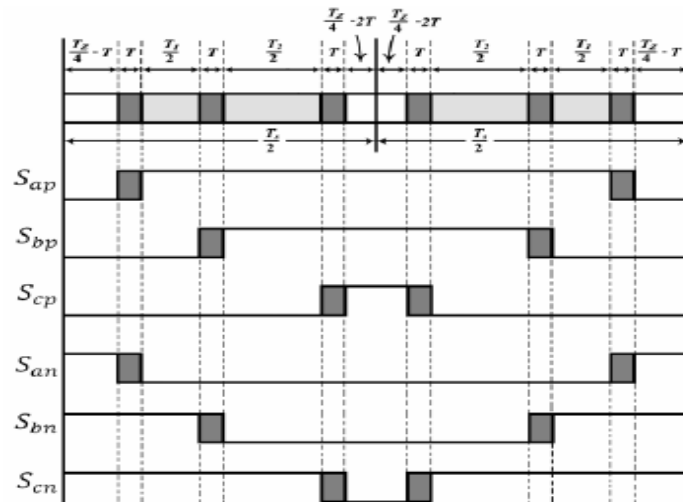


Figure 4.3: Switching form of MSVPWM-1.

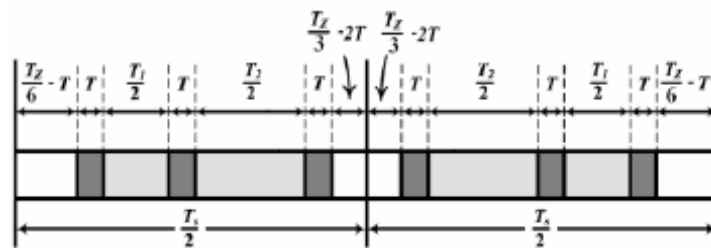
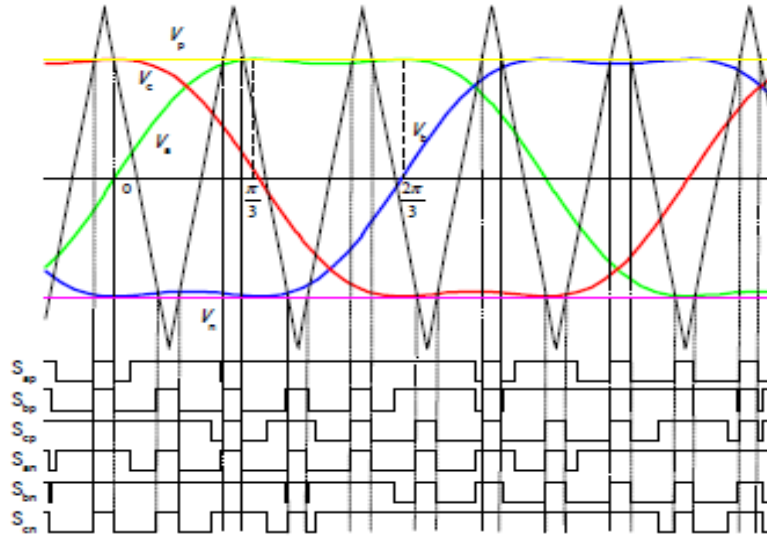


Figure 4.4: Switching form of MSVPWM-2.

#### 4.2.4 Maximum Constant Boost Control Method

Figure 4.5 showed the scheme of the Maximum Constant Boost Control (MCBC) strategy with the third harmonic injection. This technique has some features above other control strategies; with specified the cost and the volume, should be kept the shoot through duty ratio constant. MCBC is utilized in order to decrease the cost and the volume. In the meantime, a greater voltage boost (step-up) for any modulation index is required in order to decrease the voltage stress across the switches. MCBC

obtained the max. voltage gain while keeping the shoot through duty ratio constant [10]. This method using third harmonic injection, that's only two straight lines positive ( $V_p$ ) and negative ( $V_n$ ) voltages are necessary to control the shoot through duty time with 1/6 of the third harmonic injection.



**Figure 4.5:** Waveforms of maximum constant boost control strategy (MCBC) with third harmonic injection.

With the decreasing the boost factor ( $B$ ) and increasing the modulation index ( $M$ ) as much as probable, can be maximize the voltage gain and minimize the voltage stress across the inverter bridge.

All the boost control schemes that have been investigated for the conventional z-source inverter (i.e. SBC, MBC, and MCBC) can be used for the quasi z-source control in a similar way [10, 51, 52, and 53].

Among these boost control schemes, the maximum boost control makes the most use of the conventional zero vectors, so it has the higher modulation index ( $M$ ) and the lower voltage stress ( $V_s$ ) on the inverter bridge with same voltage gains.

However, MBC has the disadvantage of low frequency ripples on the passive elements of the z-source inverter and quasi z-source inverter, which requests a big volume and weight, and higher cost capacitor and inductor in the z-source and quasi z-source network. SBC has evenly spread shoot-through vectors, accordingly it doesn't include the low-frequency ripples related with output frequency but its voltage stress is largest with a specified ( $G$ ). MCBC makes a compromise of the two mentioned control methods.

MCBC with third harmonic injection strategy was selected as the control scheme to decrease the voltage stress across the inverter bridge and keep a high voltage gain.

#### **4.2.4.1 Principle of operation of the maximum constant boost control method**

MCBC scheme with third harmonic injection method is devised to produce a higher constant boost with lower voltage stress. Figure 4.6 illustrates the ST pulses produced. ST pulses can be created by applying triangular waveform at the input of a comparator. The time of ST keep almost constant from switching cycle to another and is chosen by the two reference voltage levels known as ST level. If the triangular carrier signal surpasses the upper ST level or under lower ST level, the ST pulse is created. These ST pulses are evenly spread in conventional PWM signal to get PWM signal with ST.

Figure 4.5 shows third harmonic injected PWM with shoot through and the control scheme is referred as MCBC with third harmonic injection. The third and higher harmonic component can be added into fundamental in order to reduce harmonic distortion in the output waveform [33]. The third harmonic component with 16.6% of the fundamental one is added into the modulating signals.

From the figure 4.5, it can be clearly seen that the upper ST level is always higher than or equal to the max. value of the control waveforms, and the lower ST level is always higher than or equal to the min. value of the control waveforms. Therefore, the ST vectors occur only through the traditional zero vectors. So that, this control method achieves the output voltage signal. As shown in figure 4.5, at an angle of  $(\pi/3)$  of modulating signal the third harmonic component crosses zero and then increases towards negative peak. Therefore at  $(\pi/3)$ ,  $(Va)$  reaches its peak value  $(\sqrt{3}/2)M$ , while  $(Vb)$  is at its min. value  $-(\sqrt{3}/2)M$ . In this scheme only two straight lines are required to control the ST time with third harmonic injection.

The boosting factor depends on the ST duty cycle. If the ST duty cycle is kept the same from switching cycle to switching cycle boost factor remains constant. Thus, maximum boosting factor ( $B$ ) can be obtained while keeping it constant all the time.

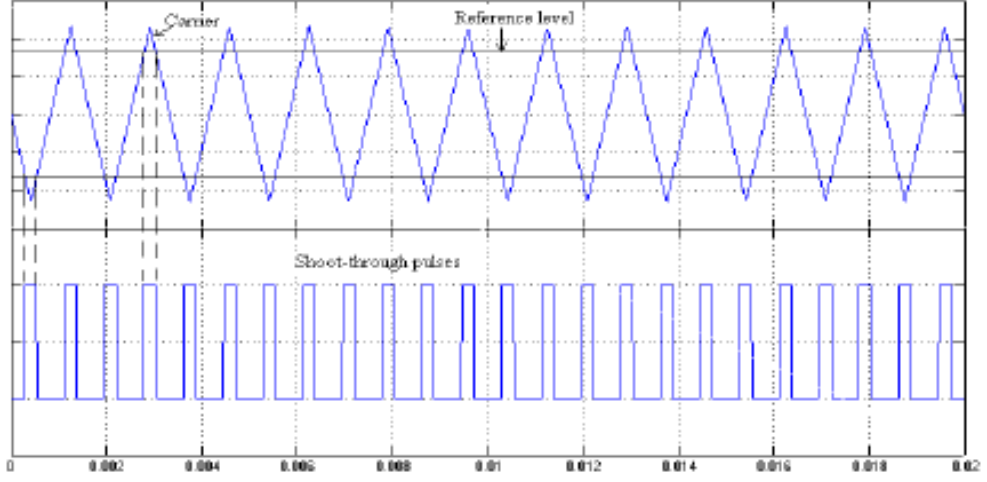


**Figure 4.6:** Shoot through pulses.

The separation between these two reference levels deciding the ST duty ratio is always constant  $((\sqrt{3}/2)M - (-\sqrt{3}/2)M)$  for a specified modulation index ( $M$ ), that is  $(\sqrt{3}M)$ . So that, the ST duty ratio is constant and can be obtained from the graph as;

$$\frac{T_o}{T} = \left( \frac{2 - \sqrt{3}M}{2} \right) = \left( 1 - \frac{\sqrt{3}M}{2} \right) \quad (4.1)$$

The boosting factor ( $B$ ) and the voltage gain ( $G$ ) can be estimated as follows:

$$B = \frac{1}{1 - 2\frac{T_o}{T}} = \frac{1}{\sqrt{3}M - 1} \quad (4.2)$$

$$G = \frac{Vacp}{Vdc/2} = M \cdot B = \frac{M}{\sqrt{3}M - 1} \quad (4.3)$$

Where:

( $Vacp$ ): is the peak value of the output phase voltage.

( $Vdc$ ): is the input dc voltage.

( $B$ ): is the boost factor decided by the ST time period ( $T_o$ ) through a switching cycle ( $T$ ), or decided by the ST duty ratio ( $T_o/T$ ).

Equation (4.2) gives relation between modulation index and boosting factor for this method. The third harmonic injection control scheme has a higher modulation index range, which can be increased from 0.577 to 1.154. Equation (4.3) shows that voltage gain is infinite for  $M = \sqrt{3}/3$  or 0.57 and decreases as the  $M$  is increased. At  $M = 2/\sqrt{3}$  or (1.154) gain of inverter becomes zero.

As can be clearly seen from figure 4.8, the maximum constant ST boost control scheme will apply a slightly higher voltage stress through the devices than the max. control scheme, but a much lower voltage stress than the simple control method. So that, since the maximum constant ST boost control strategy excludes line frequency related ripple. The passive elements in the Z network will be reduced, which will be much useful in many applications. Table 4.1 illustrates a summary of all expressions for the different shoot through control schemes. Where ( $D_o$ ) is the shoot through duty ratio, ( $G$ ) is the voltage gain, and ( $V_s$ ) is the voltage stress on the switch [57].

**Table 4.1:** The summary of different ST control methods expressions.

Control Method	SBC	MBC	MCBC	MSVPW-M1	MSVPW-M2
$D_o$	$1 - M$	$\frac{2\pi - 3\sqrt{3}M}{2\pi}$	$\frac{2 - \sqrt{3}M}{2}$	$\frac{3}{4} \cdot \frac{2\pi - 3\sqrt{3}M}{2\pi}$	$\frac{2\pi - 3\sqrt{3}M}{2\pi}$
$B$	$\frac{1}{2M - 1}$	$\frac{\pi}{3\sqrt{3}M - \pi}$	$\frac{1}{\sqrt{3}M - 1}$	$\frac{4\pi}{9\sqrt{3}M - 2\pi}$	$\frac{\pi}{3\sqrt{3}M - \pi}$
$G$	$\frac{M}{2M - 1}$	$\frac{\pi M}{3\sqrt{3}M - \pi}$	$\frac{M}{\sqrt{3}M - 1}$	$\frac{4\pi M}{9\sqrt{3}M - 2\pi}$	$\frac{\pi M}{3\sqrt{3}M - \pi}$
$M_{max}$	$\frac{G}{2G - 1}$	$\frac{\pi G}{3\sqrt{3}G - \pi}$	$\frac{G}{\sqrt{3}G - 1}$	$\frac{2\pi G}{9\sqrt{3}G - 4\pi}$	$\frac{\pi G}{3\sqrt{3}G - \pi}$
$V_s$	$(2G - 1)V_{in}$	$\frac{3\sqrt{3}G - \pi}{\pi} V_{in}$	$(\sqrt{3}G - 1)V_{in}$	$\frac{9\sqrt{3}G - 4\pi}{2\pi} V_{in}$	$\frac{3\sqrt{3}G - \pi}{\pi} V_{in}$

Figure 4.7 shows voltage gain ( $G$ ) against modulation index ( $M$ ) of PWM control strategies, and fig. 4.8 illustrates voltage stress ( $V_s$ ) against voltage gain ( $G$ ) of PWM control strategies for different shoot through control schemes. At high voltage gain, the MSVPWM-1 has the greatest voltage stress.

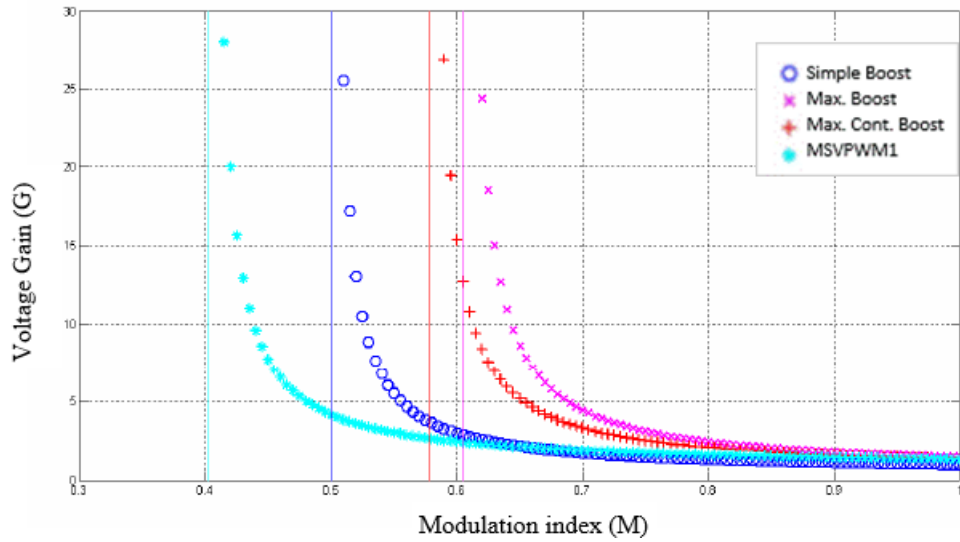


**Figure 4.7:** Voltage gain against modulation index of PWM control strategies.

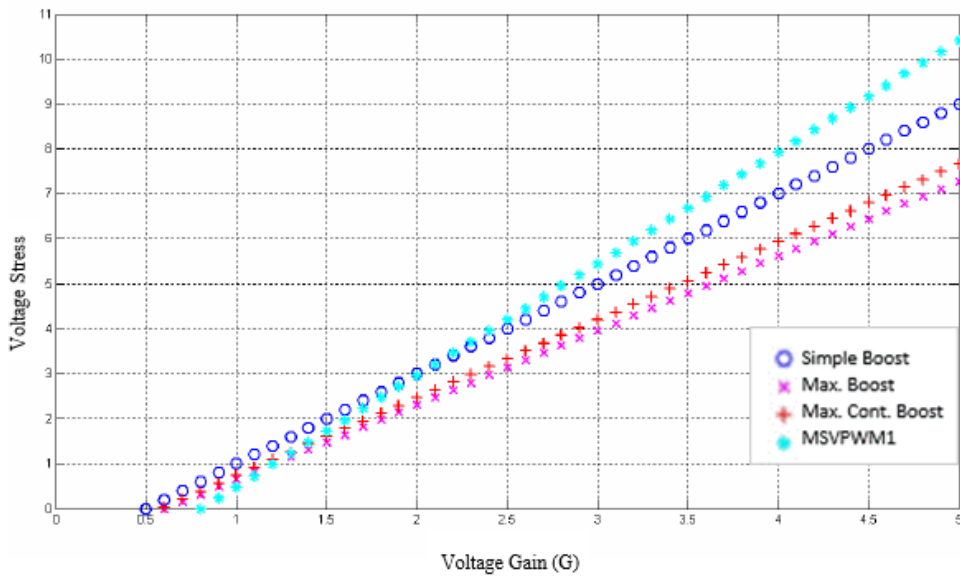


**Figure 4.8:** Voltage stress against voltage gain of PWM control strategies.

### 4.3 Efficiency Comparison

Efficiency comparison is a main task through design of inverter. Inverter losses are distributed essentially on the semiconductor devices. The losses of the semiconductor devices includes switching losses and conduction losses.

The unique process principle makes the losses estimation of the z-source inverter is different from that of the voltage source inverter, and different shoot through control schemes have a significant effect on the losses estimation. When the z-source inverter operates in buck (step-down) mode, it works as a voltage source inverter, and the losses

of the IGBTs and the freewheeling diodes are estimated in the similar manner as the voltage source inverters. While, in the boost (step-up) mode, the shoot vectors are needed to boost the input voltage. Through the ST vector, all six switches IGBTs (for the simple maximum and constant maximum ST boost control schemes) or two IGBTs (for modified space vector modulation ST boost- control scheme) are simultaneously conducting and the dc link is short circuited. In this case the current through one IGBT is the superimposition of the sinusoidal ac current and the high frequency ST current [63].

So that, there is a different way to estimate the losses of the z-source inverter when working in the boosting mode [61, 62].

The conduction losses are estimated according to the following equations [64]:

$$P_{CIGBT} = V_{CEo} \cdot i_{av} + r_{CE} \cdot i_{rms}^2 \quad (4.4)$$

$$P_{CDiode} = V_{Fo} \cdot i_{av} + r_F \cdot i_{rms}^2 \quad (4.5)$$

Where ( $V_{CEo}$ ) and ( $V_{Fo}$ ) formed the IGBT's and diode's threshold voltages, ( $r_{CE}$ ) and ( $r_F$ ) formed their differential ohmic resistance and ( $i_{av}$ ), ( $i_{rms}$ ) are the mean and RMS current flowing during the IGBT or the diode.

By a linearized model of the switching losses. The losses of the switching are directly proportional to the switching frequency and they depend on the selection shoot through control scheme and the switching loss energies of the IGBT ( $E_{on}$ ,  $E_{off}$ ) and the diode ( $E_{rec}$ ), can be given by [64]:

$$P_{SIGBT} = \frac{1}{\pi} f_S (E_{on} + E_{off}) \frac{V_v}{V_{ref}} \frac{I_v}{I_{ref}} \quad (4.6)$$

$$P_{SDiode} = \frac{1}{\pi} f_S E_{rec} \frac{V_v}{V_{ref}} \frac{I_v}{I_{ref}} \quad (4.7)$$

In datasheets the switching loss energy are only given for a reference voltage ( $V_{ref}$ ) and a current ( $I_{ref}$ ).

## **CHAPTER FIVE**

### **CALCULATIONS AND RESULTS**

#### **5.1 Arrangement of Results**

The work in this thesis is arranged in this chapter based on the simulation for three types of VSI, conventional two stage buck-boost dc-ac VSI controlled by sinusoidal pulse width modulation control, Z-source and Quasi Z-source topologies controlled by maximum constant boost with third harmonic injection. In addition, it is presented how to get a desired output ac voltage from high or low input dc values based on suitable selection of the modulation index. The work in this thesis is focused on three-phase voltage source inverters with a 120V output peak phase voltage, 60 HZ, and with a switching frequency of 10 KHz to drive a resistive star-connected load of  $10 \Omega$  at a modulation index of 0.755, 0.812, 1.0, and 1.1.

The simulation is implemented by MATLAB-Simulink software. The Insulated Gate Bipolar Transistor (IGBTs) is utilized as a switching device. The duty cycle variation is achieved by using pulse width modulation. All the simulation and theoretical results are presented in tables.

#### **5.2 Results of Three Phase Conventional Two Stage VSI**

##### **5.2.1 Matlab Simulink Model of Buck-Boost System**

Figure 5.1 illustrates MATLAB/Simulink model of conventional two stage buck-boost (BB) DC-AC VSI. This system is constructed from two stage; the first is dc-dc converter which comes just after the input dc voltage on the left side of the Simulink model. The model also consists of IGBT switch, diode, capacitor and inductor components. The function of the first stage is to get either boost or buck voltage with respect to the input voltage. The second stage is dc-ac inverter that is

composed of three legs of a six IGBTs switch each of them is equivalent to a power transistor and an antiparallel diode in order to provide bidirectional current flow and capability of unidirectional voltage blocking. Each IGBT is controlled by sinusoidal pulse width modulation (PWM) technique. The target of the second stage to get a sinusoidal output signal and pure sinusoidal signal by using a suitable LC filter to fed star connected resistive load.

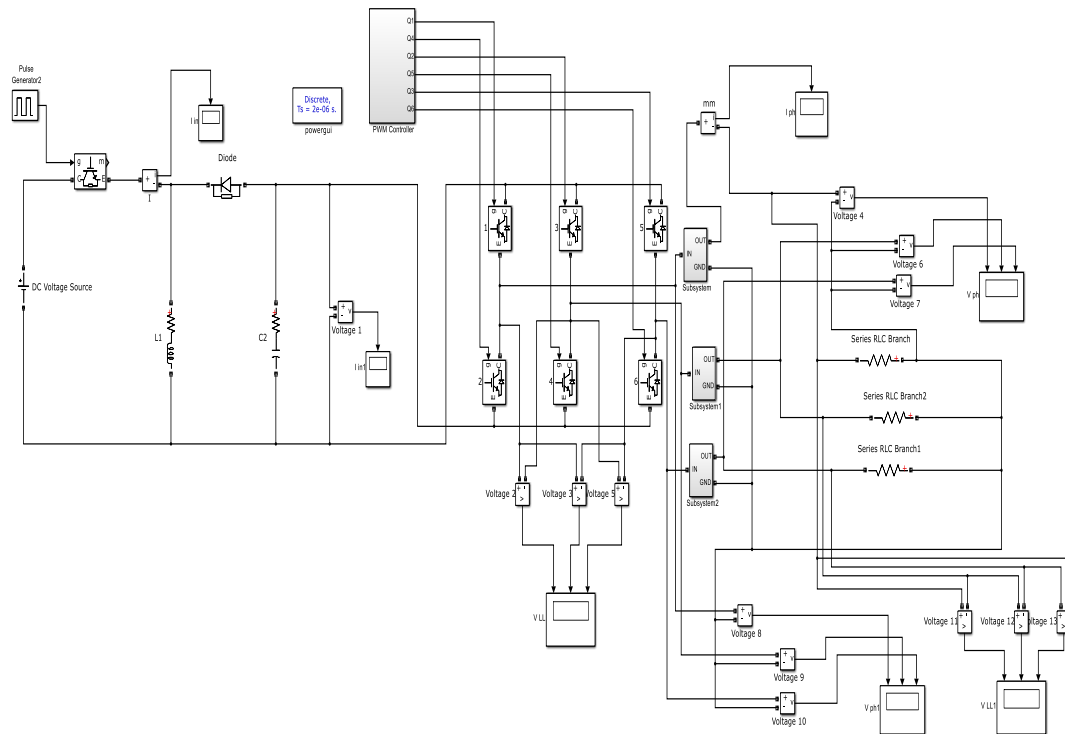


**Figure 5.1:** Simulink model of conventional buck-boost DC-AC VSI.

Figure 5.2 represents MATLAB/Simulink model of sinusoidal PWM controller for the above system. The main goal of any modulation strategy is to get a varying output with a maximum fundamental component and with minimum harmonics. Sinusoidal pulse width modulation (SPWM) is utilized in power electronics, it is widely used to digitize the power. By applying this technique, a sequence of voltage pulses can be produced by the ON and OFF of the power switching devices.

Analog PWM control is implemented by generating control and carrier waveforms that is applying on a comparator inputs that resulting an output based on the difference between the two waveforms. The control signal has a sinusoidal waveform and set at the frequency of the required output (here, it is set at 60 Hz), and the carrier waveform is triangular waveform has a high frequency than the control

signal (here, it's chosen to be 10 KHz). When the carrier waveform is larger than the control signal, the comparator gives output waveform at one case, and when the control waveform is larger than carrier waveform voltage, the output is at its second case, this process as illustrates in figure 2.2.

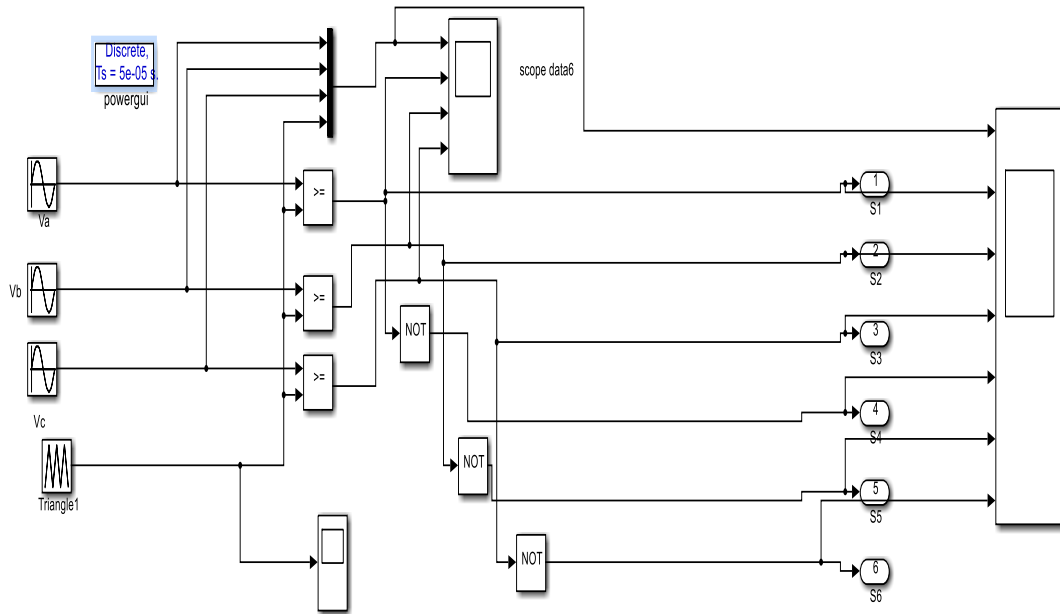


**Figure 5.2:** Sinusoidal PWM controller.

### 5.2.2 Calculations and Results of Conventional BB

The calculations have done for the dc-link voltage across the inverter bridge of the system 120V output peak phase voltage, 60 HZ, switching frequency is 10 KHZ, the load are resistors of 10  $\Omega$  star connected. It is calculated by equation (5.1) at specified values of the modulation index as shown in table 5.1:

$$V_o = \frac{M * V_{dc\ link}}{2} \quad (5.1)$$

Where:

$V_o$  – The output peak phase voltage of the inverter.

$M$  – The modulation index.

$V_{dc\ link}$  – The dc link voltage (output dc voltage).

**Table 5.1:** DC link voltage vs modulation index of conventional BB VSI.

M	0.755	0.812	1.0
$V_{dc\ link}$	318	296	240

Calculation of the duty cycle is carried out by equation (5.2) for each case with different values of the dc input voltage to maintain an output voltage of  $120 V_{ph}$  (peak) as shown in table 5.2:

$$\frac{V_{dc\ link}}{V_{in}} = \frac{D}{1 - D} \quad (5.2)$$

Where:  $V_{in}$  - the dc input voltage, and  $D$  - the duty cycle.

**Table 5.2:** Duty cycle vs input voltage of conventional BB VSI.

Case	M	$V_{dc\ link}$ volt	$V_{in}$ volt	D %
1	0.755	318	98	76.44
			145	68.68
			250	55.98
			318	50.00
			400	44.28
2	0.812	296	120	71.15
			145	67.12
			250	54.21
			296	50.00
			400	42.52
3	1.0	240	145	62.33
			176	57.69
			240	50.00
			250	48.97
			400	37.50

Calculation of the critical value of the inductor ( $L_c$ ) comes below:

$$L_c = \frac{V_{in} * D * T_{sw}}{\Delta I_L} \quad (5.3)$$

Where:

$\Delta I_L$  - The ripple of the inductor current = 10%  $I_L$

$$T_{sw} = \frac{1}{f_{sw}} \quad ; \quad f_{sw} - \text{The switching frequency}$$

$$I_i = \frac{P_i}{V_{in}} \quad (5.4)$$

Considering lossless system;

$$P_i = P_o$$

$P_i$  - The input power.

$P_o$  - The output power = 4320 KW

$I_i$  - The input current.

$$I_i = \frac{4320 \text{ KW}}{98 \text{ V}} = 44 \text{ A}$$

The dc link voltage at  $M = 1.0$  is ( $V_{dc \text{ link}} = 240 \text{ V}$ ), and the duty cycle at  $V_{in} = 98$  volt is:  $D = 0.71$ .

$$I_o = \frac{4320 \text{ KW}}{240 \text{ V}} = 18 \text{ A}$$

$$I_L = \frac{I_o}{1 - D} \quad (5.5)$$

$$I_L = \frac{18}{1 - 0.71} = 62 \text{ A}$$

$$L_c = \frac{98 * 0.71}{0.1 * 62 * 10000} = 1.122 \text{ mH}$$

$$\omega = \frac{1}{\sqrt{L * c}} \quad (5.6)$$

$$\omega = 2 * \pi * f_{sw} \quad (5.7)$$

The above value of the inductor is critical; for this reason, we set it in our design at:  $L = 6.820 \text{ mH}$  and the value of the capacitor at  $C = 250 \text{ uF}$ . Also, we set the values of the inductor ( $L_f$ ) and the capacitor ( $c_f$ ) of filter at:  $L_f = 1.0 \text{ mH}$  ;  $c_f = 100 \text{ uF}$ .

Table 5.3 shows the calculations of the voltage stress ( $V_s$ ) by equation (5.8), it is the maximum blocking voltage across the device when it is turned off.

$$V_s = \frac{V_{in}}{1 - D} \quad (5.8)$$

**Table 5.3:** Voltage stress vs input voltage of conventional BB VSI.

$M$	0.755	0.812	1.0
$V_{in}$	98	120	176
$V_s$	416	416	416

Table 5.4 illustrates the results of the simulation at the specified values of modulation index with variant input voltage and duty cycle to obtain on the output phase voltage  $120 V_{ph}$  (peak), line to line voltage  $V_{LL}$ , phase load current  $I_{ph}$  and the total harmonic distortion  $THD$ . From this table we note that at a certain value of  $M$  we can use a wide range of input voltages. The mode of the circuit is boost or buck so that we got the desired output. At  $M=0.812$  we got the output waveform with less harmonic distortion.

**Table 5.4:** Simulation results of conventional BB VSI.

<i>Theoretical</i>					<i>Simulation</i>				
<i>Case</i>	<i>M</i>	<i>V<sub>dc link</sub></i> <i>volt</i>	<i>V<sub>in</sub></i> <i>volt</i>	<i>D</i> <i>%</i>	<i>V<sub>o dc</sub></i> <i>volt</i>	<i>I<sub>ph</sub></i> <i>ampere</i>	<i>V<sub>LL</sub></i> <i>volt</i>	<i>V<sub>ph</sub></i> <i>volt</i>	<i>THD</i> <i>%</i>
1	0.755	318	98	76.44	310	11	208	115	2.57
			145	68.68	318	11	208	117	2.54
			250	55.98	320	11.5	208	120	2.52
			318	50.00	322	11.5	208	120	2.52
			400	44.28	325	12	208	120	2.51

**Table 5.4 (Continue):** Simulation results of conventional BB VSI.

<i>Theoretical</i>				<i>Simulation</i>					
2	0.812	296	120	71.15	296	11.5	208	120	1.22
			145	67.12	296	12	208	120	1.21
			250	54.21	296	12	208	120	1.18
			296	50.00	300	12	208	120	1.17
			400	42.52	300	12	208	120	1.19
3	1.0	240	145	62.33	240	11.5	208	118	2.10
			176	57.69	240	11.5	208	118	2.08
			240	50.00	240	11.5	208	118	2.03
			250	48.97	240	11.5	208	118	2.03
			400	37.50	240	11.5	208	118	1.99

Power losses calculations ( $P_{T_{losses}}$ ) of the system:

i- The losses of the diode ( $P_D$ ) :

$$I_i = 44 A \quad \text{from (5.4)}$$

$$I_L = 62 A \quad \text{from (5.5)}$$

$$I_D = I_L - I_i = 18 A \quad (5.9)$$

$$I_{D_{rms}} = 0.707 * I_D = 12.726 A \quad (5.10)$$

$I_D$  – The current of the diode.

- Forward Power losses in the diode ( $P_{vf}$ ):

$$P_{vf} = V_f * I_{D_{rms}} \quad (5.11)$$

$V_f = 0.7 \text{ volt}$ ; for the diode in the forward biase.

$$P_{vf} = 0.7 * 12.762 = 8.9334 W$$

- Reverse Power losses in the diode ( $P_{Rf}$ ):

$$P_{Rf} = R_f * I_{D_{rms}}^2 \quad (5.12)$$

$$P_{Rf} = 0.001 * (12.762)^2 = 0.1629 \text{ W}$$

- Total Power losses of the diode ( $P_D$ ):

$$P_D = P_{Rf} + P_{vf} \quad (5.13)$$

$$P_D = 0.1629 + 8.9334 = 9.0963 \text{ W}$$

- ii- IGBT losses ( $P_{IGBT}$ ):

- We choose: FS100R07PE4 Low Switching Losses -IGBT module of the dc-ac inverter bridge in our design. Therefore, from datasheet [66]:

$$\text{Power dissipation} = 335 \text{ W}$$

- We choose: BSM 75 GB 60 DLC – Flexibility, Highest reliability IGBT module of the dc-dc voltage converter in our design. Therefore, from the datasheet [67]:

$$\text{Power dissipation} = 177.5 \text{ w}$$

- Total power losses in IGBT<sub>s</sub> ( $P_{IGBT}$ ):

$$P_{IGBT} = 335 + 177.5 = 512.5 \text{ W}$$

- iii- The losses of the inductor ( $P_L$ ):

We choose the internal resistance of the inductor  $R_L=0.005 \Omega$

$$P_L = R_L * I_{Lrms}^2 \quad (5.14)$$

$$I_{Lrms} = 0.707 * I_L = 0.707 * 62 = 43.834 \text{ A}$$

$$P_L = 0.005 * (43.834)^2 = 9.607 \text{ W}$$

- iv- Total Power Losses ( $P_{Tlosses}$ ):

$$P_{Tlosses} = P_D + P_{IGBT} + P_L \quad (5.15)$$

$$P_{Tlosses} = 9.0963 + 512.5 + 9.607 = 531.2033 \text{ W}$$

Calculations of the efficiency ( $\eta$  %):

$$\eta = \frac{P_{out}}{P_{out} + P_{T_{losses}}} * 100 \% \quad (5.16)$$

$$\eta = \frac{4320}{4320 + 531.2033} * 100 \% = 89.05 \%$$

The simulation results associated to table 5.4 are obtained, at input voltage 98volt, duty cycle 0.7644, modulation index 0.755 and the output dc voltage from the first stage 318 volt. We obtained the following signals, Figure 5.3 presents the output dc voltage after the first stage of the converter. It is observed that the output dc voltage is raised up than the input dc voltage due to performance of dc-dc converter. Figure 5.4 represents the load current after the second stage. Figures 5.5, 5.6 show three phase and line to line load voltage respectively, and Fig. 5.7 shows the total harmonic distortion of the system. In this case the input voltage 98v is boosted to get the output phase voltage 120v.

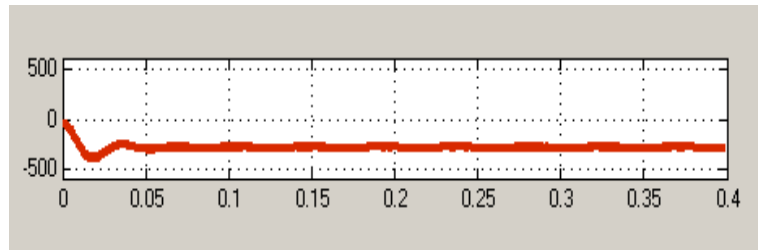


**Figure 5.3:** Output DC voltage at  $M=0.755$ ,  $V_{in}=98$  v.

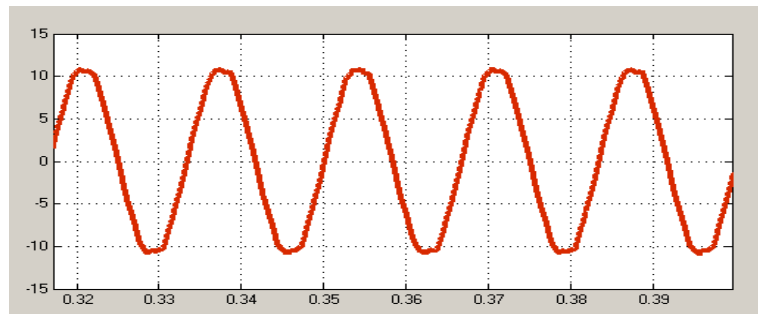


**Figure 5.4:** Load current at  $M=0.755$ ,  $V_{in}=98$  v.

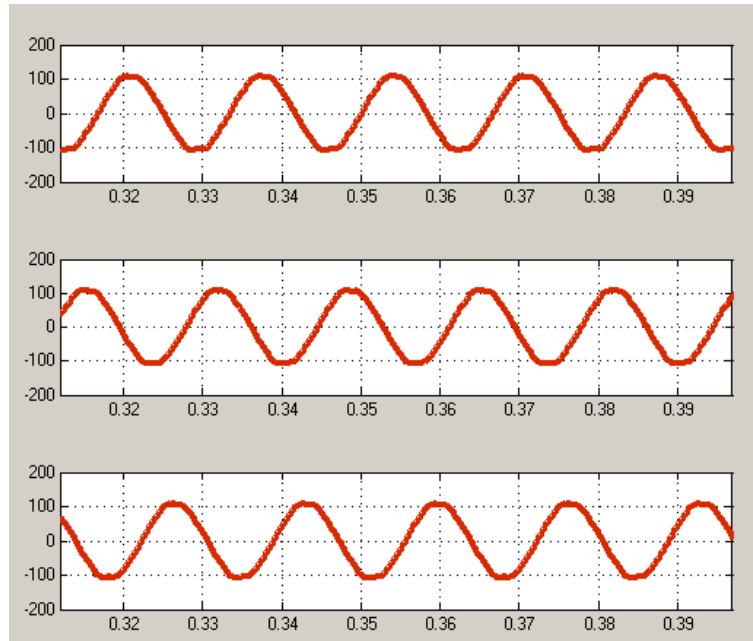


**Figure 5.5:** Three phase load voltage at  $M=0.755$ ,  $V_{in}=98$  v.

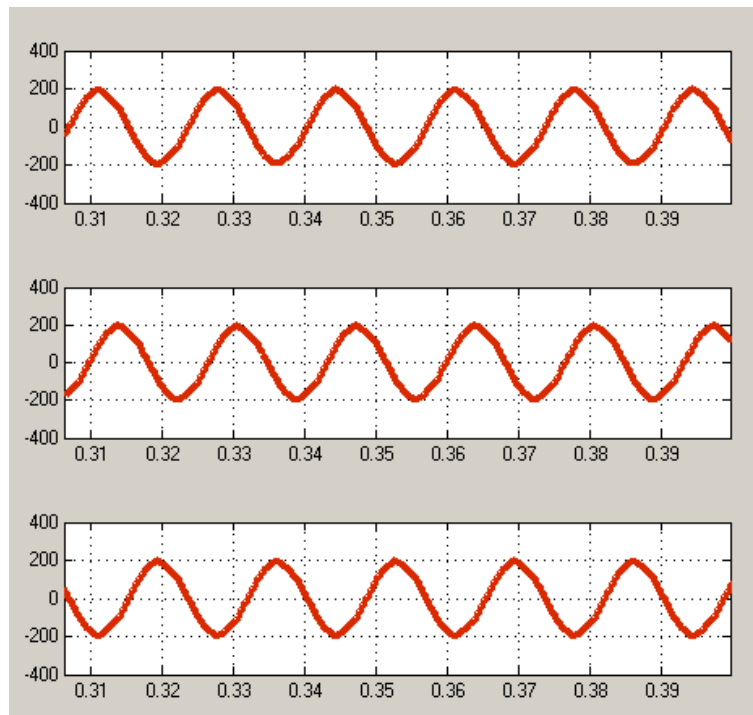


**Figure 5.6:** Line to line load voltage at  $M=0.755$ ,  $V_{in}=98$  v.

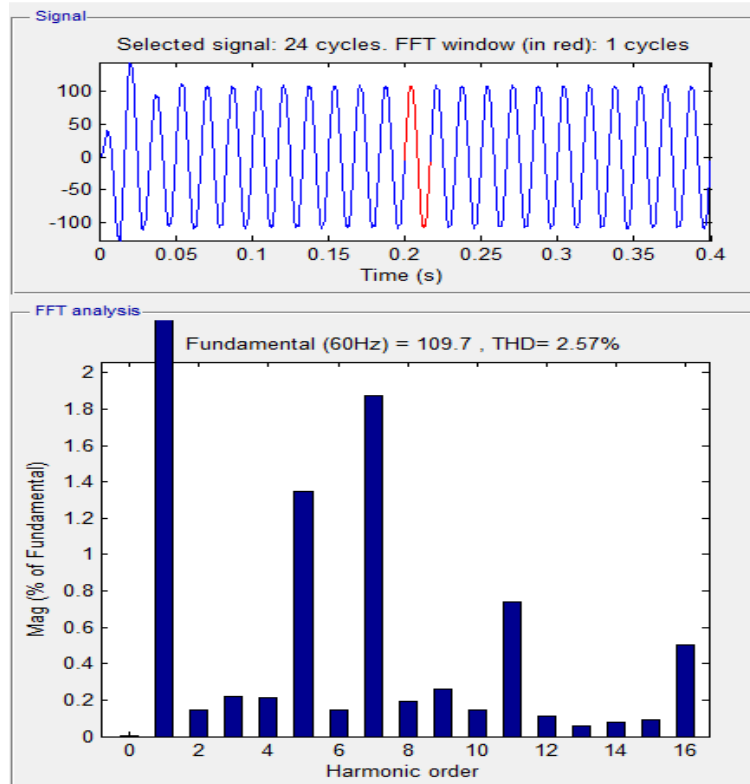


**Figure 5.7:** Total Harmonic at  $M=0.755$ ,  $V_{in}=98$  v.

From the simulation results illustrates in table 5.4, we obtained the following waveforms at an input voltage of 120 volt,  $D= 0.7115$ ,  $M= 0.812$  and the output dc voltage from the first stage 296 volt. Figure 5.8 illustrates the output dc voltage after the first stage of the converter, we note that the output dc voltage is raised up than the input dc voltage due to performance of dc-dc converter. Fig. 5.9 represents the load current, and figures 5.10, 5.11 show three phase and line to line load voltage respectively, and fig. 5.12 shows the total harmonic distortion of the system. In this case the input voltage is boosted to get an output phase voltage of 120v.

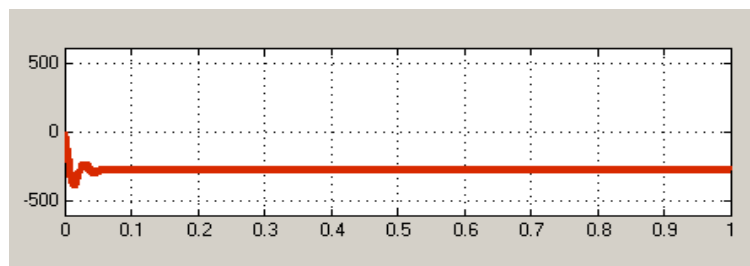


**Figure 5.8:** Output DC Voltage at  $M=0.812$ ,  $V_{in}=120$  v.

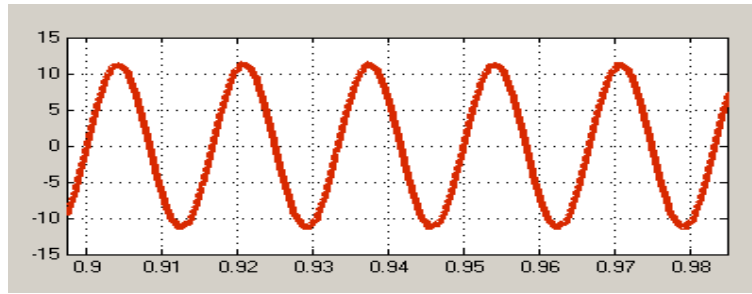


**Figure 5.9:** Load Current at  $M=0.812, V_{in}=120$  v.

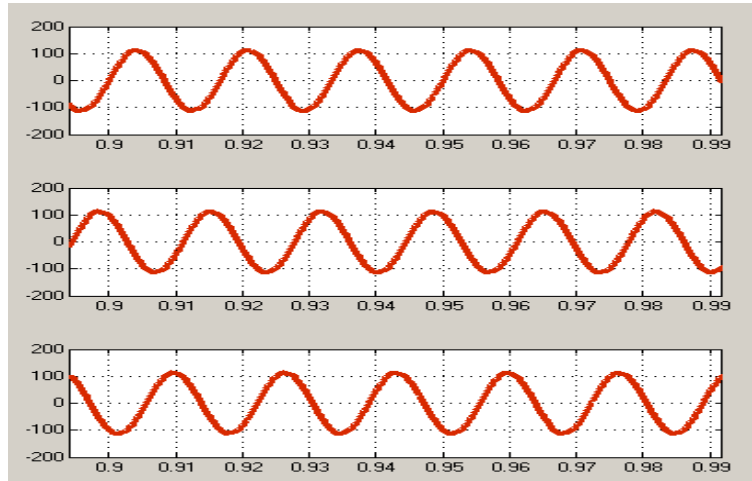


**Figure 5.10:** Three Phase Load Voltage at  $M=0.812, V_{in}=120$  v.

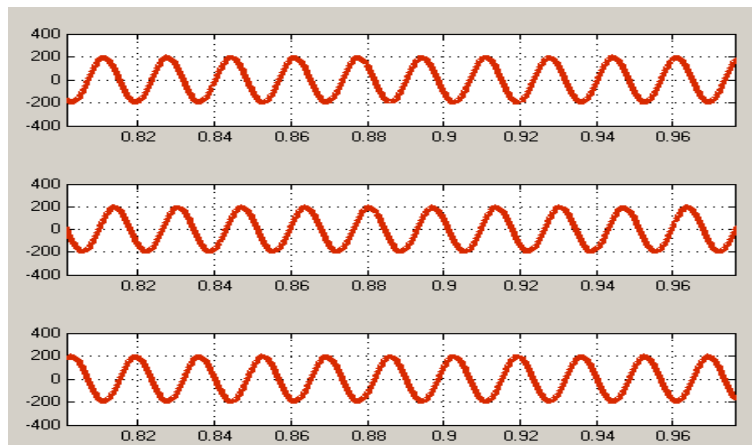


**Figure 5.11:** Line to Line Load Voltage at  $M=0.812, V_{in}=120$  v.

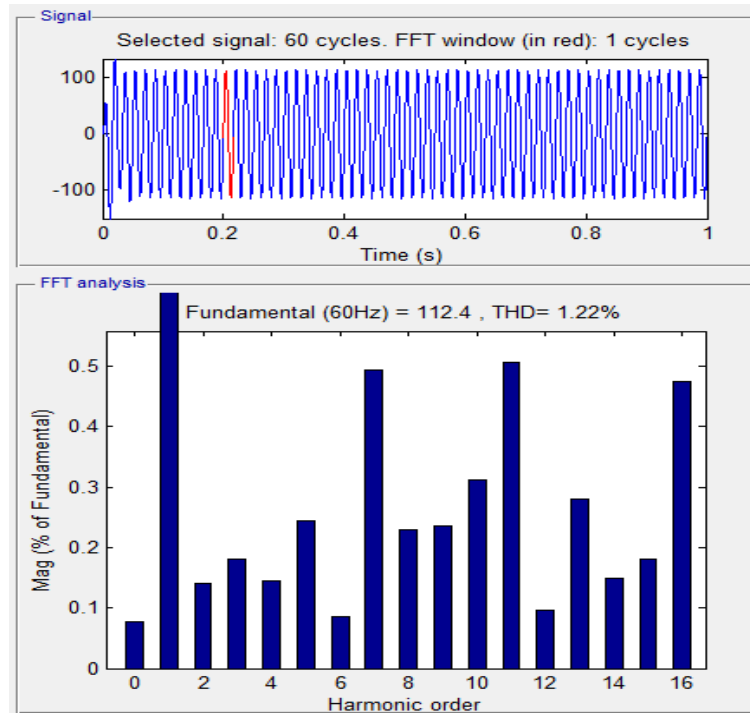


**Figure 5.12:** Total Harmonic at  $M=0.812$ ,  $V_{in}=120$  v.

From the simulation results associated to table 5.4, at input voltage 176 volt,  $D=0.5769$ ,  $M=1.0$ , the output dc voltage after the first stage is 240 volt. Figure 5.13 illustrates the output dc voltage after the first stage of the converter. It is observed that the output dc voltage is raised up and more than the input dc voltage due to performance of dc-dc converter. Fig. 5.14 represents the load current after the second stage, and figures 5.15, 5.16 show three phase load voltage, line to line load voltage respectively, and fig. 5.17 shows the total harmonic distortion of the output. In this case there is buck of the input voltage to get an output phase voltage of 120v.



**Figure 5.13:** Output DC Voltage at  $M=1.0$ ,  $V_{in}=176$  v.

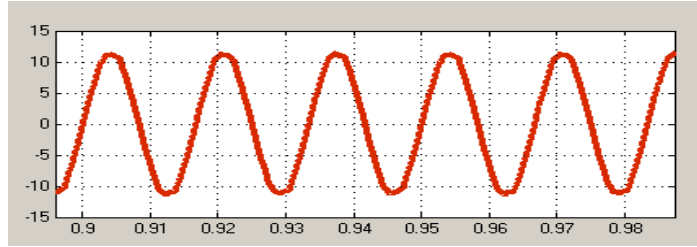


**Figure 5.14:** Load current at  $M=1.0$ ,  $V_{in}=176$  v.

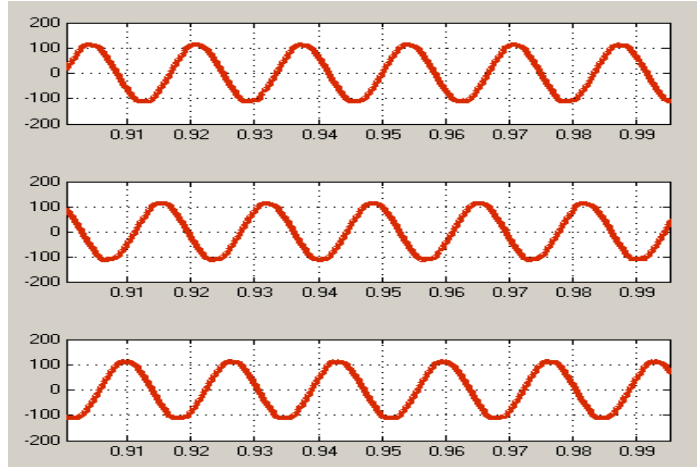


**Figure 5.15:** Three phase load voltage at  $M=1.0$ ,  $V_{in}=176$  v.

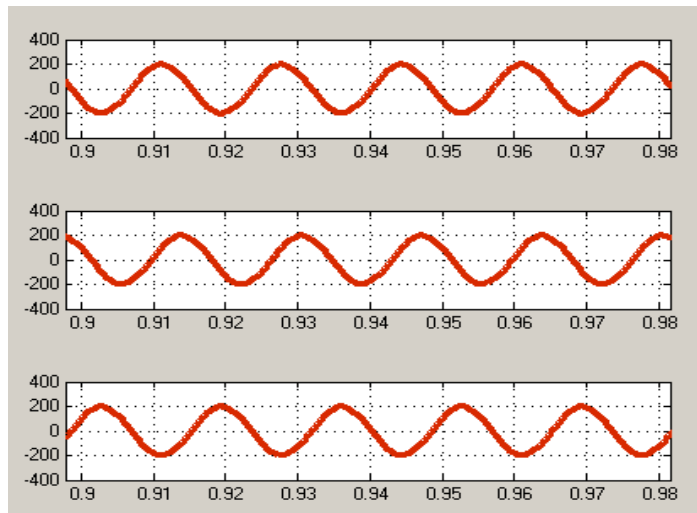


**Figure 5.16:** Line to line load voltage at  $M=1.0$ ,  $V_{in}=176$  v.

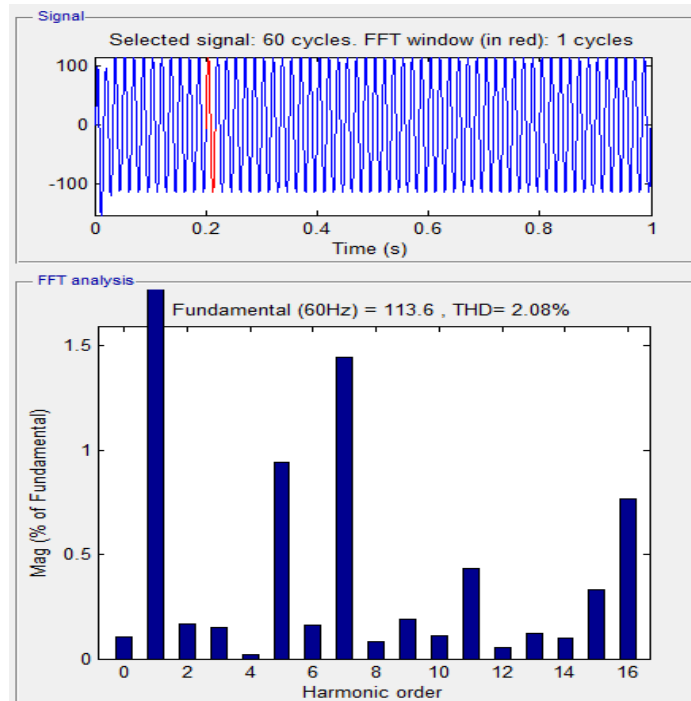


Figure 5.17: Total harmonic at  $M=1.0$ ,  $V_{in}=176$  v.

## 5.3 Results of Three Phase Z-Source Inverter

### 5.3.1 Matlab Simulink Model of ZSI System

Figure 5.18 illustrates the MATLAB/Simulink software model of ZSI controlled by MCBC with third harmonic injection. It consists of DC input voltage, impedance network, and conventional three phase inverter providing a resistive load. DC voltage source is fed to the impedance network which contains two identical inductors ( $L1$ ,  $L2$ ) and two identical capacitors ( $C1$ ,  $C2$ ). The capacitors of the network are coupled diagonally and the inductors are linked in series arms.

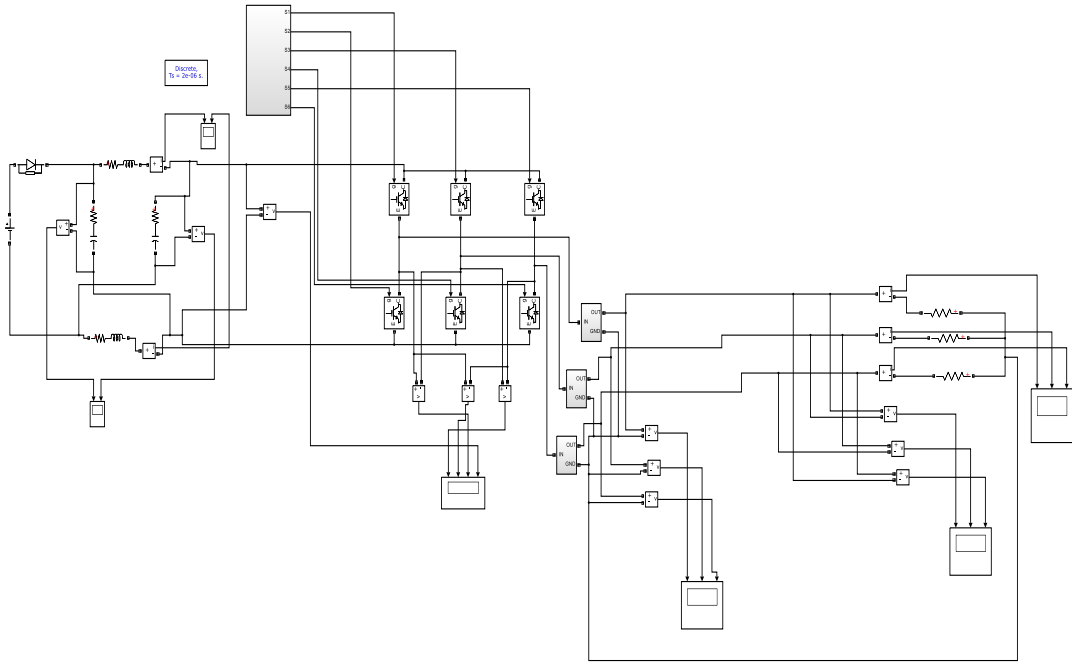


Figure 5.18: Simulink model of ZSI.

Figure 5.19 illustrates MATLAB/Simulink software model of MCBC strategy with third harmonic injection controller for the ZSI system.

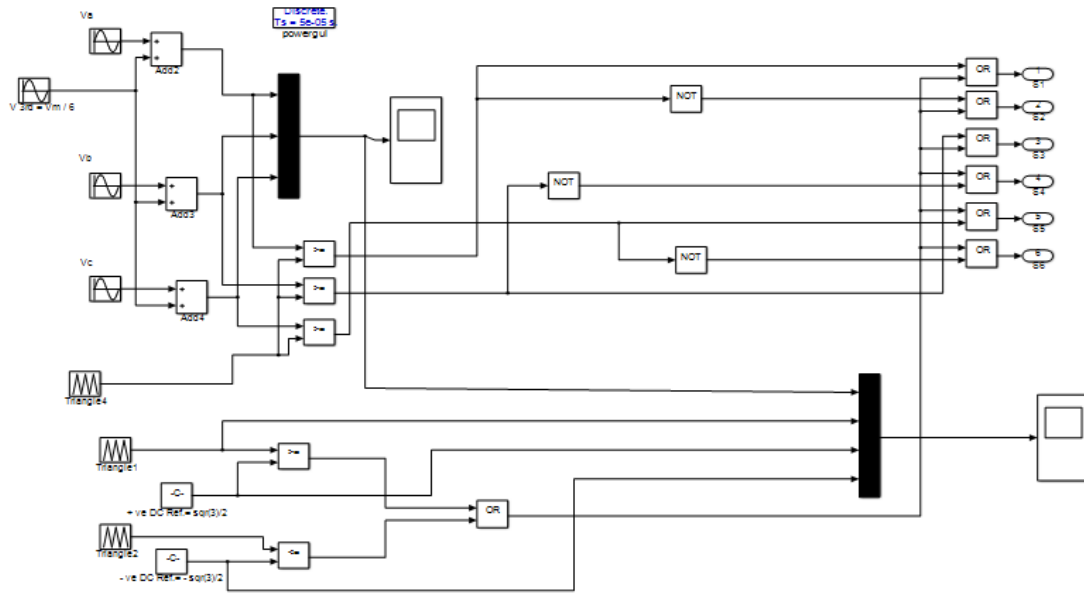


Figure 5.19: Maximum constant boost strategy with 3<sup>rd</sup> harmonic injection controller.

### 5.3.2 Calculations and results of ZSI

Table 5.5 illustrates the calculation of the input voltage ( $V_{in}$ ) by equation (5.17) when selected values of modulation index ( $M$ ) of the system 120 peak phase output voltage, 60 HZ, switching frequency 10 KHz, resistance load 10  $\Omega$  star connected are chosen.

$$\frac{2V_{ph}}{V_{in}} = \frac{M}{\sqrt{3}M - 1} \quad (5.17)$$

**Table 5.5:** Modulation index vs input voltage of ZSI.

$M$	0.755	0.812	1.0	1.1
$V_{in}$	98	120	176	198

Table 5.6 illustrates the calculation of the shoot through duty cycle ( $D_o$ ) by equation (5.18) at the selected values of modulation index.

$$D_o = \frac{2 - \sqrt{3}M}{2} \quad (5.18)$$

**Table 5.6:** Modulation index vs shoot through duty Cycle of ZSI.

$M$	0.755	0.812	1.0	1.1
$D_o$	0.3461	0.2967	0.1339	0.0473

Table 5.7 illustrates the calculation of the boost factor ( $B$ ) at the selected values of modulation index and at the shoot through duty cycle given by:

$$B = \frac{1}{\sqrt{3}M - 1} \quad (5.19)$$

$$B = \frac{1}{1 - 2 * D_o} \quad (5.20)$$

**Table 5.7:** Modulation index vs boost factor of ZSI.

<i>M</i>	0.755	0.812	1.0	1.1
<i>B</i>	3.249	2.460	1.366	1.104

Table 5.8 shows the calculation of the voltage stress ( $V_s$ ) given by equation (5.20), it is the maximum blocking voltage across the device when it is turned off, with the given values of boost factor.

$$V_s = B * V_{in} \quad (volt) \quad (5.20)$$

**Table 5.8:** Voltage stress vs input voltage of ZSI.

$V_{in}$	98	120	176	198
<i>B</i>	3.249	2.460	1.366	1.104
$V_s$	318	296	240	218

$$G = M * B \quad (5.21)$$

$$V_{ph} = \frac{M * B * V_{in}}{2} \quad (5.22)$$

All the theoretical calculations was obtained as shown in table 5.9.

**Table 5.9:** Theoretical calculations of ZSI.

<i>Case</i>	<i>M</i>	<i>B</i>	$D_o$	$V_{in}$	$V_s$
1	0.755	3.249	0.3461	98	318
2	0.812	2.460	0.2967	120	296
3	1.0	1.366	0.1339	176	240
4	1.1	1.104	0.0473	198	218

The Z-source network parameters are [25]:

$$L_1 = L_2 = L = 500 \mu H ; C_1 = C_2 = C = 400 \mu F$$

And the values of inductor and the capacitor of filter are:

$$L_f = 1.0 \text{ mH} ; C_f = 100 \text{ uF}$$

We calculate the positive dc voltage ( $V_p$ ) and the negative voltage ( $V_n$ ) for the control circuit by the equations:

$$V_p = \frac{\sqrt{3}}{2} M \cdot V_{tri} \quad (5.23)$$

$$V_n = -\frac{\sqrt{3}}{2} M \cdot V_{tri} \quad (5.24)$$

$$\text{Amplitude of Third Harmonic injection} = \frac{\text{Amplitude of the fundamental}}{6}$$

The simulation results of ZSI controlled by MCBC with 3<sup>rd</sup> harmonic injection from MATABL/SIMULINK software are shown in table 5.10. The mode of the circuit is boost or buck so that we got the desired output. At  $M=1.1$  for the input voltage 198v we got the output waveform with less harmonic distortion. The voltage across the capacitors  $C_1$  and  $C_2$  have equal values signed as  $V_C$  and the same currents across the inductors  $L_1$  and  $L_2$  signed as  $I_L$ .

**Table 5.10:** Simulation results of ZSI.

<i>Theoretical</i>			<i>Simulation</i>						
<i>Case</i>	<i>M</i>	<i>V<sub>in</sub></i>	<i>V<sub>dc</sub></i>	<i>I<sub>L</sub></i>	<i>V<sub>C</sub></i>	<i>V<sub>LL</sub></i>	<i>V<sub>ph</sub></i>	<i>I<sub>ph</sub></i>	<i>THD %</i>
1	0.755	98	325	28	205	208	122	12	2.03
2	0.812	120	265	18	190	204	112	10.5	3.56
3	1.0	176	235	14	202	208	116	11.5	2.22
4	1.1	198	220	12	205	209	123	12	1.52

Power losses calculations ( $P_{T_{losses}}$ ):

i. The losses of the diode ( $P_D$ ) :

$$I_i = \frac{P_i}{V_{in}} \quad (5.25)$$

$$I_i = \frac{4320}{98} = 44 \text{ A}$$

$$I_D = I_i = 44 \text{ A}$$

$$I_{D_{rms}} = 0.707 * I_D = 31 \text{ A} \quad (5.26)$$

• Forward Power losses in the diode ( $P_{vf}$ ):

$$P_{vf} = V_f * I_{D_{rms}} \quad (5.27)$$

$V_f = 0.7 \text{ volt}$ ; for the diode in the forward biase.

$$P_{vf} = 0.7 * 31 = 21.7 \text{ W}$$

• Reverse Power losses in the diode  $P_{Rf}$ :

$$P_{Rf} = R_f * I_{D_{rms}}^2 \quad (5.28)$$

$$P_{Rf} = 0.001 * (31)^2 = 0.961 \text{ W}$$

• Total Power losses of the diode ( $P_D$ ):

$$P_D = P_{Rf} + P_{vf} \quad (5.29)$$

$$P_D = 0.961 + 21.7 = 22.661 \text{ W}$$

ii. IGBT losses ( $P_{IGBT}$ ):

We choose: FS100R07PE4 Low Switching Losses -IGBT module for the dc-ac inverter bridge in our design, Hence from datasheet:

Power dissipation = 335 W

iii. The losses of the inductor ( $P_L$ ):

We choose the internal resistance of the inductor  $R_L=0.005 \Omega$

$$P_L = R_L * I_{L_{rms}}^2 \quad (5.30)$$

$$I_{L_{rms}} = 0.707 * I_L \quad (5.31)$$

$$I_{L_{rms}} = 0.707 * 28 = 19.796 A$$

$$P_L = 0.005 * (19.796)^2 = 1.959 W$$

$$P_{LT} = 1.959 * 2 = 3.918 W$$

iv. Total Power Losses ( $P_{T_{losses}}$ ):

$$P_{T_{losses}} = P_D + P_{IGBT} + P_{LT} \quad (5.32)$$

$$P_{T_{losses}} = 22.661 + 335 + 3.918 = 361.579 W$$

Calculations of the efficiency ( $\eta$  %):

$$\eta = \frac{P_{out}}{P_{out} + P_{T_{losses}}} * 100 \% \quad (5.33)$$

$$\eta = \frac{4320}{4320 + 361.579} * 100 \% = 92.276 \%$$

From the simulation results associated to table 5.10, at input voltage 98volt,  $D_o=0.3461$ ,  $M=0.755$  and the dc link voltage 325 volt, the following waveforms are obtained. Figure 5.20 illustrates the dc link voltage, we note that the dc voltage is raised up more than the input dc voltage due to performance Z network. Fig. 5.21 represents the voltage across  $C_1$  and  $C_2$  of the Z network. Figure 5.22 shows the currents flow through the inductors  $L_1$  and  $L_2$  of the Z network. Figure 5.23 shows the load current, and figures 5.24, 5.25 represent three phase and the line to line load voltage respectively, and fig. 5.26 shows the total harmonic distortion of the output waveform. From above, the mode of circuit is boost.

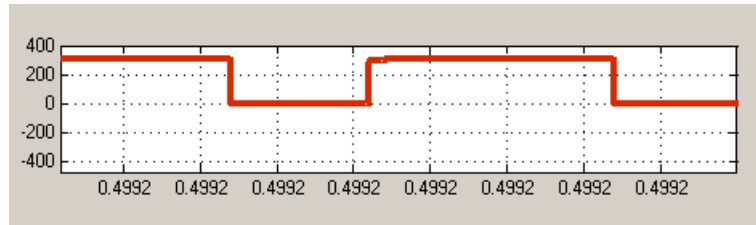


**Figure 5.20:** The DC link voltage at  $M=0.755$ ,  $V_{in}=98$  v.



**Figure 5.21:** The voltage across  $C_1$  and  $C_2$  at  $M=0.755$ ,  $V_{in}=98$  v.



**Figure 5.22:** The Inductors current at  $M=0.755$ ,  $V_{in}=98$  v

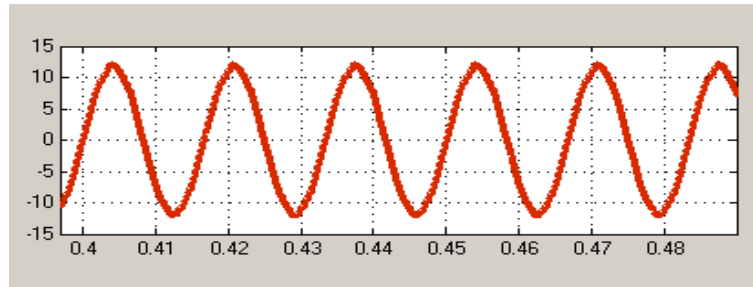


**Figure 5.23:** The load current at  $M=0.755$ ,  $V_{in}=98$  v

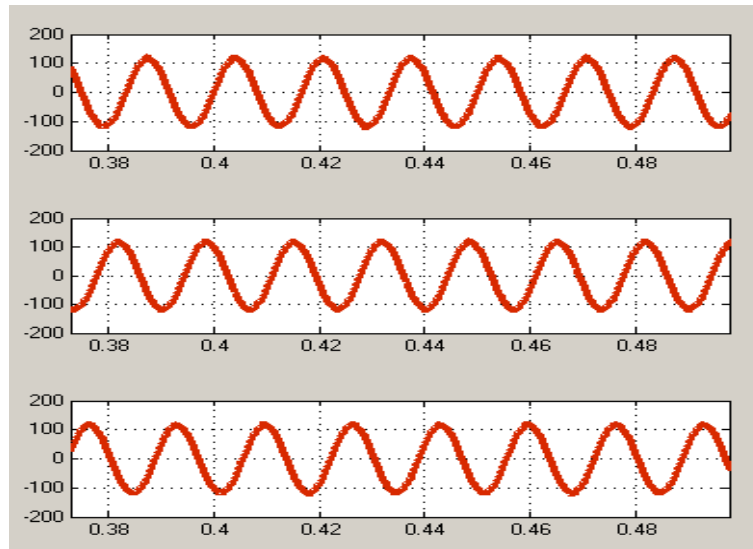


**Figure 5.24:** Three phase load voltage at  $M=0.755$ ,  $V_{in}=98$  v.

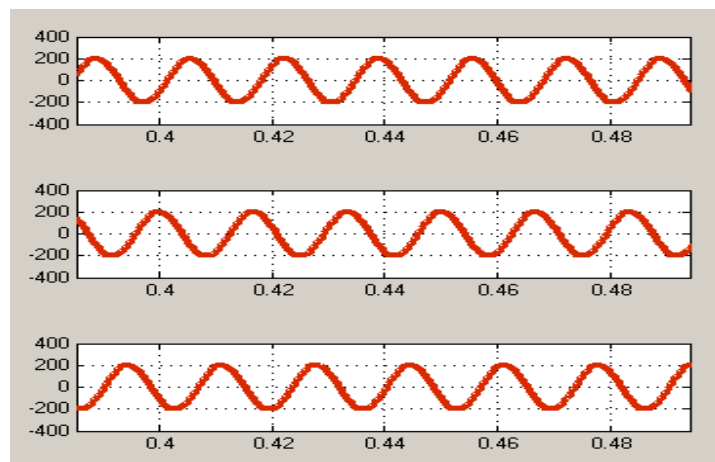


**Figure 5.25:** Line to Line load Voltage at  $M=0.755$ ,  $V_{in}=98$  v.

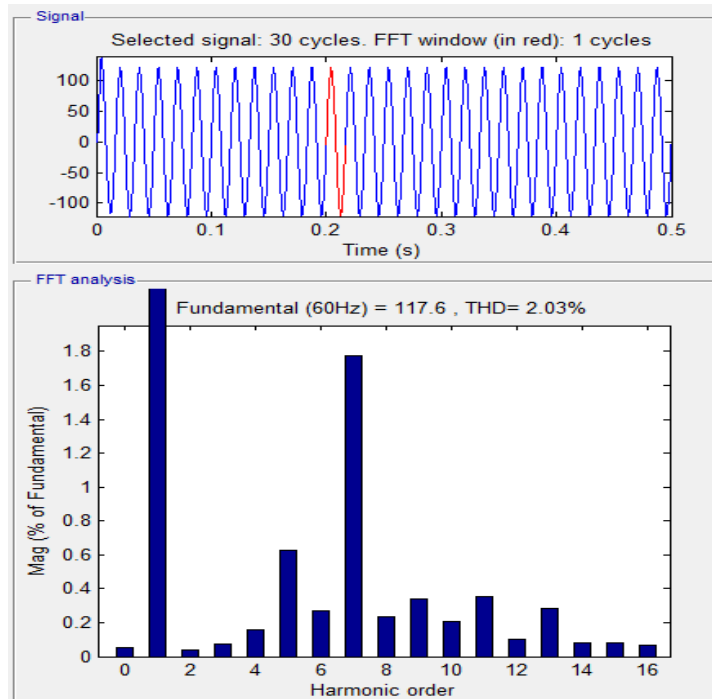


**Figure 5.26:** Total harmonic at  $M=0.755$ ,  $V_{in}=98$  v.

From the simulation results associated to table 5.10, at input voltage 120 volt,  $D_o=0.2967$ ,  $M=0.812$  and the dc link voltage 265 volt, we obtained the following waveforms. Figure 5.27 illustrates the dc link voltage. It is important to note that the dc voltage is raised up more than the input dc voltage due to performance Z network. Fig. 5.28 represents the voltage across  $C_1$  and  $C_2$  of the Z network. Figure 5.29 shows the currents flow through the inductors  $L_1$  and  $L_2$  of the Z network. Fig. 5.30 shows the load current, and figures 5.31, 5.32 represent three phase and the line to line load voltage respectively, and fig. 5.33 shows the total harmonic distortion of the output waveform. From above, the mode of circuit is boost.

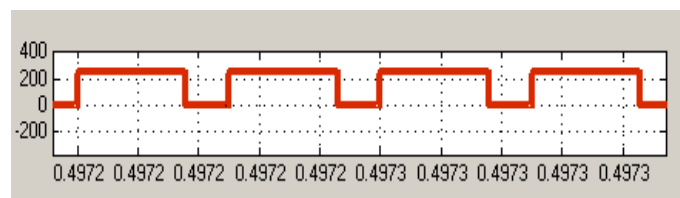


**Figure 5.27:** The DC link voltage at  $M=0.812$ ,  $V_{in}=120$  v.

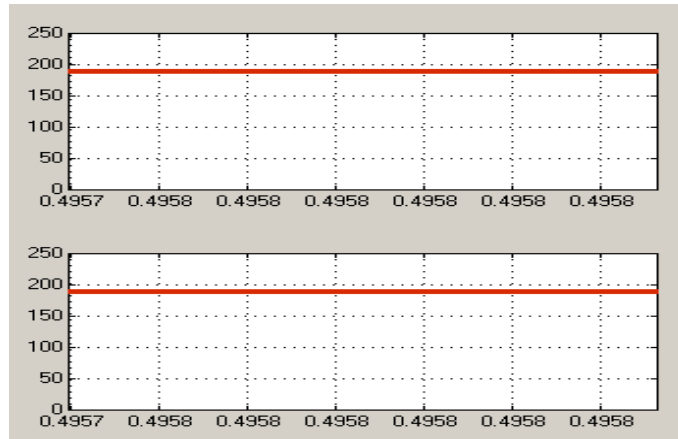


**Figure 5.28:** The voltage across  $C_1$  and  $C_2$  at  $M=0.812$ ,  $V_{in}=120$  v.

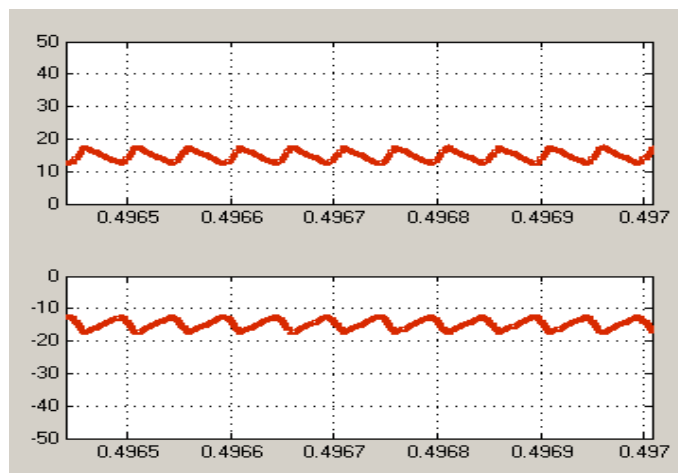


**Figure 5.29:** The inductors current at  $M=0.812$ ,  $V_{in}=120$  v.

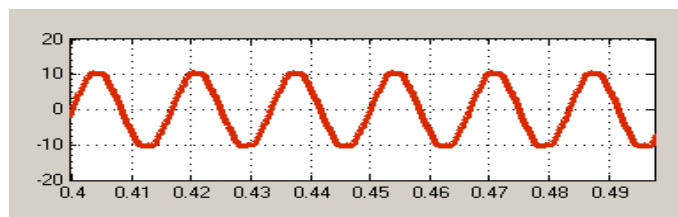


**Figure 5.30:** The load current at  $M=0.812$ ,  $V_{in}=120$  v.

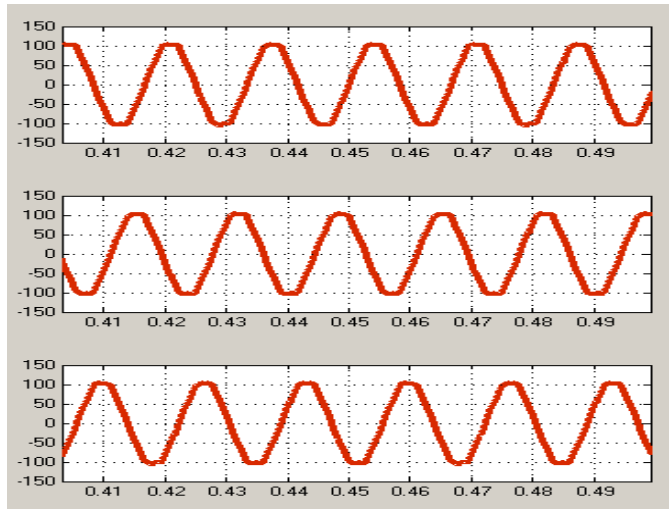


**Figure 5.31:** Three phase load voltage at  $M=0.812$ ,  $V_{in}=120$  v.

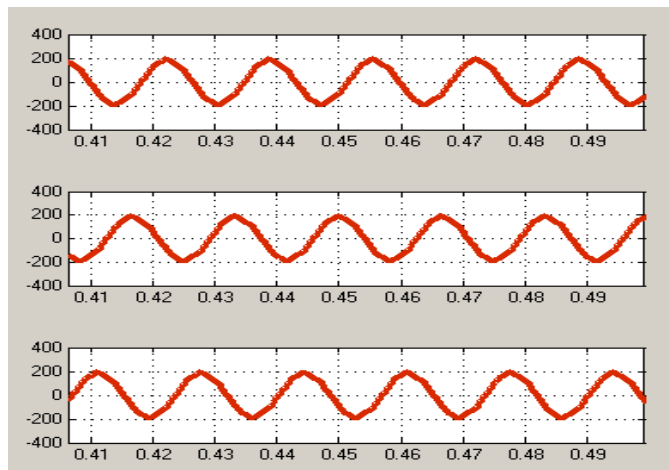


**Figure 5.32:** Line to line load voltage at  $M=0.812$ ,  $V_{in}=120$  v.

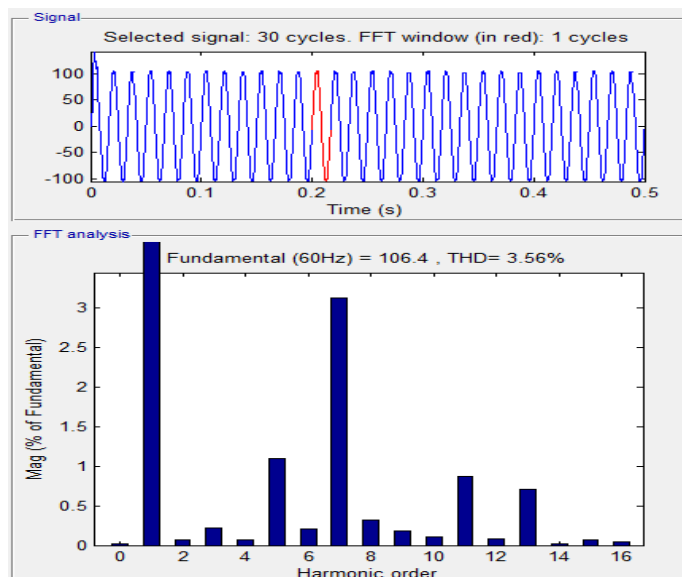


**Figure 5.33:** Total harmonic at  $M=0.812$ ,  $V_{in}=120$  v.

From the simulation results associated to table 5.10, at input voltage 176 volt,  $D_o= 0.1339$ ,  $M= 1.0$  and the dc link voltage 235 volt, we obtained the following waveforms. Figure 5.34 illustrates the dc link voltage. Fig. 5.35 represents the voltage across  $C_1$  and  $C_2$  of the Z network, and figure 5.36 shows the currents in the inductors  $L_1$  and  $L_2$  of the Z network. Fig. 5.37 shows the load current, and figures 5.38, 5.39 represent three phase and the line to line load voltage respectively, and fig. 5.40 shows the total harmonic distortion of the output waveform. From above, the mode of circuit is buck.



**Figure 5.34:** The voltage across  $C_1$  and  $C_2$  at  $M=1.0$ ,  $V_{in}=176$  v.

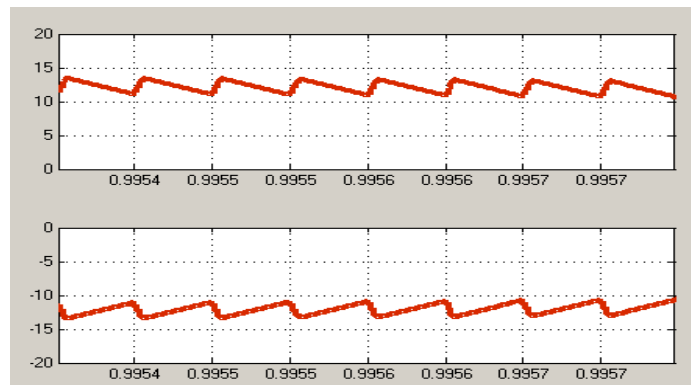


**Figure 5.35:** The inductors current at  $M=1.0$ ,  $V_{in}=176$  v.

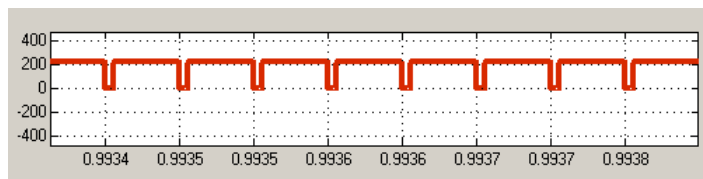


**Figure 5.36:** The DC link voltage at  $M=1.0$ ,  $V_{in}=176$  v.

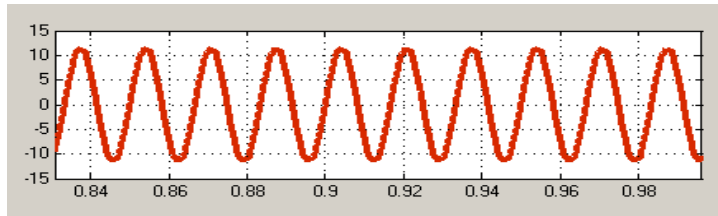


**Figure 5.37:** The load current at  $M=1.0$ ,  $V_{in}=176$  v.

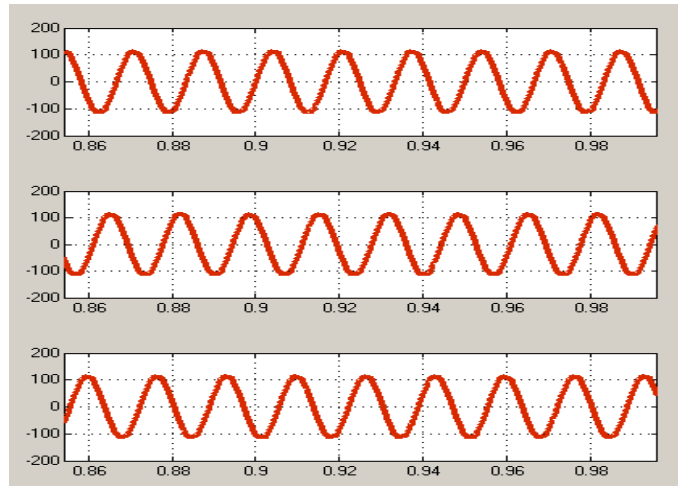


**Figure 5.38:** Three phase load voltage at  $M=1.0$ ,  $V_{in}=176$  v.

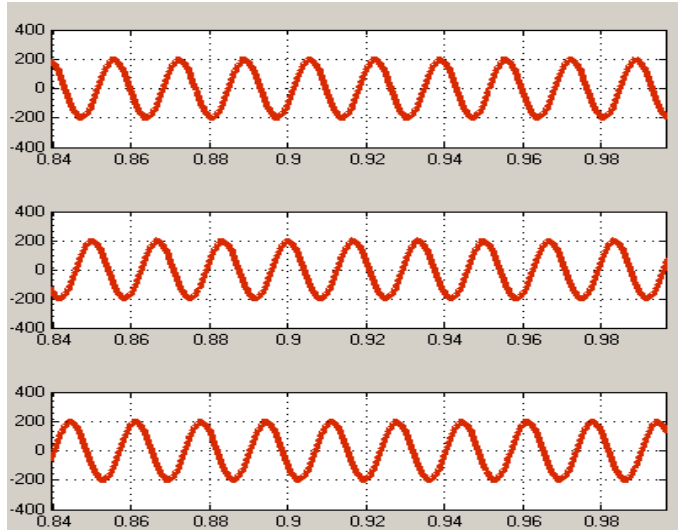


**Figure 5.39:** Line to line load voltage at  $M=1.0$ ,  $V_{in}=176$ v.

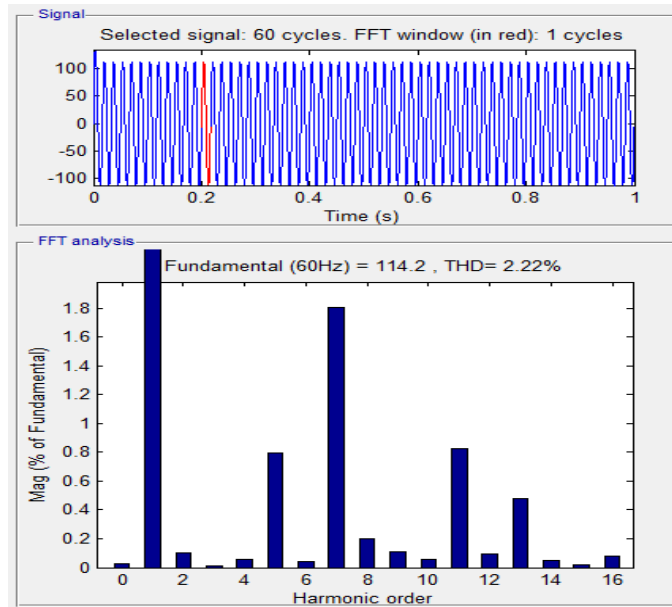


Figure 5.40: Total harmonic at  $M=1.0$ ,  $V_{in}=176$  v.

From the simulation results associated to table 5.10, at input voltage 198 volt,  $D_o= 0.0473$ ,  $M=1.1$  and the dc link voltage 220 volt, we obtained the following waveforms: Figure 5.41 illustrates the dc link voltage. Fig. 5.42 represents the voltage across  $C_1$  and  $C_2$  of the Z network. Figure 5.43 shows the currents in the inductors  $L_1$  and  $L_2$  of the Z network, and fig. 5.44 shows the load current, while figures 5.45, 5.46 represent three phase and the line to line load voltage respectively, and fig. 5.47 shows the total harmonic distortion of the output waveform. From above, the mode of circuit is buck.

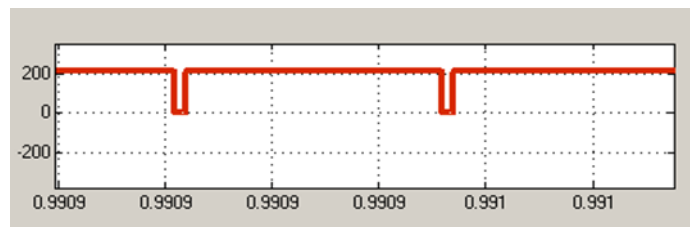
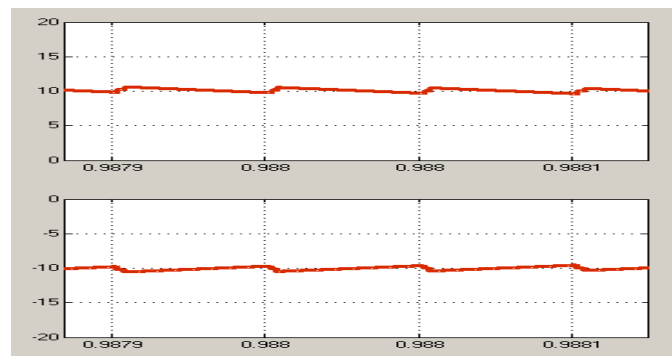


Figure 5.41: The DC link voltage at  $M=1.1$ ,  $V_{in}=198$  v.



**Figure 5.42:** The voltage across  $C_1$  and  $C_2$  at  $M=1.1$ ,  $V_{in}=198$  v.



**Figure 5.43:** The Inductors Current at  $M=1.1$ ,  $V_{in}=198$  v.

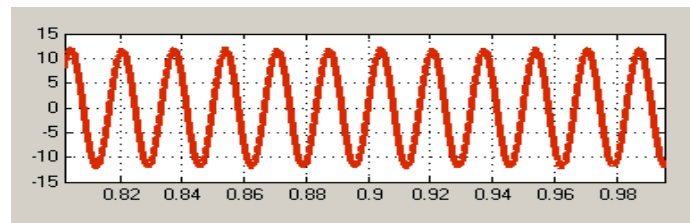


**Figure 5.44:** The Load Current at  $M=1.1$ ,  $V_{in}=198$  v.

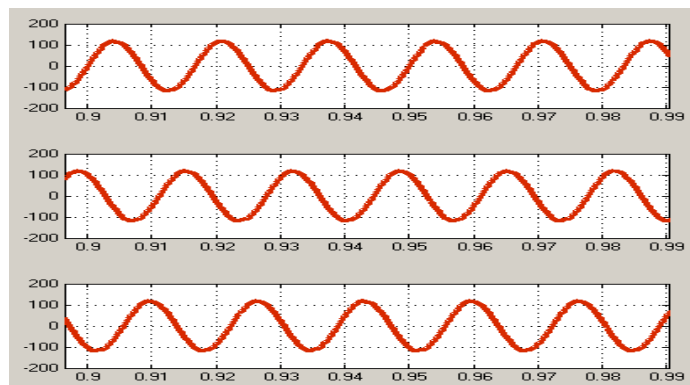


**Figure 5.45:** Three phase load voltage at  $M=1.1$ ,  $V_{in}=198$  v.

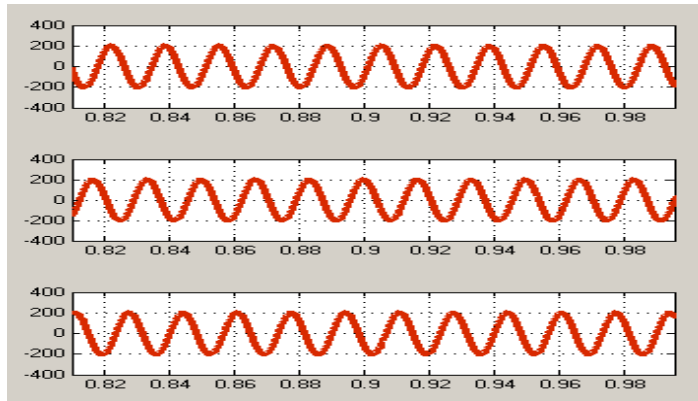


**Figure 5.46:** Line to Line load Voltage at  $M=1.1$ ,  $V_{in}=198$  v.

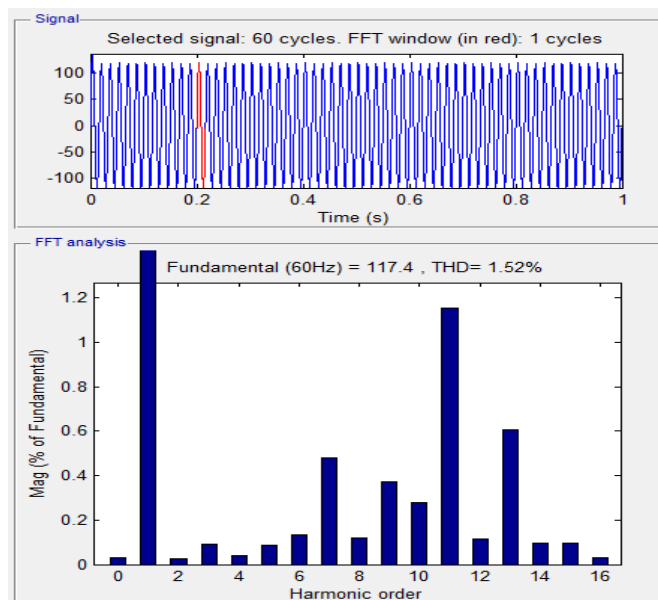


**Figure 5.47:** Total harmonic at  $M=1.1$ ,  $V_{in}=198$  v.

## 5.4 Results of Three Phase Quasi Z-Source Inverter

### 5.4.1 Matlab Simulink Model of QZSI System

Figure 5.48 illustrates the MATLAB/Simulink software model of QZSI MCBC strategy with third harmonic injection control. It consists of DC input voltage, impedance network, and conventional three phase inverter providing a resistive load.

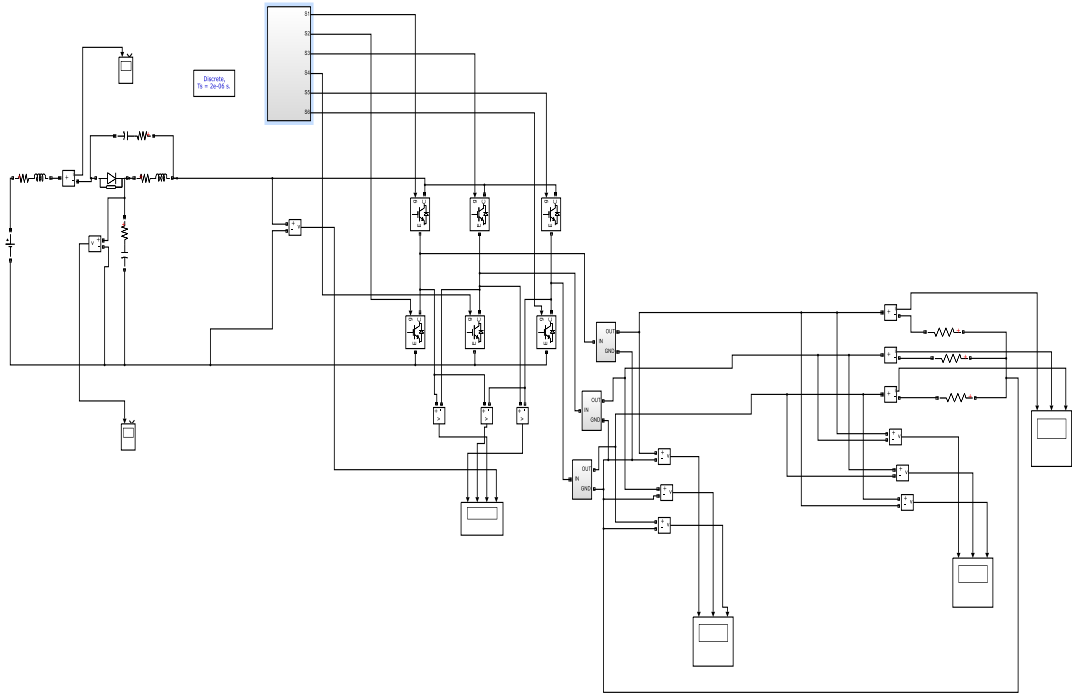


**Figure 5.48:** Simulink model of QZSI.

### 5.4.2 Calculations and Results of QZSI

We used the same controller associated with ZSI and the same procedure to get the results of QZSI as shown in table 5.11. The mode of the circuit is boost or buck so that we got the desired output. At  $M=1.1$  for input voltage 198v we got the output waveform with less harmonic distortion. The voltage across the capacitor  $C_2$  less than  $C_1$  and the same currents across the inductors  $L_1$  and  $L_2$ .

**Table 5.11:** Simulation results of QZSI.

<i>Theoretical</i>			<i>Simulation</i>								
<i>CASE</i>	<i>M</i>	<i>V<sub>in</sub></i>	<i>V<sub>dc</sub></i>	<i>I<sub>L1</sub></i>	<i>I<sub>L2</sub></i>	<i>V<sub>c1</sub></i>	<i>V<sub>c2</sub></i>	<i>I<sub>ph</sub></i>	<i>V<sub>LL</sub></i>	<i>V<sub>ph</sub></i>	<i>THD %</i>
1	0.755	98	300	28	28	200	100	12	208	122	2.03
2	0.812	120	265	18	18	185	65	10.5	204	112	3.56
3	1.0	176	245	14	14	200	25	11.5	208	116	2.22
4	1.1	198	225	11	11	207	6	12	209	123	1.52

From the simulation results associated to table 5.11, at the input voltage 98volt,  $M= 0.755$  and the dc link voltage 300 volt. We obtained the following waveforms: Figure 5.49 illustrates the dc link voltage, fig. 5.50 represents the voltage across  $C_1$  and  $C_2$  , figure 5.51 shows the currents in the inductors  $L_1$  and  $L_2$ . From above, the mode of circuit is boost.

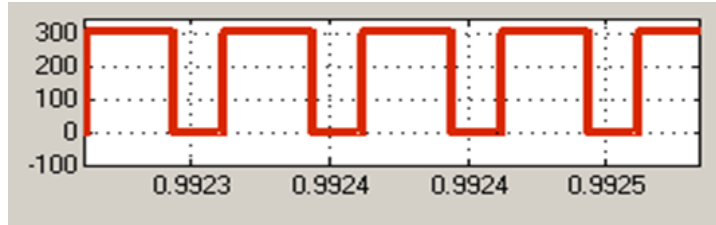


**Figure 5.49:** The DC link voltage at  $M=0.755$ ,  $V_{in}=98$  v.

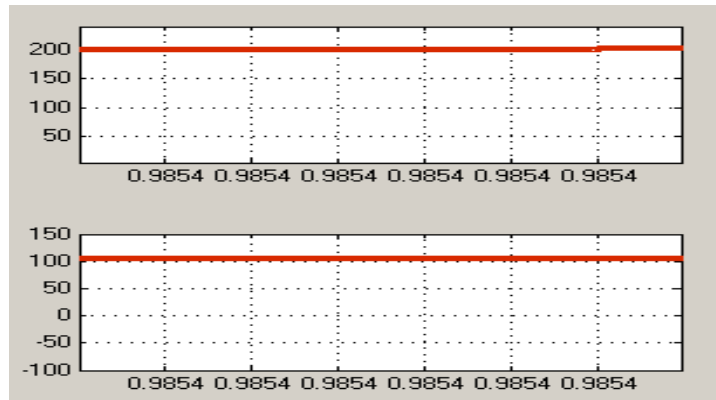


**Figure 5.50:** The voltage across  $C_1$  and  $C_2$  at  $M=0.755$ ,  $V_{in}=98$  v.

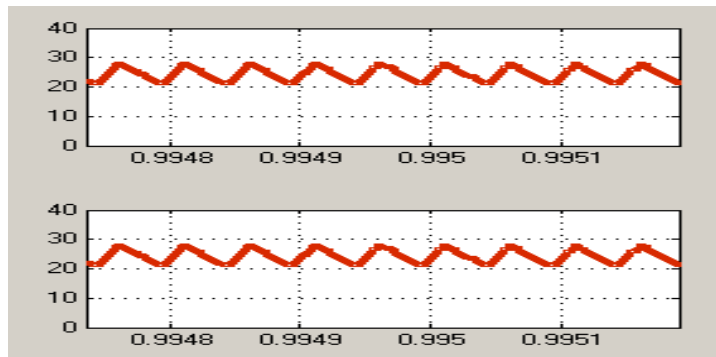


**Figure 5.51:** The inductors current at  $M=0.755$ ,  $V_{in}=98$  v.

The simulation results associated to table 5.11, at the input voltage 120volt,  $M=0.812$  and the dc link voltage 265 volt. We obtained the following waveforms: Figure 5.52 shows the dc link voltage, fig. 5.53 represents the voltage across  $C_1$  and  $C_2$ , figure 5.54 shows the currents in the inductors  $L_1$  and  $L_2$ . From above, the mode of circuit is boost.

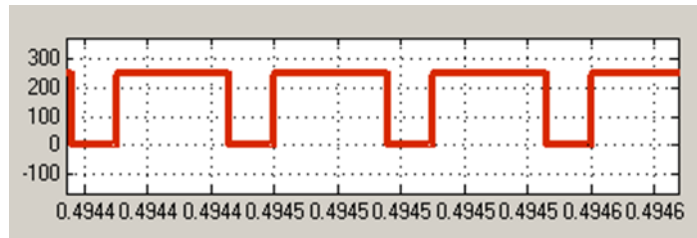


**Figure 5.52:** The DC link voltage at  $M=0.812$ ,  $V_{in}=120$  v.



**Figure 5.53:** The voltage across  $C_1$  and  $C_2$  at  $M=0.812$ ,  $V_{in}=120$  v.

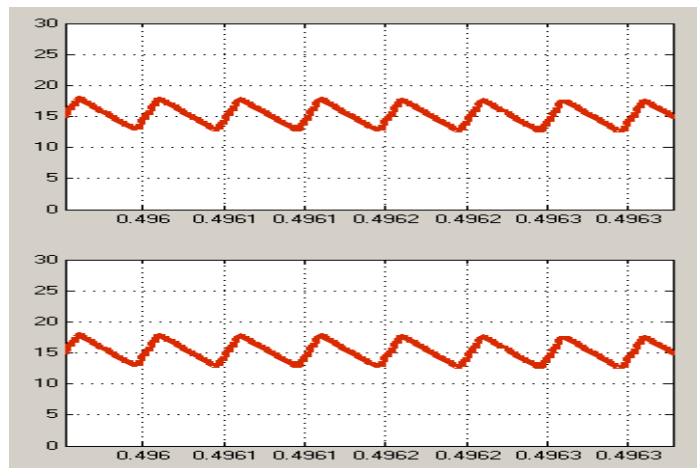


**Figure 5.54:** The inductors current at  $M=0.812$ ,  $V_{in}=120$  v.

From simulation results associated in table 5.11, at the input voltage 176volt,  $M= 1.0$  and the dc link voltage 245 volt. We obtained the following waveforms: Figure 5.55 represents the dc link voltage, fig. 5.56 shows the voltage across  $C_1$  and  $C_2$  and figure 5.57 shows the currents in the inductors  $L_1$  and  $L_2$ . From above, the mode of circuit is buck.



**Figure 5.55:** The DC link voltage at  $M=1.0$ ,  $V_{in}=176$  v.

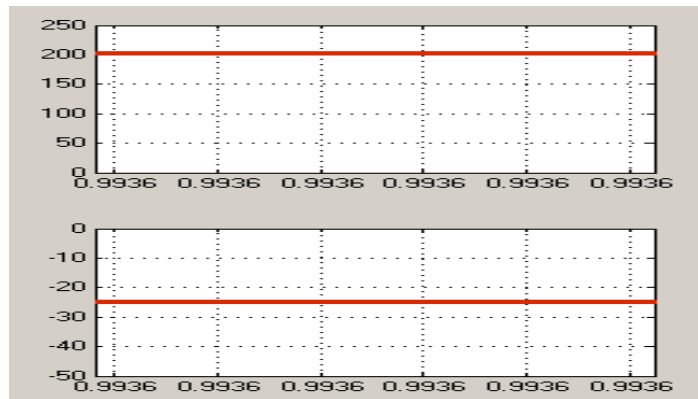


**Figure 5.56:** The voltage across  $C_1$  and  $C_2$  at  $M=1.0$ ,  $V_{in}=176$  v.

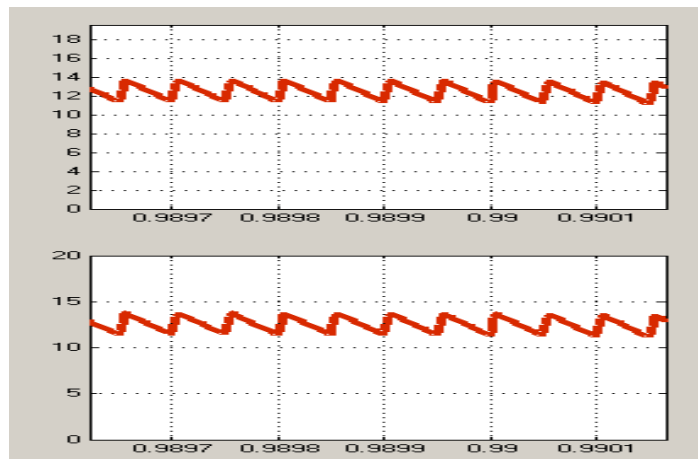


**Figure 5.57:** The inductors current at  $M=1.0$ ,  $V_{in}=176$  v.

The simulation results associated to table 5.11, at input voltage 198volt,  $M= 1.1$  and the dc link voltage 225 volt. We obtained the following waveforms: Figure 5.58 illustrates the dc link voltage, fig. 5.59 shows the voltage across  $C_1$  and  $C_2$  and figure 5.60 represents the currents in the inductors  $L_1$  and  $L_2$ . From above, the mode of circuit is buck.

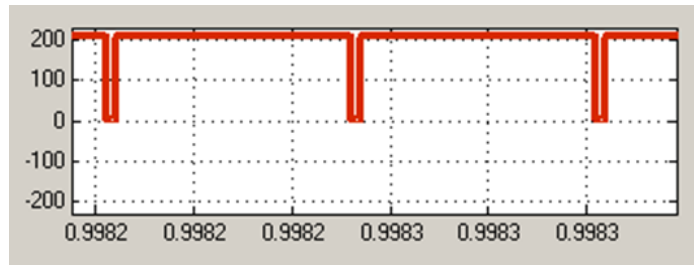


**Figure 5.58:** The DC link voltage at  $M=1.1$ ,  $V_{in}=198$  v.



**Figure 5.59:** The voltage across  $C_1$  and  $C_2$  at  $M=1.1$ ,  $V_{in}=198$  v.



**Figure 5.60:** The inductors current at  $M=1.1$ ,  $V_{in}=198$  v.

## 5.5 Comparison Among Conventional Two Stage BB VSI, ZSI AND QZSI

From the above and from the tables 5.4, 5.10 and 5.11, we obtained the tables 5.12 and 5.13. We observe that three types of topologies do buck or boost with the variant values of input voltage to get the desired output voltage 120v phase voltage. However, the first type performs that by two stages, while the last two types perform buck or boost in one stage. In the first topology, we note that at a certain value of  $M$ , we can use a wide range of input voltages, and with modulation index  $M= 0.812$  it provided a better output waveform because of less harmonic distortion with input voltage 120v. For ZSI and QZSI we got the desired output voltage with less harmonic distortion at  $M=1.1$  at an input voltage of 198v. In addition, conventional two stage VSI has higher voltage stress than ZSI and QZSI, they are have the same voltage stress as shown in table 5.13.

**Table 5.12:** The comparison results of conventional BB, ZSI and QZSI.

<i>Type of inverter</i>	$M$	$V_{in}$	$V_{LL}$	$V_{ph}$	$I_{ph}$	$THD \%$
Conventional--al two stage VSI	0.755	98	208	115	11	2.57
	0.812	120	208	120	11.5	1.22
	1.0	176	208	118	11.5	2.08
ZSI with 3rd harmonic injection	0.755	98	208	122	12	2.03
	0.812	120	204	112	10.5	3.56
	1.0	176	208	116	11.5	2.22
	1.1	198	209	123	12	1.52
Q-ZSI with 3rd harmonic injection	0.755	98	208	122	12	2.03
	0.812	120	204	112	10.5	3.56
	1.0	176	208	116	11.5	2.22
	1.1	198	209	123	12	1.52

**Table 5.13:** Comparison the input voltage and the voltage stress.

<i>Case</i>	<i>M</i>	<i>V<sub>in</sub></i>	<i>Voltage stress</i>		
			<i>Conventional Two stage</i>	<i>ZSI</i>	<i>QZSI</i>
1	0.755	98	416	318	318
2	0.812	120	416	296	296
3	1.0	176	416	240	240
4	1.1	198	-	218	218

## CHAPTER SIX

### CONCLUSIONS AND FUTURE WORKS

#### 6.1 Conclusions

The work in this thesis is focused on the simulation and comparison among three types of VSI; conventional two stage buck-boost VSI controlled by sinusoidal pulse width modulation, Z-source and Quasi Z-source topologies controlled by maximum constant boost with third harmonic injection. In addition, it is presented how to get a desired output ac voltage from higher or lower input dc values based on suitable selection of the modulation index. The work in this thesis considers three-phase voltage source inverters with a 120V output peak phase voltage, 60 HZ, and with a switching frequency of 10 KHz to drive a resistive star-connected load of 10  $\Omega$  at the modulation index values of 0.755, 0.812, 1.0, and 1.1. Also, it focuses on the effect of shoot through of the traditional Z-source and Quasi Z-Source inverters.

The simulation is implemented by MATLAB/Simulink software. The Insulated Gate Bipolar Transistors (IGBTs) is utilized as a switching device. The duty cycle variation is achieved by using pulse width modulation. All the simulation and theoretical results are presented in tables.

Two pulse width modulation control strategies are implemented; Sinusoidal carrier-based PWM and maximum constant boost with third harmonic injection control methods. These methods are described in details and compared on the basis of simulation in MATLAB / Simulink software.

This thesis investigated the voltage gain of the three types of inverters topologies at a specified boost factor. The voltage gain of any type of topology were calculated. Then, the simulation waveforms of the output line to line voltage, line to neutral voltage and current of the inverter is presented to verify the theoretical analysis.

The simulation results for three types of VSI are stated as follows: from the simulation results of conventional BB inverter illustrated in table 5.4, we note that at a certain value of  $M$  a wide range of input voltages can be used. The mode of the circuit is boost or buck so that we got the desired output. At  $M= 0.812$  we got the output waveform with less harmonic distortion.

The simulation results of ZSI associated to table 5.10 show that the mode of the circuit is boost or buck. So that, we got the desired output. At  $M=1.1$ , the output waveform has less harmonic distortion. The voltage across the capacitors  $C_1$  and  $C_2$  have equal values and the same currents flow through the inductors  $L_1$  and  $L_2$ .

From the simulation results of QZSI illustrates in table 5.11. The mode of the circuit is boost or buck. So that, we got the desired output. At  $M=1.1$  we got the output waveform with less harmonic distortion. The voltage across the capacitor  $C_2$  is less than  $C_1$  and the same current passes through the inductors  $L_1$  and  $L_2$ .

We observe that three types of topologies have done buck or boost with the variant values of input voltage to get the desired output voltage 120v phase voltage. However, the first type performs that by two stages, while the last two types perform buck or boost in one stage. In the first topology, we note that at a certain value of  $M$ , we can use a wide range of input voltages, and with modulation index,  $M= 0.812$  it provides a better output waveform because of the less harmonic distortion. For ZSI and QZSI we got the desired output voltage with less harmonic distortion at  $M=1.1$  at an input voltage of 198v. In addition, conventional two stage VSI has higher voltage stress than ZSI and QZSI, they are have the same voltage stress as shown in table 5.12 and 5.13.

The last two types of inverters studied in this thesis present several benefits when compared to the conventional voltage source inverter. Traditional VSIs have many disadvantages if used in variant applications. In particular, they should have an input voltage which is more than the output peak phase voltage to get the desired output.

Often, to solve these issues and to get the desired outputs, an additional stage dc-dc converter is utilized in front of the inverter to deliver the required DC link voltage that help the second stage (i.e. voltage source inverter) to produce the desired output voltage.

Lately, the voltage provide for z-source inverters, have been suggested to treat these issues. They are substitute the dc-dc input stage with a unique LC network to permits the input voltage to be changed as desired.

Furthermore, it has the ability to act as a voltage source inverter or a current source inverter based on the applications and requirements, and the output voltage can be changed from zero to infinity.

The z-source inverter has some disadvantages, it has intermittent input current in the boost mode and the capacitors of the network must support high voltage. Also, the intermittent input current is not suitable for many applications and may need a large input filter.

Quasi ZSI topologies presented in this thesis, inherits the advantages of the ZSI. It can execute boost (step-up) and/or buck (step-down) conversion in one stage with a wide range of voltage gain, and it has several benefits and features when compared to the conventional voltage source inverter. These advantages include decreased component count, decrease passive component ratings, and enhanced input profiles. QZSI topology has been introduced recently to treat some of the drawbacks and issues of the ZSI. The quasi z-source inverter offers some benefits over the ZSI as lower component ratings, continuous input current and higher reliability. This topology of the inverter is known as one of the greatest suitable power interfaces between the PV system and the power grid

The Problems faced by the z-source inverter is treated by a QZSI topology. This inverter can give joint earthing of dc link and input source; in this manner, a lessening in the common mode noise can happen. Also, the input inductor buffers the source current and the voltage on one of the capacitors in the Z network is lower than in the case of Z source inverter. Consequently there is no drawback for QZSI when compared with ZSI; and subsequently, QZSI can be utilized where ZSI finds its application.

The ZSI and quasi ZSI were suggested to treat the issues of conventional voltage source inverters. In this way, the systems become so easier and less cost. As well as, a shoot through vector, that means if both the upper and the lower switches of any one leg or any two legs or all three legs are shorted such as both switches are turned ON at the same time, this conduction will cause a short at load terminals, without burning the power devices.

The comparison results show that the Z-Source and QZ-Source inverters may increase inverter conversion efficiency by 3% than conventional BB because the last have an extra switch. In addition, the ZSI and QZSI have lower voltage stress and higher voltage gain. For this reason, ZSI and QZSI Provide a small cost, higher reliability and efficient conversion with one stage for boost (step-up) and buck (step-down) conversions.

The maximum constant boost with third harmonic injection control (MCBC) method has the highest modulation index and thus has the highest voltage gain and lower voltage stress. Many researchers developed and modified few topologies that derived from ZSI and QZSI to develop and enhance the performance when they used in various applications, specifically for renewable energy applications. Furthermore, efforts have been made to develop or find new control methods of PWM that can made the controlling of these inverters more effective and easier to handle with.

## **6.2 Future Works**

In this thesis, the simulation model is built in MATLAB / Simulink software to verify the conventional two stage buck-boost dc-ac VSI, Z-source network, and Quasi Z-Source inverter topologies performance.

For the future research, the following improvement can be implemented:

By using optimization, the inductor and the capacitor values of the Z-Source and Quasi Z-Source could be minimized to the suitable value, which could reduce the total cost of the proposed topology for the experimental research. Other enhance will be done in future research is that modify the control methods to get better performance with minimizing the cost.

## REFERENCES

- [1] Tan K. Kwang, Syafrudin B. Masri, "Grid Tie Photovoltaic Inverter for Residential Application", *Modern Applied Science*, Vol. 5, No. 4, pp. 200-211, August 2011.
- [2] Muhammad H. Rashid, "*Power Electronics: Circuits, Devices and Applications*", (3rd Edition). s.l.: Prentice Hall, 2004.
- [3] K.V. Kumar, P.A. Michael, J.P. John and S.S. Kumar, "Simulation and Comparison of SPWM and SVPWM control for Three Phase Inverter", *Asian Research Publishing Network*, Vol. 5, No. 7, pp. 61-74, July 2010.
- [4] Yan Z., Jinjun L., Chaoyi Z. , "Comparison of Traditional Two-Stage Buck-Boost Voltage Source Inverter and Diode-Assisted Buck-Boost Voltage Source Inverter", Twenty-Seventh Annual IEEE Applied Power Electronics Conference and Exposition (APEC), pp. 141 – 148, 5-9 Feb. 2012.
- [5] Omar E., Joeri V. M., and Philippe L., "Experimental Study of Shoot-Through Control Methods for Z-Source Inverter" *EPE Journal*, Vol. 21, No 2, June 2011.
- [6] H. Rostami, D. A. Khaburi, "Voltage Gain Comparison of Different Control Methods of the Z-Source Inverter", Electrical and Electronics Engineering, ELECO. International Conference, I-268 - I-272, 5-8 Nov. 2009.
- [7] Miaosen S., Alan J., Jin W., Fang Z. P., and Donald J. A, "Comparison of Traditional Inverters and Z-Source Inverter for Fuel Cell Vehicles", *Power Electronics in Transportation*, pp. 125 – 132, 21-22 Oct. 2004.
- [8] B. Justus Rabi and R. Arumugam, "Harmonics Study and Comparison of Z-source Inverter with Traditional Inverters", *American Journal of Applied Sciences* 2 (10): pp. 1418-1426, 2005.
- [9] Mohd. Shafie B., Nasrudin Abd. R., and Kamarul H. G., "Analysis of various PWM controls on single-phase Z-source inverter", Research and Development (SCORED), IEEE Student Conference, pp. 448 – 451, 13 - 14 Dec. 2010.

- [10] Miaosen S., Jin W., Alan J., and Fang Z. P. , "Constant Boost Control of the Z-Source Inverter to Minimize Current Ripple and Voltage Stress", *IEEE transactions on industry applications*, Vol. 42, No. 3, pp. 770-778, May/June 2006.
- [11] Selva K., and Priyaa D., "High Performance PV Power Generation Using Z Source Inverter", *International Journal of Advanced Research in Electrical and Electronics Engineering*, Volume 2, Issue 2 08-Apr. 2014.
- [12] Anh-Vu H., Tae-Won C. , Hong-Hee L., and Heung-Geun K., "Active Switched Quasi-Z-Source Inverter with High-Boost Ability for Low-Voltage Renewable Energy Sources", *Clean Electrical Power (ICCEP)*, International Conference , pp. 627 – 632, 16-18 June 2015.
- [13] A. S. Kumar, and G. M. Gowd , "Simple Boost Control of Five-Level Z-Source Diode-Clamped Inverter by Multi-Carrier PWM Methods", *International Journal of Engineering Research and Applications (IJERA)*, Vol. 3, Issue 4, pp.2162-2167, Jul-Aug 2013.
- [14] M. A. Kumar, and M. Barai , "Performance Analysis of Control and Modulation Methods of Z-source Inverter", *Signal Processing, Informatics, Communication and Energy Systems (SPICES)*, IEEE International Conference , pp. 1 – 5, 19-21 Feb. 2015.
- [15] Miaosen S., Jin W., Alan Joseph, Fang Z. P., Leon M. Tolbert, and Donald J. Adams , "Maximum Constant Boost Control of the Z-Source Inverter" , *Industry Applications Conference, 39th IAS Annual Meeting. Conference Record of the 2004 IEEE*, Volume 1, pp. 142-147, 3-7 Oct. 2004.
- [16] S. Rajakaruna, and Y. R. L. Jayawickrama, "Designing Impedance Network of Z-Source Inverters", *International Power Engineering Conference*, Vol. 2, pp. 962 – 967, Nov. 29 2005-Dec. 2 2005.
- [17] E. C. dos Santos Jr. , M. Pacas , and M. G. Molina , "Two-Phase Motor Drive Systems with Z-Source Inverter and Hybrid PWM", *IEEE Energy Conversion Congress and Exposition* , pp. 3877 – 3882 , 12-16 Sept. 2010.
- [18] U. Shajith Ali, and V. Kamaraj, "Z-Source Inverter with Improved Performance for Photovoltaic Applications", *Industrial Electronics and Applications (ISIEA)*, IEEE Symposium, pp. 681 – 686, 25-28 Sept. 2011.
- [19] K. Supraja, and K. Suresh, "An Optimizing Methodology of ZSI with Suitable PWM Control Techniques", *International Journal of Science and Research (IJSR)*, Volume 3 Issue 9, pp. 1828- 1834, September 2014.

- [20] Fang Zheng Peng, "Z-Source Inverter", *IEEE Transactions on Industry Applications*, Vol. 39, No. 2, pp. 504-510, March/April 2003.
- [21] Atul K., and Mohd. Arif K., "Z- Source Inverter Simulation and Harmonic Study", *Global Journal of Advanced Engineering Technologies*, Vol. 1, Issue 1, pp. 5-9, 2012.
- [22] Sumedha R., and Laksumana J., "Steady-State Analysis and Designing Impedance Network of Z-Source Inverters", *IEEE Transactions on Industrial Electronics*, Vol. 57, No. 7, pp. 2483- 2490, July 2010.
- [23] D. Vinnikov, I. Roasto, T. Jalakas, S. Ott, "Extended Boost Quasi-Z-Source Inverters: Possibilities and Challenges", 2012 13th Biennial Baltic Electronics Conference, pp. 259 – 262, 3-5 Oct. 2012.
- [24] Sunpho G., and Jani D., "Analysis of Sinusoidal Pulse Width Modulation Control Strategies for Quasi Z Source Inverter", *International Journal of Advanced Research in Electrical, Electronics and Instrumentation Engineering*, Vol. 2, Issue 9, pp. 4355- 4362, September 2013.
- [25] Yuan Li1, Joel Anderson, Fang Z. Peng, and Dichen Liu, "Quasi-Z-Source Inverter for Photovoltaic Power Generation Systems", Applied Power Electronics Conference and Exposition, APEC 2009. Twenty-Fourth Annual IEEE, pp. 918 – 924, 15-19 Feb. 2009.
- [26] Yam P. Siwakoti and Fang Zheng Peng, "Impedance-Source Networks for Electric Power Conversion Part I: A Topological Review", *IEEE Transactions on Power Electronics*, Vol. 30, No. 2, pp. 699-716, Feb. 2015.
- [27] X. P. Fang, Z. M. Qian, Gao. B. Gu., F. Z. Peng, and X. M. Yuan, "Current Mode Z-Source Inverter-Fed ASD System", *IEEE PESC*, Vol. 4, pp. 2805-2809, April 2004.
- [28] F. Z. Peng , A. Joseph, J. Wang , M. Shen , L. Chen, Z. Pan , E. Ortiz-Rivera , and Y. Huang, "Z-source inverter for motor drives", *IEEE Transactions on Power Electronics* , Volume 20 , Issue 4 , pp. 857 – 863 , July 2005.
- [29] Yushan L., Baoming Ge, Haitham Abu-Rub, and Fang Z. P., "Control System Design of Battery-Assisted Quasi-Z-Source Inverter for Grid-Tie Photovoltaic Power Generation", *IEEE Transactions on Sustainable Energy*, vol. 4, No. 4, October 2013.

- [30] Hooman Z., and Alfred B., "A New Quasi z-source inverter Topology to improve Voltage boost ability", *Technical Journal of Engineering and Applied Sciences*, Available online at [www.tjeas.com](http://www.tjeas.com).
- [31] Young-Cheol L., and Sung-Jun P., "Improved Trans-Z-Source Inverter with Continuous Input Current and Boost Inversion Capability", *IEEE Transactions on Power Electronics*, Volume 28, Issue 10, pp. 4500 – 4510, Oct. 2013.
- [32] Zulhani R., M. F. Rahman, "Design and Simulation of Quasi-Z Source Grid connected PV Inverter with Battery Storage", *Power and Energy (PECon), IEEE International Conference*, pp. 303 – 308, 2-5 Dec. 2012.
- [33] Muhammad H. Rashid, "*Power electronics: Circuits, Devices and Applications*", Pearson Education India, 01-Sep-2003.
- [34] N. Mohan, T.M. Undeland, W.P. Robbins, "*Power Electronics: Converters, Applications, and Design*", John Wiley and Sons, Singapore, 1995.
- [35] M. H. Rashid, "*Power Electronics, Circuits, Devices, and Applications*", 3rd Ed. New Delhi: Prentice-Hall of India Private Limited, pp.253-256, 2007.
- [36] B. Panda et. al., "Soft-Switching DC-AC Converters a Brief Literature Review", *International Journal of Engineering Science and Technology*, Vol. 2(12), pp. 7004-7020, January 2010.
- [37] Fang.Z. Peng, "Z-Source Inverter", *IEEE Transactions on Industry Applications*, Vol. 39, No. 2, pp.504-510, March/April 2003.
- [38] Jingquan Chen, Dragan Maksimovic, and Robert W. Erickson, "Analysis and Design of a Low-Stress Buck-Boost Converter in Universal-Input PFC Applications", *IEEE Transactions on Power Electronics*, Vol. 21, No. 2, March 2006.
- [39] Yan Zhang, Jinjun Liu, Chaoyi Zhang, "Comparison of Traditional Two-Stage Buck-Boost Voltage Source Inverter and Diode-Assisted Buck- Boost Voltage Source Inverter", *Twenty-Seventh Annual IEEE Applied Power Electronics Conference and Exposition (APEC)*, pp. 141 – 148, 5-9 Feb. 2012.
- [40] Bindeshwar Singh, S. P. Singh, J. Singh, and Mohd Naim, "Performance evaluation of three phase induction motor drive fed from z-source inverter", *International Journal on Computer Science and Engineering (IJCSE)*, Vol. 3 No. 3 , pp. 1227-1289, Mar 2011.

- [41] Anderson J., Peng F. Z. , "Four quasi-Z-Source inverters ", IEEE Power Electronics Specialists Conference (PESC'2008), pp. 2743–2749, 2008.
- [42] Yuan Li, Anderson J., Peng F. Z., Dichen Liu., " Quasi-Z-Source Inverter for Photovoltaic Power Generation Systems", Twenty-Fourth Annual IEEE Applied Power Electronics Conference and Exposition (APEC'09), pp. 918–924, 2009.
- [43] Jong Hyoung Park, Heung Geun Kim, Eui Cheol Nho, Tae Won Chun, Jaeho Choi. "Grid-Connected PV System Using a Quasi-Z-Source Inverter", Twenty-Fourth Annual IEEE Applied Power Electronics Conference and Exposition (APEC'09), pp. 925–929, 2009.
- [44] J. Anderson and F. Z. Peng, "A class of quasi-Z-source inverters", in Proc. IEEE Industry Applications Society Annual Meeting (IAS'08), Edmonton, AB, Canada, Oct. 5–9, pp. 1–7, 2008.
- [45] Y. Li, J. Anderson, F. Z. Peng, and D. Liu, "Quasi-Z-source inverter for photovoltaic power generation systems", in Proc. 24th Ann. IEEE Applied Power Electronics Conf. Exposition (APEC2009), Washington, DC, Feb. 15–19, pp. 918–924, 2009.
- [46] J. Park, H. Kim, E. Nho, T. Chun, and J. Choi, "Grid-connected PV system using a quasi-Z-source inverter", in Proc. 24th Ann. IEEE Applied Power Electronics Conf. Exposition (APEC2009), Washington, DC, Feb. 15-19, pp. 925–929, 2009.
- [47] J.-H. Park, H.-G. Kim, E.-C. Nho, and T.-W. Chun, "Power conditioning system for a grid connected PV power generation using a quasi Z source inverter", *J. Power Electron*, Vol. 10, No. 1, pp. 79–84, Jan. 2010.
- [48] D. Vinnikov, I. Roasto, T. Jalakas, S. Ott, "Extended Boost Quasi-Z-Source Inverters: Possibilities and Challenges", *Electronics and Electrical Engineering*, Vol. No. 6 (112), pp. 51-56.
- [49] W.-Toke Franke, Malte Mohr, Friedrich W. Fuchs, "Comparison of a Z-Source Inverter and a Voltage-Source Inverter Linked with a DC/DC Boost-Converter for Wind Turbines Concerning Their Efficiency and Installed Semiconductor Power", IEEE Conf. (PESC'08), pp.1814–1820, 2008.
- [50] J. Anderson and F.Z. Peng, "Four Quasi-Z-Source Inverters", in Proc. IEEE PESC'08, Rhodes, Greece, pp. 2743-2749, June 2008.
- [51] FY 2005 report, "Z-source inverter for fuel cell vehicles, Oak Ridge National Laboratory", pp. 1-77, September 2005.

- [52] F. Z. Peng, M. Shen, and Z. Qian, "Maximum boost control of the Z-source inverter", *IEEE Transactions on Power Electronic*, Vol. 20, No. 4, pp. 833-838, July 2005.
- [53] Poh Chiang Loh, D. Mahinda Vilathgamuwa, Yue Sen Lai, Geok Tin Chua, and Yunwei Li, "Pulse-Width Modulation of Z-Source Inverters", *IEEE Transactions on Power Electronics*, Vol. 20, No. 6, pp. 1346-1355, November 2005.
- [54] T.W. Chun, Q.V. Tran, J.R. Ahn, and J.S. Lai, "AC Output Voltage Control with Minimization of Voltage Stress Across Devices in the Z-Source Inverter Using Modified SVPWM", *IEEE Power Electronics Specialists Conference, PESC*, Jeju, Korea, pp. 3030-3034, June 2006.
- [55] Jin Li, Jinjun Liu, and Zeng Liu, "Loss Oriented Evaluation and Comparison of Z-Source Inverters Using Different Pulse Width Modulation Strategies", the twenty-fourth annual IEEE Applied Power Electronics Conference and Exposition, APEC, pp. 851-856, Feb. 2009.
- [56] Jin Li, Jinjun Liu, and Zeng Liu, "Comparison of Z-source inverter and traditional two-stage boost-buck inverter in grid-tied renewable energy generation", *IEEE 6th International Power Electronics and Motion Control Conference, IPEMC*, pp. 1493-1497, May 2009.
- [57] Omar Ellabban, Joeri Van Mierlo and Philippe Lataire, "Comparison between Different PWM Control Methods for Different ZSource Inverter Topologies", the 13th European Conference on Power Electronics and Applications, Barcelona-Spain, pp. 1-11, Sept. 2009.
- [58] Jacek Rabkowski, "Improvement of Z-source inverter properties using advanced PWM methods", the 13th European Conference on Power Electronics and Applications, Barcelona-Spain, pp. 1-9, Sept. 2009.
- [59] H. Rostami and D. A. Khaburi, "Voltage Gain Comparison of Different Control Methods of the Z-Source Inverter", *International Conference on Electrical and Electronics Engineering, ELECO*, pp. 268-272, Nov. 2009.
- [60] T. Meenakshi and K. Rajambal, "Identification of an Effective Control Scheme for Z-source Inverter", *The Asian Power Electronics Journal*, Vol. 4, No.1, pp. 22-28, April 2010.
- [61] W.-T. Franke, M. Mohr and F. W. Fuchs, "Comparison of a Z-Source Inverter and a Voltage-Source Inverter Linked with a DC/DC Boost-Converter for Wind Turbines Concerning Their Efficiency and Installed Semiconductor Power",

IEEE 39th Power Electronics Specialists Conference, PESC08, Rhodes, pp. 1814 – 1820, June 2008.

- [62] Keping You and M. F. Rahman, "Analytical Model of Conduction and Switching Losses of Matrix-Z-Source Converter", *Journal of Power Electronics*, Vol. 9, No. 2, pp. 275-287, March 2009.
- [63] Omar Ellabban, Joeri Van Mierlo and Philippe Lataire, "Experimental Study of the Shoot-Through Boost Control Methods for the Z-Source Inverter", *EPE Journal*, Volume 21, Issue 2, pp. 18-29, June 2011.
- [64] Malte Mohr, and Friedrich W. Fuchs, "Comparison of Three Phase Current Source Inverters and Voltage Source Inverters Linked with DC to DC Boost Converters for Fuel Cell Generation Systems", the European Conference on Power Electronics and Applications, Dresden, pp. 1-10, 2005.
- [65] Amol R. Sutar, Satyawan R. Jagtap, and Jakirhusen Tamboli, "Performance Analysis of Z-source Inverter Fed Induction Motor Drive", *International Journal of Scientific and Engineering Research*, Issue 5, Volume 3, pp. 1-6, May-2012.
- [66] Technical Information, "Infineon-FS100R07PE4", DATA SHEET OF IGBT-Module.
- [67] Technical Information, "Infineon-BSM 75 GB 60 DLC", DATA SHEET OF IGBT-Module.
- [68] Shobanadevi Nagarajan, Krishnamurthy Venkatachalapathy, Stalin Narayanasamy, "A Simple Boost Shoot through Control for Single phase Quasi ZSI DC-DC Converters Based on Voltage Doubler Rectifier", *przełąd elektrotechniczny*, pp.242-246, 2015.
- [69] K. Thorborg, "*Power Electronics*", London, U.K.: Prentice-Hall International (U.K.) Ltd., 1988.

## CURRICULUM VITAE

### PERSONAL INFORMATION

Name, Surname : Israa Hussein  
Date and Place of Birth : 26.10.1972/Iraq - Baghdad  
Marital Status : Married  
Phone : 00905340220668  
E-mail : eng.israismaeel@gmail.com



### EDUCATION

High School : Shohada AL- jaish Secondary School, 1990.  
Undergraduate : University of Technology / Electrical Engineering Department,  
1996.

### PUBLISHED PAPERS

Raad S. Jawad, Israa I. Hussein, I. Mahariq , "Design and Simulation of Three Phase and Single Phase Z-Source Inverters", ICEEPIV, researchgate.net, pp. 58-64, 6-7 April 2016.  
Raad S. Jawad, Israa I. Hussein, I. Mahariq , "FACTS Technology: Current Challenges and Future Trends", ICEEPIV, researchgate.net, pp. 45-50, 6-7 April 2016.